Photosynthetic response of Southern Ocean phytoplankton under Iron and light limitations: Bioassay experiments

By Natasha Van Horsten

Thesis presented in fulfilment of the requirements for the degree of Master of Geology at the Stellenbosch University

Supervisor: Dr Susanne Fietz

Co-supervisors: Dr Thato Mtshali & Prof. Alakendra Roychoudhury

December 2015

Declaration

By submitting this thesis electronically, I declare that the entirety of the work contained therein is my own, original work, that I am the authorship owner thereof (unless to the extent explicitly otherwise stated) and that I have not previously in its entirety or in part submitted it for obtaining any qualification.

Signature: ……

Date: 19-11-2015

Abstract

The Southern Ocean (SO) is of significant interest in the understanding of the global carbon cycle and therefore many studies have been conducted to determine the limiting factors controlling the biological pump within the region. During photosynthesis phytoplankton require various nutrients such as NO_3, PO_4, inorganic carbon and the micronutrient Fe. The SO is a High-Nutrient Low-Chlorophyll region, therefore no macronutrient limitation is experienced by resident phytoplankton but instead the micronutrient Fe is a significant limiting factor within these waters due to limited inputs. Due to deep mixed layer depths, ice cover, low sun angles and cloud cover throughout parts of the year, light is also considered a limiting factor in the SO. Fe and light limitation cause a decrease in photosynthetic efficiency and therefore a decrease in carbon fixation capabilities. During this study we conducted five bioassay shipboard incubation experiments during two cruises along the Greenwich meridian between South Africa and the ice edge, SOSCEx during March and SAFePool during January to February, in which we varied Fe concentrations and light levels to determine the effects of Fe and light limitation or co-limitation within resident phytoplankton. Spatial and temporal variations in phytoplankton response were studied to determine varying effects of limitation across water masses and different stages of bloom decline within the study area. The combined addition of Fe and light gave the largest increase in biomass, photosynthetic capacity and nutrient uptake. In support of the hypotheses tested changes in the photosynthetic apparatus led to changes in the photosynthetic efficiency and growth of the SO phytoplankton, as a result of variations in Fe and light availability. Variability was also observed in the response of phytoplankton to Fe and light amendments due to spatial and temporal variation in resident phytoplankton communities. It was therefore concluded that both Fe and light are significant controls in the resident phytoplankton photosynthetic apparatus, photosynthetic capabilities, organic carbon fixation and therefore the biogeochemical cycles within the Atlantic sector of the SO.

Opsomming

Die Suidelike Oseaan (SO) is van beduidende belang in die begrip van die globale koolstofsiklus en dus is baie studies gedoen om die beperkende faktore te bepaal wat die biologiese pomp in die streek beheer. Tydens fotosintese benodig fitoplankton verskillende voedingstowwe soos NO_3, PO_4, anorganiese koolstof en die mikrovoedingstof Fe. Die SO is 'n High-Nutrient Lae-Chlorofil streek, dus word geen makrovoedingstof beperking ervaar deur inwoner fitoplankton maar in plaas daarvan is die mikrovoedingstof Fe 'n beduidende beperkende faktor binne hierdie waters weens beperkte insette. As gevolg van diep gemengde laag dieptes, ysbedekking, lae son hoeke en wolkbedekking deur dele van die jaar, word lig ook beskou as 'n beperkende faktor in die SO. Fe en lig beperking veroorsaak 'n afname in die fotosintetiese doeltreffendheid en dus 'n afname in koolstof binding vermoëns. Tydens hierdie studie het ons vyf biotoets inkubasie eksperimente aan boord die skeep gedoen tydens twee vaarte langs die Greenwich meridiaan tussen Suid-Afrika en die ys rand, SOSCEx gedurende Maart en SAFePool gedurende Januarie tot Februarie, waarin ons Fe konsentrasies en lig vlakke gewissel het om die gevolge van Fe en lig beperking, of mede-beperking, binne inwoner fitoplankton te bepaal. Ruimtelike en temporale variasies in fitoplankton reaksie was bestudeer om wisselende gevolge van die beperking oor watermassas en verskillende stadiums van bloei afname in die studie area te bepaal. Die gekombineerde byvoeging van Fe en lig het die grootste toename in biomassa, fotosintetiese kapasiteit en voedingsopname gegee. Ter ondersteuning van die getoetste hipoteses, veranderinge in die fotosintetiese apparaat het gelei tot veranderinge in die fotosintetiese doeltreffendheid en groei van die SO fitoplankton, as 'n gevolg van variasies in Fe en lig beskikbaarheid. Veranderlikheid is ook waargeneem in die reaksie van fitoplankton om Fe en lig wysigings weens die ruimtelike en tydelike variasie in inwoner fitoplankton gemeenskappe. Dus was dit by die gevolgtrekking gekom dat beide Fe en lig beduidende kontrole in die inwoner fitoplankton fotosintetiese apparaat, fotosintetiese vermoëns, organiese koolstof binding en daarom die biogeochemiese siklusse binne die Atlantiese sektor van die SO.

Acknowledgements

I would like to thank the National Research Foundation (NRF), the South African National Antarctic Programme (SANAP), the Department of Environmental Affairs (DEA), the Southern Ocean Climate and Carbon Observatory (SOCCO) research group and the Council of Scientific and Industrial Research (CSIR) for making this study possible through financial support. The Smit Amandla crew of the SA Agulhas I & II and all the scientific participants of the SOSCEx and SAFePool cruise, for their assistance in sampling and conducting of experiments and analyses. Dr Sandy Thomalla and Emma Bone for their much appreciated assistance and input. My supervisors Dr Susanne Fietz, Dr Thato Mtshali and Prof. Alakendra Roychoudhury for their valuable supervision. Lastly, I would like to thank my family and friends for all their support throughout my studies.

Table of Contents

List of Figures

List of Tables

List of Abbreviations

ATP	-	Adenosine triphosphate
AZ	-	Antarctic Zone
C-B cycle	-	Calvin-Benson cycle
Chl *a*	-	Chlorophyll *a*
CTD	-	Conductivity, Temperature and Depth
F_0	-	Minimum fluorescence
FIRe	-	Fluorescence Induction and Relaxation
F_m	-	Maximum fluorescence
FRRf	-	Fast Repetition Rate fluorometry
F_v	-	Variable fluorescence
F_v/F_m	-	PSII photochemical efficiency
HL	-	High Light
HL-HFe	-	High Light – High Fe
HL-LFe	-	High Light – Low Fe
HNLC	-	High-Nutrient Low-Chlorophyll
HNLSiLC	-	High-Nutrient Low-Silicate Low-Chlorophyll
LL	-	Low Light
LL-HFe	-	Low Light – High Fe
LL-LFe	-	Low Light – Low Fe
MLD	-	Mixed Layer Depth
NADPH	-	Nicotinamide adenine dinucleotide phosphate
P. antarctica	-	*Phaeocystis antarctica*
PAR	-	Photosynthetically Active Radiation
PFZ	-	Polar Frontal Zone
POC	-	Particulate Organic Carbon
PSI	-	Photosystem I

PSII	-	Photosystem II
$R\sigma_{PSII}$	-	Probability of PSII reaction centre being closed during first flashlet during FRRf
SA	-	SubAntarctic
SAFePool	-	South Atlantic Fe Pool
SAZ	-	SubAntarctic Zone
SCM	-	Subsurface Chlorophyll Maximum
SO	-	Southern Ocean
SOSCEx	-	Southern Ocean Seasonal Cycle Experiment
σ_{PSII}	-	PSII functional absorption cross-section

1. Introduction

1.1 Background

The Southern Ocean (SO) is the largest High-Nutrient Low-Chlorophyll (HNLC) region in which, through various studies, it has been reported that the bioavailability of the micronutrient Fe significantly impacts the in situ phytoplankton growth (Berg *et al.* 2011; Cassar *et al.* 2004; Boyd & Abraham 2001; Boyd *et al.* 1999; Feng *et al.* 2010). The organic fixation of inorganic carbon is driven by phytoplankton and therefore this is significant to the global atmospheric CO_2 levels. Based on climate change predicted scenarios there will be multiple concurrent changes in the physical and chemical environment of the SO, affecting light, macro- and micronutrient supply, pH and CO_2 concentrations, all affecting the regulation of phytoplankton carbon fixation, biomass and export. Thus it is important to understand the effects of these changes due to their synergistic and antagonistic effects on future phytoplanktonic responses (Boyd *et al.* 2010)

The micronutrient Fe is of crucial importance to the photosynthesis and biosynthesis processes of phytoplankton, including the photosynthetic electron transport chain, respiratory processes and the reduction of nitrate and phosphate (Falkowski & Raven 2007). Dissolved Fe concentrations in most parts of the SO are relatively low throughout the year due to its low solubility in oxic seawater, fast photo-redox chemistry, organic complexation and low internal and external inputs, therefore reducing bioavailable Fe concentrations (Klunder *et al.* 2011; Tagliabue *et al.* 2014). Much focus has been put on Fe as the main factor limiting phytoplankton growth in the SO and it has become evident that photosynthetically active radiation (PAR) is another key limiting factor due to strong wind mixing that causes deep mixed layer depths (MLDs), sea-ice cover, cloud cover and low sun angles experienced to different levels throughout the year. Both these co-factors play a key role in phytoplankton photosynthetic apparatus of the electron transport chain, and have been reported to have significant interactive effects on phytoplankton biomass accumulation in the HNLC regions of the SO. Many in situ Fe fertilization experiments and shipboard incubation experiments have been conducted to better understand the interactive effects of limiting factors on phytoplankton growth throughout the SO (Berg *et al.* 2011; Boyd *et al.* 1999; Feng *et al.* 2010; Moore *et al.* 2007).

The section of the water column of biological interest is the lower euphotic zone. This is the section of relatively higher phytoplankton biomass due to nutrient supply from deeper

waters and irradiance sufficient for photosynthesis to proceed, creating the Subsurface Chlorophyll Maximum (SCM) (Boyd & Abraham 2001). Spatial and temporal variations in limiting factors are reported to affect in situ phytoplankton, where Fe controls growth in shallow MLDs of SubAntarctic (SA) waters during summer and Fe and light co-limitation controls growth in polar regions of deeper MLDs (Boyd *et al.* 2001). A seasonal progression of limiting factors in SA waters is reported to be; Fe and light co-limitation in spring, Fe limitation in summer as MLDs shoal and Fe and Si co-limitation in late summer, during bloom decline, under higher irradiance (Boyd *et al.* 2010).

1.2 Objectives and aim

In this study our aim was to understand the interactive effects of Fe and light co-limitation in SO phytoplankton of the Atlantic sector and how phytoplankton adapt to these limiting conditions. To do this a number of shipboard Fe/light bioassay incubation experiments were conducted across the different water masses of the SO, from the SubAntarctic zone (SAZ) to the Antarctic zone (AZ). A bioassay incubation is the process by which phytoplankton biological activity is measured against a standard. Shipboard bioassay incubation experiments were to be run during the Southern Ocean Seasonal Cycle Experiment (SOSCEx) and South Atlantic Fe Pool (SAFePool) cruises, by incubating resident phytoplankton from the SO at in situ and increased Fe and light levels to determine the response of the resident phytoplankton to changes of these two limiting factors, separately and interactively, during early and late bloom decline within the SAZ and the AZ. Chlorophyll *a* (chl *a*) and particulate organic carbon (POC) was measured in lieu of actual phytoplankton counts to determine growth response and fluorescence was measured to determine photosynthetic response.

The following hypotheses were tested:

Hypothesis 1:

Changes in photosynthetic apparatus, as a result of variations in Fe and light availability, lead to changes in photosynthetic efficiency and therefore phytoplankton growth in the SO, thereby affecting the biogeochemical cycles within the SO.

This hypothesis was tested with the following two questions in mind:

(i) How does SO phytoplankton growth respond and adapt to Fe and light deprivation, and

(ii) How does their photosynthetic apparatus respond to these co-limiting factors?

Hypothesis 2:

SO phytoplankton show variability in response to Fe and light amendments due to spatial and temporal variation in resident phytoplankton communities.

To test this hypothesis Fe and light bioassay incubation experiments were conducted at different times of the season in the SAZ and at different water masses to compare phytoplankton community response to Fe and light variability.

2. Literature Review

2.1 Introduction

Marine biogeochemistry is the study of the elements present in the ocean and the processes that affect these elements. The element of most interest is carbon due to the effects of anthropogenic CO_2, as a greenhouse gas, on climate change. The ocean is of significant importance in this regard due to it acting as a reservoir for anthropogenic CO_2. It is believed that the ocean takes up about 30% of global anthropogenic CO_2 produced (Falkowski & Raven 2007). CO_2 is regulated by various processes in the ocean, namely, the solubility pump, biological pump and the carbonate counter pump (Figure 2.1). The solubility pump is the process of dissolution and dissociation of CO_2 between the atmosphere and the ocean. This process is mainly controlled by temperature and, to a lesser extent, salinity. CO_2 concentration in seawater is inversely proportional to temperature and directly proportional to salinity, therefore more CO_2 is found in polar and deep waters. The biological pump is the process by which photosynthetic organisms take up and release dissolved inorganic carbon through photosynthesis and respiration; carbon is either stored in the deep ocean or remineralized and released through upwelling. The biological pump comprises two reactions, photosynthesis and respiration. These processes are further discussed in subsection 2.3. The carbonate counter pump is partly a biological mechanism where calcium carbonate, which is produced by specific photosynthetic organisms, remineralizes and CO_2 is released (Sarmiento & Gruber 2006).

The carbon flux through phytoplankton is about a thousand times faster than through terrestrial plants and is therefore a very significant factor in the regulation of global CO_2 levels (Falkowski & Raven 2007). Phytoplankton play a major role in the cycling of the elements in the ocean and are particularly important in the uptake of CO_2 through photosynthesis. There are many factors that limit the uptake of CO_2 through photosynthesis in the global oceans and therefore much research is done to understand this intricate web of factors to better understand climate change.

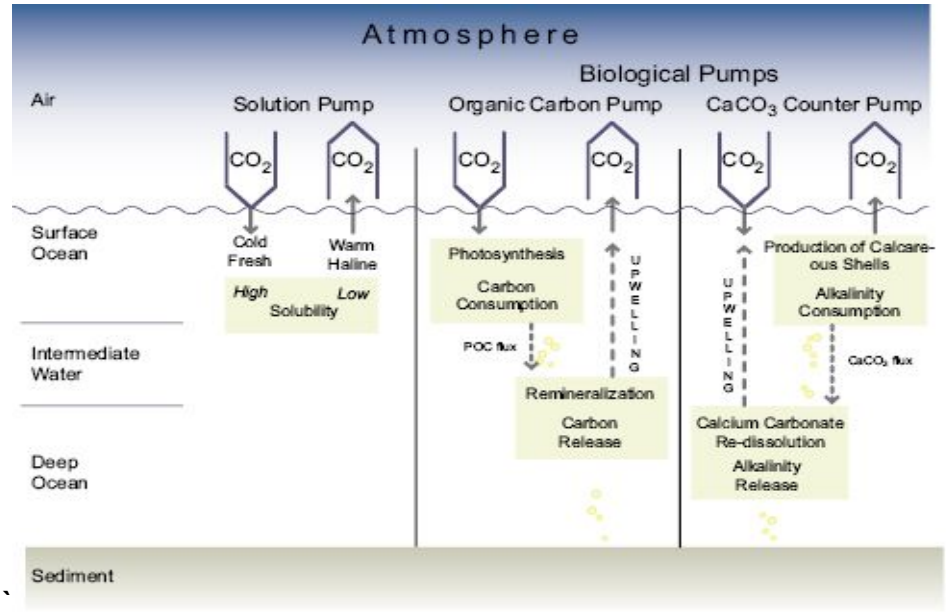

Figure 2.1 Diagram illustrating the solubility pump, biological pump and carbonate counter pump regulating CO_2 in the ocean (Lagzi *et al.* 2013)

The thermohaline circulation is another process by which the elements of the ocean are affected and transported throughout the global oceans (Figure 2.2). This process is controlled by temperature and salinity, and the effects of these two factors on the density of seawater. Warm equatorial surface waters are transported towards the poles thereby creating a flux. As the warm water reaches the cold polar regions the high salinity waters cool and sink and are then transported back towards the equator as deep water. Due to upwelling, an enhanced nutrient flux is created to the euphotic zone at the edges of the rotating fields of the circulation (Falkowski & Raven 2007; Sarmiento & Gruber 2006).

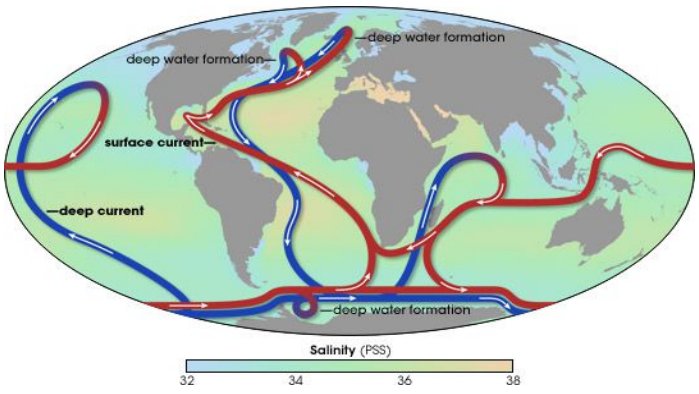

Figure 2.2 The general location and direction of the global ocean warm surface (red) currents and the cold deep (blue) currents, of the thermohaline circulation (Riebeek & Simmon 2006)

2.2 The Southern Ocean

The ocean is an important element in the regulation of anthropogenic CO_2 uptake and the SO has been reported to be of particular significance to the global carbon cycle, with up to 40% of the global ocean anthropogenic CO_2 passing through the SO (Caldeira & Duffy 2000). The SO is a HNLC region which has been shown to be high in macronutrients namely, nitrate, phosphate and silicate (Bentaleb *et al.* 1998; Le Moigne *et al.* 2013) but due to low micronutrients and other environmental controls such as light and temperature there is limited photoautotrophic biomass (Boyd *et al.* 2010) (Figure 2.3). Deep MLDs, sea-ice cover and low sun angles are a few reasons for light limitation being an environmental factor controlling biomass accumulation, therefore limiting the use of available macronutrients in the SO (Sigman *et al.* 1999). Micronutrient limitation, specifically Fe, has also been reported in numerous studies as a limiting factor in the SO, with concentrations being subnanomolar throughout most of the year and therefore playing a significant role in the limited biomass observed in this HNLC region (Boyd *et al.* 1999, Boyd & Abraham 2001; Browning *et al.* 2014; Hopkinson *et al.* 2007; Moore *et al.* 2007; Sosik & Olson 2002). The main new Fe inputs in the HNLC waters of the SO are through dust deposits but due to spatial vastness, low dust inputs limit Fe concentrations throughout the year and therefore most dissolved Fe is supplied to surface waters from subsurface reservoirs (Falkowski & Raven 2007; Tagliabue *et al.* 2014). Seasonal Si limitation has been reported in SA waters, whereas Si concentrations in Antarctic polar waters are high throughout the year (Boyd *et al.* 2001, 2010; Hutchins *et al.* 2001; Klunder *et al.* 2011).

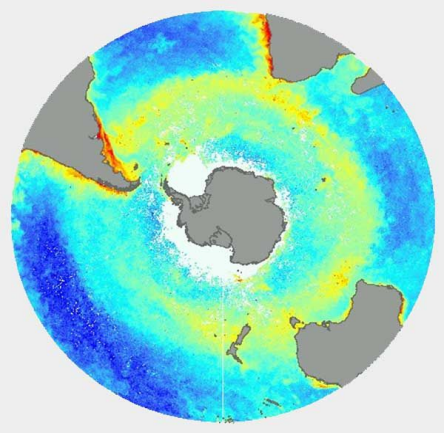

Figure 2.3 Chlorophyll concentration of the SO measured by the SeaWiFS project, showing areas of relatively high chlorophyll in yellow and green (British Antarctic Survey n.d.)

The dominant phytoplankton in the SO have been reported to be diatoms and *Phaeocystis antartica* (*P. antarctica*), as seen in Figure 2.4 (Alvain *et al.* 2008; Bentaleb *et al.* 1998; Hopkinson *et al.* 2007). The distribution of phytoplankton species is controlled by many factors such as temperature, MLD and micro- and macronutrient availability (Falkowski & Raven 2007). Diatoms are considered to be cosmopolitan and are present throughout most of the SO, prone to areas of shallow MLDs, whereas *P. antarctica* are more specific to higher latitudes with deeper MLDs and lower temperatures. The varying phytoplankton community structure has been shown to have a large effect on results of different in situ and incubation experiments, due to Fe enrichment not being equally beneficial to all species. It has however been reported that both diatom and *P. antarctica* growth tend to be stimulated by the combined addition of Fe and light (Boyd *et al.* 2010; Sosik & Olson 2002). Little is known however about the environmental factors and the interactive effects of these factors, that control the growth of phytoplankton throughout the SO (Feng *et al.* 2010).

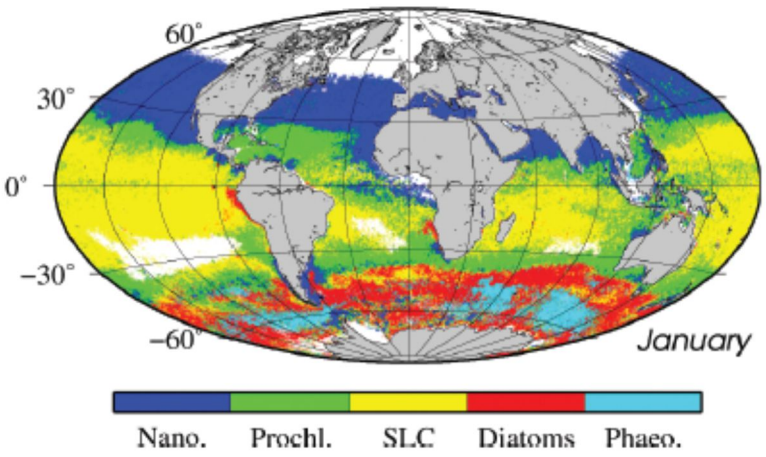

Figure 2.4 Climatology map (1997 – 2008, SeaWiFS) of dominant phytoplankton for January, using PHYSAT. Nano. = nanophytoplankton, Prochl. = *Prochlorococcus*, SLC = *Synechococcus*-like cyanobacteria and *Phaeo.* = *Phaeocystis* (Alvain *et al.* 2011)

2.3 Photosynthesis

Photosynthesis is the process by which photoautotrophic organisms use PAR to reduce CO_2 to carbohydrates for biosynthesis, food and respiration. Through oxygenic photosynthesis CO_2 is taken up and O_2 is released, where CO_2 becomes reduced and H_2O becomes oxidized, along the general redox reaction equation:

$$2H_2O + CO_2 + PAR \xrightarrow{\text{chl } \alpha} CH_2O + H_2O + O_2 \quad \text{(i)}$$

In the absence of light, photosynthetic organisms consume O_2 and CO_2 is evolved due to respiratory processes, along the general reaction equation:

$$CH_2O + O_2 \rightarrow CO_2 + H_2O + ATP \quad \text{(ii)}$$

The rate of photosynthesis is controlled by the efficiency of light utilization to drive photosynthetic reactions. Photosynthesis is comprised of two parts, the light-dependent reactions and the light-independent/dark reactions (Figure 2.5). The light reactions are the movement of protons and electrons. These are photochemically catalysed redox reactions which follow the process described by the Z-scheme (Figure 2.6), and the dark reactions are the fixation and reduction of CO_2, through the Calvin-Benson (C-B) cycle (Figure 2.7). These processes are facilitated by a group of elements within the photosynthetic organism, called the photosynthetic apparatus and the absorption of light is facilitated by chl *a*, a chromophore, one of the compounds which give the photosynthetic organism its colour. Photosynthesis involves light harvesting via chl *a*, primary charge separation through photosystem I (PSI) and photosystem II (PSII), electron transport, adenosine triphosphate (ATP) and nicotinamide adenine dinucleotide phosphate (NADPH) formation, carbon fixation and regeneration of substrates in the C-B cycle (Falkowski & Raven 2007).

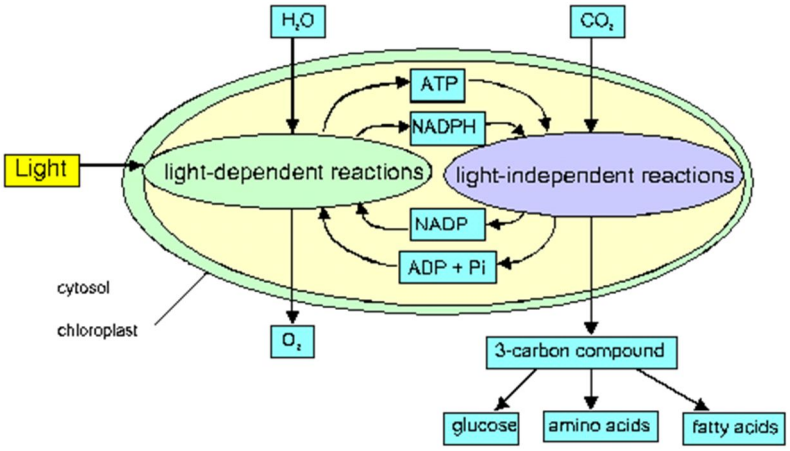

Figure 2.5 Schematic diagram of light and dark reactions that make up the photosynthesis process (Muller 2010)

Light reactions

Photons are absorbed by chl *a* molecules, the photosynthetic pigment, and the part of the photosynthetic unit which undergoes the photochemical reaction of oxygenic photosynthesis. The photosynthetic unit contains two photosystems, namely, PSI and PSII. These photosystems consist of reaction centres that are coupled to light-absorbing antennae, which absorb photons to proceed with the photochemical reactions. The reaction centre is where light is converted to photochemical energy. When a reaction centre is able to absorb a photon, it is said to be open, and fluorescence is photochemically quenched but when a reaction centre has already absorbed a photon it closes and further absorption is not possible, therefore photons are re-emitted and fluorescence is observed (Figure 2.8). When a reaction centre is open there is a high probability of trapping excitation and a flow of electrons is then generated. When a reaction centre undergoes a single photochemical reaction it is termed a single turnover. This electron transport chain yields the chemical reductant, NADPH, to assimilate inorganic carbon and the chemical energy, ATP, to sustain the metabolic activity of the organism, via the following reaction:

$$2H_2O + 2NADP^+ + 3ADP + 3P_i + \geq 8photons \rightarrow O_2 + 2NADPH + 2H^+ + 3ATP \qquad (iii)$$

(Falkowski & Raven 2007).

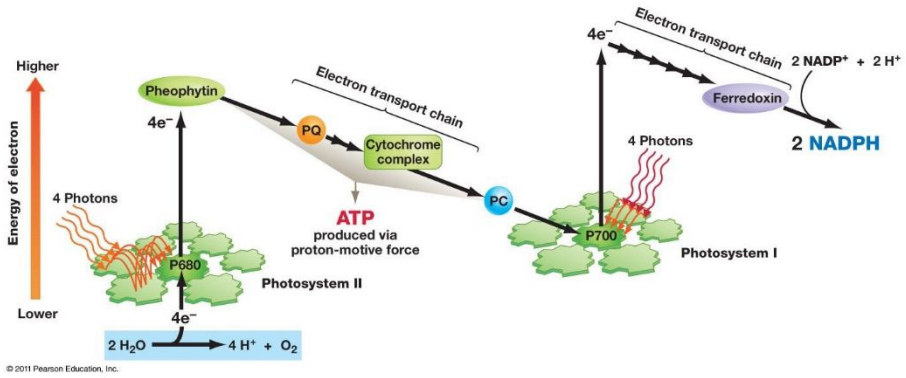

Figure 2.6 Schematic diagram of the Z-scheme, the pathway of the photosynthetic electron transport chain of photosynthesis (Muller 2010)

The Z-scheme

The Z-scheme is the pathway followed by the light reactions of oxygenic photosynthesis, in which two light reactions are coupled via an electron transport chain. Fe is an important element in the components of the Z-scheme; PSII contains three Fe atoms, PSI contains twelve and the cytochrome b_6/f complex contains five. Therefore Fe limitation will impair the functions of these components, thereby decreasing photosynthetic efficiency. The reaction in PSII generates an oxidant to oxidize H_2O and the electrons from H_2O then produce a reductant in PSI which is then used to reduce CO_2. The cytochrome b_6/f complex acts as an electron carrier and transfers electrons between the two photosystems. Ferrodoxin is a Fe-containing protein which, at the end of the electron transport chain, reduces the $NADP^+$ for use in the reduction of CO_2. When Fe availability is limited many photosynthetic organisms replace ferrodoxin with flavodoxin, a Cu-containing protein (Falkowski & Raven 2007).

Light can be a limiting factor in photosynthesis, which causes photosynthetic organisms to adapt by finding alternative pathways to proceed with physiological functions under these limiting conditions. Cyclic electron flow around PSI is a pathway which allows for the generation of ATP without the oxidation of H_2O or the reduction of CO_2. It has been suggested that 20% of absorbed photons contribute to this pathway under light limiting conditions. Temperature can affect electron transport due to the thermal effects of intermolecular collisions such as the diffusion of electron carriers (Falkowski & Raven 2007).

The Calvin-Benson cycle

The C-B cycle is the pathway followed for the photosynthetic reduction of CO_2 to carbohydrate. NADPH and ATP generated in the electron transport chain couples the light reaction and carbon fixation and ultimately cell growth. All oxygenic photosynthetic organisms incorporate CO_2 into organic carbon via the net reaction, including ATP and NADPH:

$$CO_2 + 2NADPH + 2H^+ + 3ATP \rightarrow CH_2O + H_2O + 2NADP^+ + 3ADP + 3P_i \qquad \text{(iv)}$$

The reaction occurs in a cycle, with only $^1/_6$ of carbon used to form an end product and the other $^5/_6$ are used as the substrate for the fixation of more CO_2. Overall, two moles of ATP and NADPH are used per mole CO_2 fixed. ATP is an energy source for the C-B cycle and NADPH is used to saturate double bonds. Although the C-B cycle is a dark process, it is affected by light availability due to the ATP and NADPH required for the process therefore a loss of activity will be observed in darkness due to a reduction in ATP and NADPH. This process is also temperature dependent due to enzyme activity in carbon assimilation (Falkowski & Raven 2007).

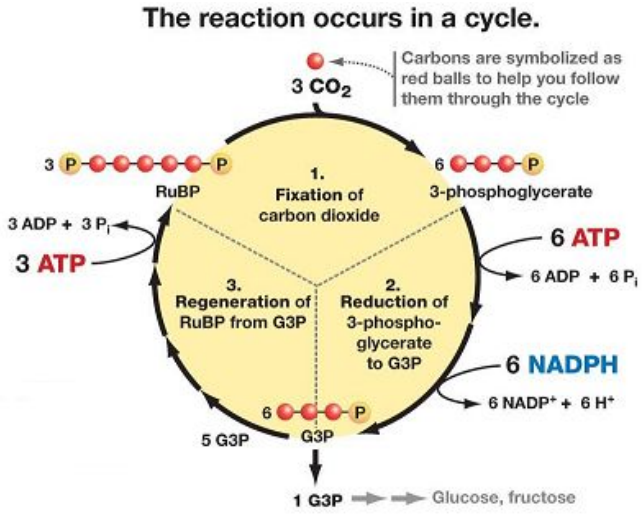

Figure 2.7 Schematic diagram of the Calvin-Benson cycle, the carbon fixation, dark reactions of photosynthesis (Muller 2010)

Photoacclimation

Phytoplankton are able to adapt to their environment effectively through many mechanisms, one of which is photoacclimation. Photoacclimation is the process by

which an organism acclimates to a light environment when exposed to a certain level of light for a long period of time, within the limits of its genetic potential. Acclimation to low light levels is usually reflected by an increase in chlorophyll proteins and a decrease in chlorophyll proteins for high light levels, which may or may not be coupled to the synthesis of reaction centres. It is expected that at extremely low light levels cells become chlorotic and as light increases slightly but remains low cellular chl *a* reaches a maximum. If light levels continue to increase a subsequent decrease in cellular chl *a* is expected until a minimum is reached. There are two possible forms of photoacclimation; acclimation due to changes in number of reaction centres without a change in functional absorption cross-section or changes in functional absorption cross-section while number of reaction centres remain unchanged. These processes can have an impact on the C-B cycle, due to the higher surface area to volume ratio of the cells of low light acclimated phytoplankton compared to high light acclimated cells, causing a limitation of ATP and NADPH substrates thereby becoming a controlling factor in carbon fixation (Falkowski & Raven 2007).

Photoinhibition

At supraoptimal light levels phytoplankton do however lack the ability to overcome damaging effects and photoinhibition occurs. At a continuous high light level PSII reaction centres turn over rapidly and electron donation from H_2O can become limiting. This limitation will lead to unfilled electron holes in donor molecules, thereby creating free radicals which can oxidize and destroy pigments and proteins in the reaction centre, causing photoinhibition. Photoinhibition causes a reduction in functional reaction centres and therefore a reduction in photochemical efficiency of PSII and a reduction in the rate of photosynthesis. This reduction in photosynthetic efficiency is observed in the upper portion of the water column, as well as a more rapid increase to maximum fluorescence due to reaction centres closing faster at the increased irradiance. A depression in photosynthetic efficiency of PSII is usually observed at midday on sunny days due to photoinhibition, where a shallow MLD is observed and cells are near to the surface of the euphotic zone. Low temperatures and nutrient stress make cells more susceptible to photoinhibition. Due to slower electron transport at low temperatures, cells become photoinhibited at lower irradiances and a reduction in functional reaction centres due to nutrient stress also leads to photoinhibition (Falkowski & Raven 2007).

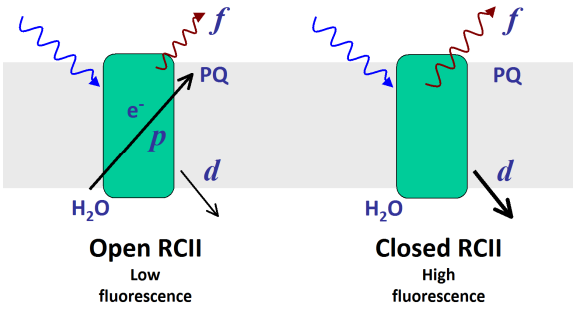

Figure 2.8 Schematic diagram depicting an open reaction centre absorbing a photon (left) and a closed reaction centre fluorescing (right) (Oxborough 2012)

Fast Repetition Rate fluorometry (FRRf)

FRRf is a technique used to determine photosynthetic efficiency of aquatic organisms. This technique uses rapid, sub-saturating pulses of light, of a specific wavelength, that cumulatively saturates PSII and allows for the measurement of photosynthetic efficiency (F_v/F_m) and functional absorption cross-section of PSII (σ_{PSII}) (Figure 2.9).

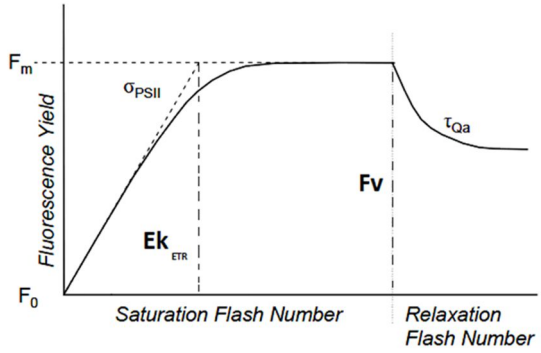

Figure 2.9 Flourescence yield produced by FRRf to measure phytoplankton photosynthetic apparatus (Falkowski & Raven 2007)

The sample is exposed to a series of short, sub-saturating flashlets, in a controlled sequence, such that ~100 pulses of light are absorbed by the reaction centre within ~100µs and the reaction centre subsequently becomes saturated. The rate at which fluorescence rises is proportional to σ_{PSII} and minimum (F_0) and maximum fluorescence (F_m) can be measured accurately. Variable fluorescence (F_v) is the difference between F_m and F_0, the ratio of F_v/F_m is measured as the photosynthetic efficiency of PSII. The functional absorption cross-section (σ) of antennae for the photochemical target corresponds to the ability of light of a given wavelength to promote a photochemical

reaction that leads to the evolution of O_2. The absorption cross-section undergoes adjustments throughout the day to acclimate to the changes in light.

F_0 is the minimum fluorescence measurable when all reaction centres are open and a maximum level of photon absorption is allowed, whereas F_m is the maximum fluorescence measurable due to closed reaction centres and minimum absorption of photons for photochemistry. Fluorescence is used to determine the physiological state of phytoplankton, in most cells a maximum F_v/F_m of ~0.65 (dimensionless) is indicative of a healthy and nutrient replete cell but this value can be significantly lower for cells growing under limiting conditions, with F_v/F_m values <0.2 (dimensionless). FRRf is also made use of to measure σ_{PSII}, by the varying of flash intensity, σ_{PSII} is measured quantitatively with a typical value of ~450 $Å^2$.quanta^{-1} in phytoplankton (Falkowski & Raven 2007).

2.4 Nutrients and limiting factors in the Southern Ocean

Marine phytoplankton require various macro- and micronutrients and environmental factors for photosynthesis and biosynthesis. A generally accepted ratio of elemental requirements of marine phytoplankton is the Redfield ratio, 106C:16N:1P, derived from the reaction equation of the oxidation of phytoplankton organic matter:

$$(CH_2O)_{106}(NH_3)_{16}H_3PO_4 + 138O_2 \rightarrow 106CO_2 + 122H_2O + 16NO_3^- + PO_4^{3-} + 19H^+ \quad (v)$$

When taking into consideration the Fe requirements of phytoplankton the “new and improved” Redfield ratio is 106C:16N:1P:0.005Fe (Hutchins *et al.* 2001). There are however variations in elemental ratios due to cell wall composition of different species, growth conditions and limiting factors (Bucciarelli *et al.* 2010; Feng *et al.* 2010; Klunder *et al.* 2013). The distribution of nutrients is controlled by many processes throughout the global oceans. Remineralisation due to biological processes and the influx of nutrients from other sources are the two major sources of nutrients in the euphotic zone. Photosynthetic biological uptake of inorganic nutrients is confined to the euphotic zone, therefore the concentrations of these nutrients are much higher at depth due to lack of biological uptake. The supply of nutrients affects photosynthetic efficiency and physiological status of phytoplankton on large spatial scales and physical factors facilitate the flow of nutrients controlling biomass accumulation. Biomass increases until an essential factor, nutrient or environmental, becomes limiting, a substrate that is least available to what is required for biosynthesis. Nutrient requirements are highly variable across species and therefore nutrient limitation creates competitive selection between

species. In high nutrient, high latitude waters large, dense cells, such as diatoms which dominate in polar regions, form large blooms and can acquire and store nutrients faster during periods of intermittent nutrient supply therefore being able to survive under limiting conditions (Bentaleb *et al.* 1998; Falkowski & Raven 2007).

As seen in the Redfield ratio, phytoplankton require three macronutrients, N, P and C, for metabolic processes and some phytoplankton, such as diatoms, require Si for the production of a silicified cell wall. As a crucial micronutrient, Fe is required by phytoplankton for various photosynthetic components of the electron transport chain, as well as in NO_3 and PO_4 reducing enzymes (Berg *et al.* 2011). Photosynthesis and biosynthesis of phytoplankton is directly proportional to irradiance and nutrient availability, as well as other environmental controlling factors (Table 2.1). Cells living under nutrient limitation become chronically stressed; by not having access to nutrients required to repair reaction centres, a larger portion of irradiance is released as fluorescence thereby decreasing the photochemical efficiency of the cells (Falkowski & Raven 2007).

Table 2.1 Environmental control factors for diatoms and *Phaeocystis antarctica*, with a suggested ranking of each factor based on evidence in the literature, from most important (1) to least important (5). Controls that are deemed not significant for each group are marked as n.s., and factors whose relative importance remains unresolved are marked with a question mark (?). Factors that share a superscripted letter have been demonstrated to have significant interactive effects. (Boyd *et al.* 2010)

Algal group	Temperature	PAR	Nitrogen	Phosphorus	Silicon	Iron	CO_2
Diatoms	?[a]	4[be]	1[d]	n.s.	3[e]	2[abcde]	5[c]
P. antarctica	?	1[f]	n.s.	n.s.	n.s.	2[f]	3

[a] Temperature and iron have been shown to have marked synergisms on diatom abundance in the Ross Sea (Rose *et al.* 2009).

[b] Numerous laboratory and field studies have demonstrated co-limitation of diatoms by light and iron (Sunda & Huntsman 1997; Maldonado *et al.* 1999).

[c] CO_2, light, and iron have a three-way interactive effect on diatom community structure in the Ross Sea (Feng *et al.* 2010).

[d] Nitrogen and iron are also potentially co-limiting for diatoms (Price *et al.* 1991; DiTullio *et al.* 1993).

[e] Silicon and iron requirements are antagonistic in diatoms (Hutchins & Bruland 1998).

[f] Light and iron have synergistic effects on the abundance of colonial *P. antarctica* (Feng *et al.* 2010).

NO_3 and PO_4 concentrations are in excess of phytoplankton requirements throughout the year in the SO. Irradiance and Fe are, however, limiting due to deep MLDs and oxidation of Fe (Boyd & Abraham 2001, Boyd *et al.* 2001; Browning *et al.* 2014; Feng *et al.* 2010; Hutchins *et al.* 2001). Irradiance is a limiting factor of SO phytoplankton throughout many parts of the year due to ice cover, cloud cover and deep MLDs and phytoplankton are therefore adapted to low light conditions (Hopkinson *et al.* 2007). Fe is the most abundant metal on earth. Its most abundant form in seawater is Fe^{3+} which

is relatively insoluble in seawater and biologically unavailable to phytoplankton. Phytoplankton have evolved to be able to substitute Fe requirements under limiting conditions. It has, however, been shown that photosynthetic yield is low under Fe limitation but cells are able to survive under balanced nutrient limitation (Boyd *et al.* 1999; Hopkinson *et al.* 2007; Sosik & Olson 2002). Increased Fe inputs in the HNLC SO have been reported to increase photosynthesis and thereby increase the biological pump (Boyd *et al.* 2001; Klunder *et al.* 2011). Fe supply to the SO is primarily due to dust inputs from land but due to the spatial vastness of the SO new Fe inputs are low. Dissolved Fe supply to surface waters in the SO is primarily from subsurface reservoirs due to the low dust inputs and low lateral supply, Fe recycling has been shown to sustain productivity in SA waters (Figure 2.10) (Tagliabue *et al.* 2014). Fe concentrations have been reported to be subnanomolar throughout much of the SO (Boyd *et al.* 1999, 2001; Klunder *et al.* 2011, 2013). Fe limitation can cause N limitation in phytoplankton due to Fe requirements in N fixation enzymes, which phytoplankton cannot substitute under limiting conditions (Falkowski & Raven 2007). Fe and light limitation has been reported to have interactive effects on SO phytoplankton, such as diatoms and *P. antarctica* (Feng *et al.* 2010; Moore *et al.* 2007). The availability of Fe in the SO significantly influences the biochemical cycling of nutrients (Klunder *et al.* 2013).

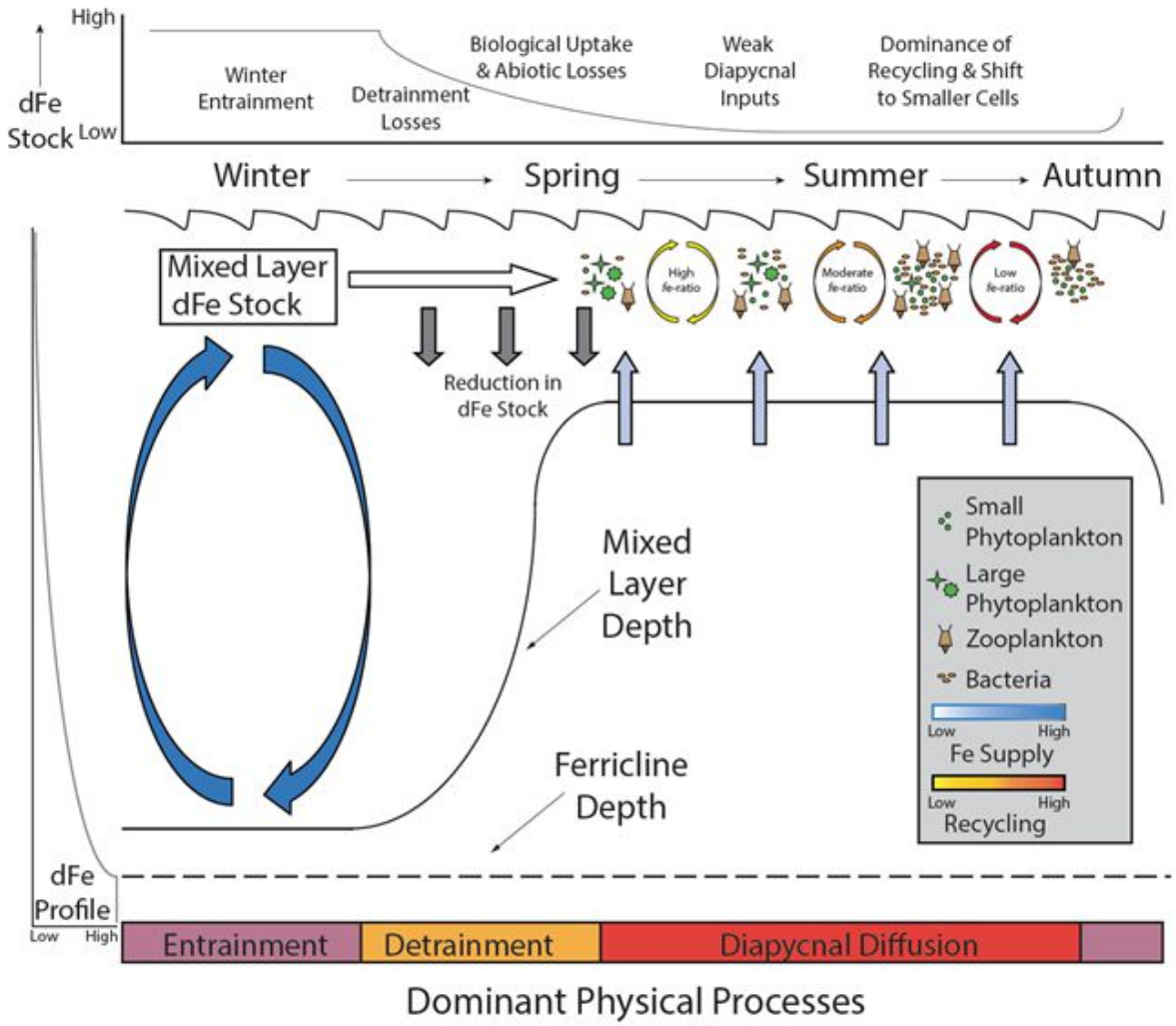

Figure 2.10 A schematic diagram of the seasonal variability in SO Fe cycling (Tagliabue *et al.* 2014)

Diatom growth is limited by light in winter and early summer and then by Fe when light levels increase in SA waters. Si has similarly been reported as a limiting factor during summer and late summer in SA waters due to high uptake by diatoms during spring, creating a High-Nutrient, Low-Si, Low-Chlorophyll (HNLSiLC) system (Boyd *et al.* 1999; Hutchins *et al.* 2001; Moore *et al.* 2007). A complex co-limitation of nutrients and environmental factors control diatom growth in these waters. Fe and light co-limitation has been reported to limit biomass throughout SA and polar waters of the SO (Boyd *et al.* 2001; Moore *et al.* 2007). Fe availability has been shown to directly affect the uptake of nutrients such as Si and N. Increased Fe availability in SO waters has been shown to decrease diatom Si uptake, creating lesser silicified diatoms and an increase in N uptake (Boyd *et al.* 2010; Brzezinski *et al.* 2002; Bucciarelli *et al.* 2010; Hopkinson *et al.* 2007; Klunder *et al.* 2013).

There are gradients in nutrient concentrations and temperature from low to high latitudes in the SO, creating separate systems across the different fronts, with varying limiting

factors, also affecting phytoplankton community and size structure (Feng *et al.* 2010; Hutchins *et al.* 2001; Sosik & Olson 2002). NO_3 concentrations in the SAZ are typically reported to be ~15μM, increasing southward to ~26μM during summer. PO_4 concentrations similarly increase southward from ~1μM to ~2μM, both nutrients being non-limiting. SiO_4 is however limiting in SA waters, as previously stated, and also increases southward with a sharp increase across the Polar Front up to ~68μM in the AZ. Fe concentrations in the upper surface mixed layer during summer, in the Atlantic sector of the SO, are reported to vary between 0.1 and 0.3nM, with sporadic increases due to dust inputs originating from South America and melting of icebergs and seasonal sea-ice. A subsurface minimum in Fe concentration has been observed between 25 to 200m, with a deeper minimum at higher latitudes, assumed to correspond with MLD and therefore confirming the biological uptake of Fe by phytoplankton (Figure 2.11) (Klunder *et al.* 2011).

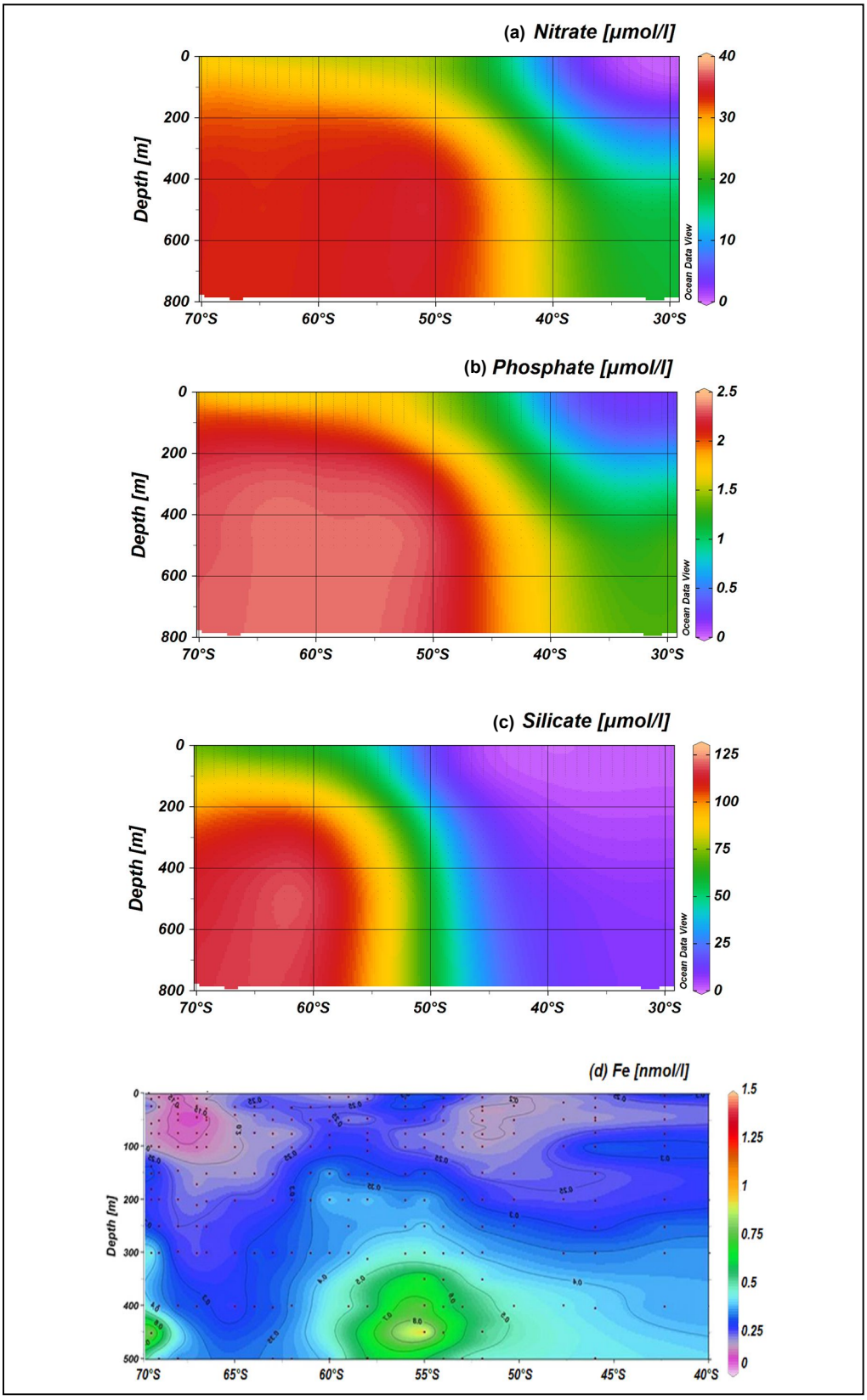

Figure 2.11 Colour plots of surface nutrient concentrations of transect along the Greenwich Meridian between 30°S and 70°S, Nitrate (a), Phosphate (b) and Silicate (c). Figures generated using Ocean Data View, plotting World Ocean Atlas Data 2013 Jan-Mar (Schlitzer, 2015). Colour and contour plot of dissolved Fe concentration (nM) of the Greenwich Meridian transect (d) in the upper 500m (Klunder *et al.* 2011)

2.5 Previous studies related to iron and light co-limitation in the Southern Ocean

In situ Fe enrichment experiments have been conducted in the SO, mainly in the Pacific region, based on the hypothesis that phytoplankton growth is limited by low Fe concentrations in these HNLC regions. A positive response to Fe enrichment has been observed in these experiments while other controlling factors, nutrient and environmental, have been brought to light. Many factors other than limiting factors, such as community composition and nutrient assimilation mechanisms, have been shown to control phytoplankton response to Fe enrichment (Browning *et al.* 2014). An increase in Fe concentration has seen a response in photophysiology, nutrient uptake and biomass accumulation. Fe enrichment has also shown to have a definite effect on the size and community structure of the in situ phytoplankton community leading to dominance of larger cells (Berg *et al.* 2011; Cassar *et al.* 2004). An increase in F_v/F_m due to Fe enrichment is observed for in situ experiments as the first response to Fe stress relief and has generally been an immediate response of in situ phytoplankton but has however been slower than what is observed in warmer HNLC regions, possibly due to low temperatures and deep MLDs in the SO (Boyd and Abraham, 2001; Moore *et al.* 2007).

Due to the high cost and practical challenges of in situ Fe fertilization, shipboard incubation experiments have come into practice to recreate in situ enrichment scenarios under a controlled environment at a fraction of the cost. Incubation experiments allow for the manipulation of various controlling factors, including environmental factors that are not possible with in situ fertilization, thereby being able to better study the intricate web of controlling factors that ultimately control phytoplankton growth in the SO (Boyd *et al.* 2010). Nutrient enrichment in incubation experiments has shown that photosynthetic yield of phytoplankton responds rapidly to increased nutrient availability (Falkowski & Raven 2007). Specifically, Fe enrichment has caused an increase in biomass accumulation, higher nutrient assimilation, improved photophysiology, a shift in phytoplankton community structure and an increase in NO_3 assimilation due to relief of Fe stress on NO_3 and NO_2 assimilation enzymes (Feng *et al.* 2010, Hopkinson *et al.* 2007; Hutchins *et al.* 2001; Moore *et al.* 2007). As observed for in situ experiments, an increase in F_v/F_m in response to Fe enrichment is also observed in shipboard incubation experiments, but this is not always the case (Boyd & Abraham 2001). In addition to Fe enrichment, many experiments conducted in SA waters have included Si enrichment due to Si limitation during summer and late summer, displaying a higher response for the combined addition of Fe and Si, specifically for diatoms (Hutchins *et al.* 2001). Light limitation has also been evident in many incubation experiments, giving a relatively low

response at in situ light levels (Boyd *et al.* 1999, 2001). Ross Sea phytoplankton have shown a significant response to the combined addition of Fe and light, as has been observed for many other areas of the SO (Feng *et al.* 2010). Fe addition has resulted in an increase in the larger size fraction of cells as seen for in situ Fe fertilization experiments (Boyd *et al.* 1999, 2001; Hopkinson *et al.* 2007).

A significant increase in cellular chl *a* upon Fe enrichment and increased irradiance is a general response observed in both incubation and in situ Fe enrichment experiments conducted across the SO (Boyd & Abraham 2001; Boyd *et al.* 1999; Browning *et al.* 2014; Hopkinson *et al.* 2007; Moore *et al.* 2007). Greater MLDs and higher cellular chl *a* in phytoplankton have been seen at higher latitudes, indicative of stronger light limitation, thereby a stronger response is reported for Fe addition under high light (HL) levels to relieve Fe and light co-limitation. Fe limitation has been reported to control phytoplankton growth in SA waters more than light limitation, due to shallower MLDs (Boyd *et al.* 2001). Phytoplankton have been shown to redevelop Fe stress after Fe fertilization due to rapid uptake of available Fe, as well as competing processes, such as oxidation and organic complexation, decreasing the amount of bioavailable Fe (Boyd *et al.* 1999; Hopkinson *et al.* 2007; Moore *et al.* 2007). Diatoms have been reported to be the phytoplankton group that are most benefitted by Fe enrichment due to their combined NO_3 assimilation mechanisms and photosynthetic Fe requirements, thereby outcompeting other species in Fe enrichment experiments, whereas *P. antarctica* has been reported to better respond to irradiance increases. Fe and light interactive effects have been shown to have significant effects on the relative abundance of diatoms and *P. antarctica* and elemental ratios of SO phytoplankton (Cassar *et al.* 2004; Hopkinson *et al.* 2007; Moore *et al.* 2007). Higher silicification of diatoms under Fe limitation has been reported in Ross Sea diatoms, therefore displaying significant interactive effects between Fe and Si availability in SO diatoms (Feng *et al.* 2010; Hopkinson *et al.* 2007). Relief of Fe stress is suggested to increase F_v/F_m and biomass increases are due to the increase in efficient NO_3 assimilation (Berg *et al.* 2011; Browning *et al.* 2014; Hutchins *et al.* 2001).

Limiting factors in the SO have been reported to be seasonal, causing shifts in community structure due to conditions becoming increasingly limited during bloom decline. Fe limitation has been consistently reported in the SO, with subnanomolar concentrations being a constant throughout the year (Browning *et al.* 2014; Feng *et al.* 2010; Hopkinson *et al.* 2007; Hutchins *et al.* 2001). A larger response to the relief of light limitation has been reported for samples at higher latitudes from areas with deeper MLDs, due to phytoplankton growth being controlled by light limitation rather than Fe limitation. A seasonal progression of limiting factors in SA waters has been evident, with

Fe and light co-limitation during spring, Fe limitation during early summer at higher irradiances levels and Fe and Si co-limitation during summer and beginning of late summer controlling phytoplankton growth (Hutchins *et al.* 2001; Moore *et al.* 2007). Fe and light co-limitation, in the presence of high Si concentrations, is reported to control phytoplankton growth in SO polar waters (Boyd *et al.* 2001). A floristic shift in community structure from diatoms toward nonsiliceous pico- and nanoplankton has been observed during bloom decline, under Si limitation. Smaller cells have also been shown to respond more rapidly to nutrient addition than larger cells (Hutchins *et al.* 2001). During end of bloom incubation experiments in SA waters, small, lightly silicified diatoms have been shown to grow after Fe addition although Si concentrations are extremely low, whereas large diatoms struggle to compete under these limiting conditions due to high Fe and Si requirements (Hutchins *et al.* 2001). An addition of 1nM dissolved Fe has been shown to be the threshold above which Fe stress becomes noticeably alleviated in SA, Fe limited, waters (Boyd *et al.* 1999).

Although irradiance has been shown to be a limiting factor in the SO, supraoptimal light conditions can lead to photoinhibition, as seen in many experiments, whereas a slight increase in irradiance can be beneficial. This response is species specific, due to various photorecovery mechanisms of different species, and is influenced by the phytoplankton light history due to photoacclimation to low light (LL) levels. Ross Sea *P. antarctica* has been shown to have faster photorecovery mechanisms and therefore outcompetes diatoms under HL conditions, where diatoms experience photoinhibition (Feng *et al.* 2010). Spatial differences in response to Fe enrichment and light level manipulation has been suggested to be due to MLD and temperature differences (Boyd *et al.* 2001). SO phytoplankton in deeper waters have been reported to have a higher photosynthetic efficiency due to Fe enrichment, than cells in near surface waters, due to photoinhibition of cells in surface waters (Boyd and Abraham, 2001; Feng *et al.* 2010; Moore *et al.* 2007).

Active fluorescence in combination with genetic analysis has been successfully used to determine Fe stress and photophysiological response to Fe enrichment in phytoplankton communities. All size classes have been reported to show an increase in F_v/F_m in response to Fe addition (Browning *et al.* 2014; Feng *et al.* 2010; Hopkinson *et al.* 2007; Moore *et al.* 2007). Low F_v/F_m of ~0.2 (dimensionless) is indicative of nutrient stressed phytoplankton. This is, however, not the only reason for a depressed F_v/F_m signal; light limitation, photoinhibition and reduced temperatures can also contribute to changes seen in F_v/F_m (Boyd *et al.* 2001; Moore *et al.* 2007). A stronger correlation between F_v/F_m and Fe:NO_3 ratios, rather than between F_v/F_m and dissolved Fe, has been reported in SA phytoplankton (Browning *et al.* 2014). In SO polar waters irradiance has been reported

to be the main factor influencing photosynthetic efficiency, instead of Fe (Feng *et al.* 2010). In the absence of Fe enrichment, a reduced response is observed in phytoplankton incubated under HL conditions and photoinhibition is instead observed, due to nutrient stress, by a decrease in F_v/F_m. High F_v/F_m values can be maintained under less severe Fe stress, due to steady-state Fe limited growth (Moore *et al.* 2007). A decrease in σ_{PSII} has been observed in response to an increase in Fe availability, possibly due to an increase in reaction centres relative to pigment, indicative of a physiological acclimation to increased Fe availability (Moore *et al.* 2007). Decreased σ_{PSII} has also been observed for increased light levels (Boyd & Abraham 2001; Hopkinson *et al.* 2007). Various responses to Fe enrichment and manipulation of limiting factors have been reported for SO phytoplankton, therefore indicating an intricate web of limiting factors and seasonal changes to these factors.

2.6 Need for further research

The Atlantic sector of the SO is the least researched area, relative to the northern hemisphere and the Pacific sector of the SO. Due to the heterogeneity of the SO, high resolution sampling is needed to better understand the separate regions and the combination of environmental factors controlling biogeochemistry of the various regions. Little is known of the seasonality of limiting factors in the SO and current findings cannot be generalised, as has been observed of reported data.

Photophysiology measurements have yielded many different results across experiments, specifically between in situ and incubation experiments, and therefore not all is understood of phytoplankton response to Fe enrichment and the interactive response with other limiting factors (Feng *et al.* 2010). In situ results have been shown to differ from shipboard incubations and contradictions have been reported (Boyd *et al.* 2001). There are however many factors that could be the cause of these discrepancies and these environmental controls have not been sufficiently resolved (Boyd *et al.* 2010; Moore *et al.* 2007).

3. Methodology

3.1 Sampling and incubation set-up

Incubation experiments were conducted during two cruises in 2013-2014; Southern Ocean Seasonal Cycle Experiment (SOSCEx) and South Atlantic Fe Pool (SAFePool) (Figure 3.1). During both cruises sampling and incubations were conducted as closely as possible to standards of the processes recommended by the GEOTRACES program (Cutter *et al.* 2010; Cutter & Bruland 2012).

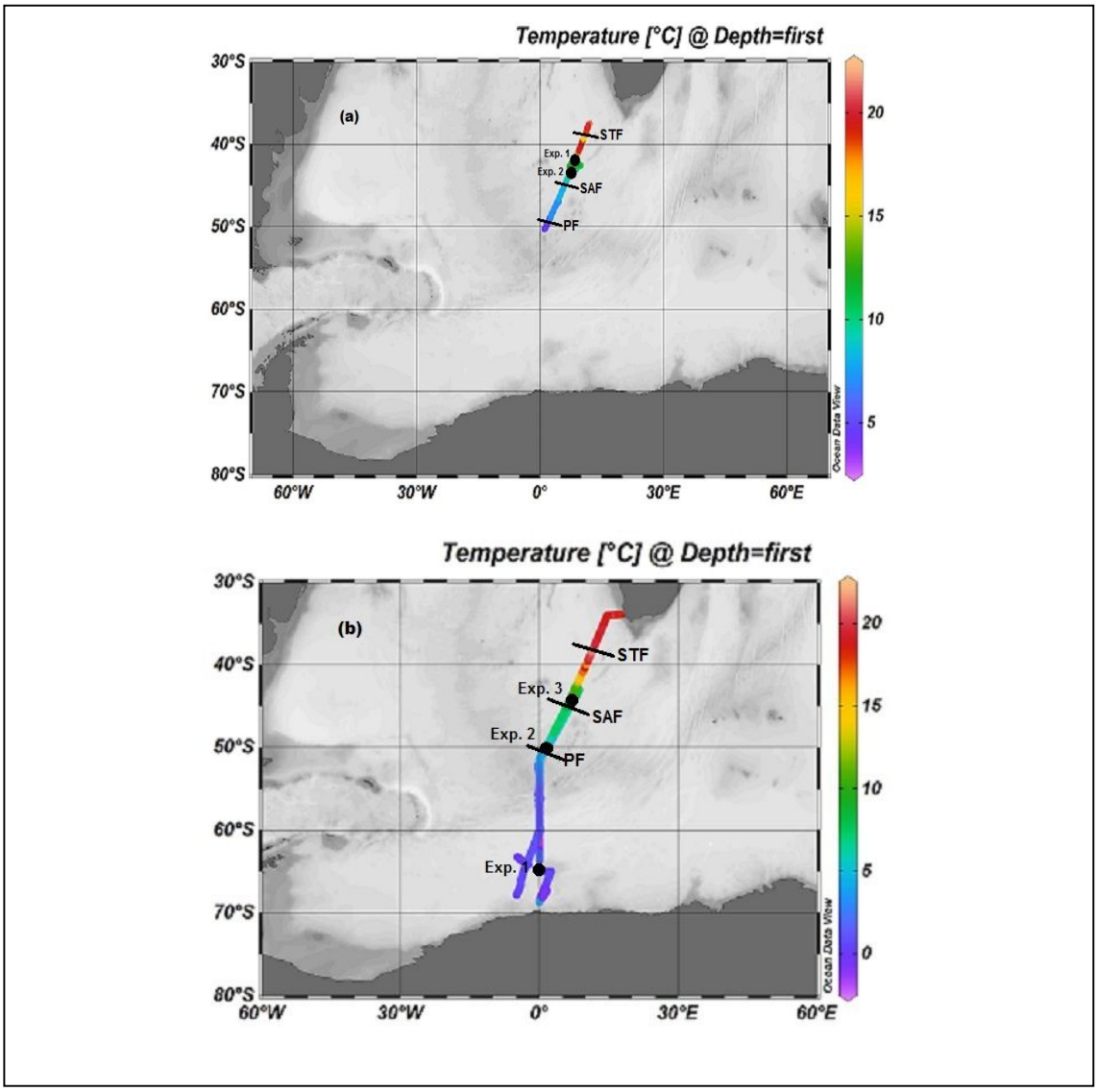

Figure 3.1 Sea surface temperature colour plot displaying the cruise track followed during the SOSCEx (a) and SAFePool (b) cruises. Black dots indicate bioassay sampling sites. Black lines cutting across the cruise tracks indicate approximate front positions estimated using the method of Orsi *et al.* (1994). Figure was generated using Ocean Data View (Schlitzer, 2015).

SOSCEx

During the SOSCEx cruise, on-board the RV SA Agulhas, two bioassay Fe and light incubation experiments were conducted within the SAZ of the SO during March 2013 (Figure 3.1(a)). Seawater was collected at ~40m depth (Table 3.1) at the SCM; the vertical profiles are further characterised in chapter 4.

Seawater samples were collected using a GEOTRACES CTD rosette equipped with 24 12L GoFlo sampling bottles, specially modified for trace metal clean sampling. A carousel Auto Fire Mode (AFM) pressure sensor was attached to trigger GoFlo bottles at sampling depths and the rosette was deployed using a Dynema hydroline (General Oceanics Inc.) and a controlled depth winch. Deployment and sampling were done with absolute contamination prevention in mind at all times and sampling of seawater from the GoFlo bottles was conducted in the trace metal clean class-100 container laboratory.

Approximately 15 of the 24 GoFlo bottles were triggered at the SCM fto collect sufficient seawater needed for the incubation experiment. Each GoFlo bottle was inverted a few times to homogenise the seawater, containing resident phytoplankton, and was then transferred into two acid washed 50L LDPE carboys (Thermo scientific) using PFA Teflon tubing (Chemfluor PFA Teflon Tubing, 9.5mm OD / 7.9mm ID; Laboratory consumables and chemical supplies) attached to the sampling valve on the GoFlo bottle while filtering sample through a 200µm mesh, to remove large zooplankton from the sample. The homogenised seawater was then redistributed into 39 acid washed 2.4L PC bottles (Nalgene; Thermo Scientific). Each bottle was filled up to approximately 2.4L with the seawater sample from the 50L carboys. Samples were incubated under four treatments, LL-LFe (control sample, no Fe added, in situ PAR), LL-HFe (1nM dissolved Fe added, in situ PAR), HL-LFe (no Fe added, 10 times in situ PAR) and HL-HFe (1nM dissolved Fe added, 10 times in situ PAR). An addition of 1nM dissolved Fe has previously been reported to be the threshold above which Fe stress becomes noticeably alleviated in SA, Fe limited, waters (Boyd *et al.* 1999). Temperature was set at in situ values for all samples (Table 3.1). Nine bottles were prepared for each treatment and three bottles were sampled for initial conditions as T_0 (Figure 3.2).

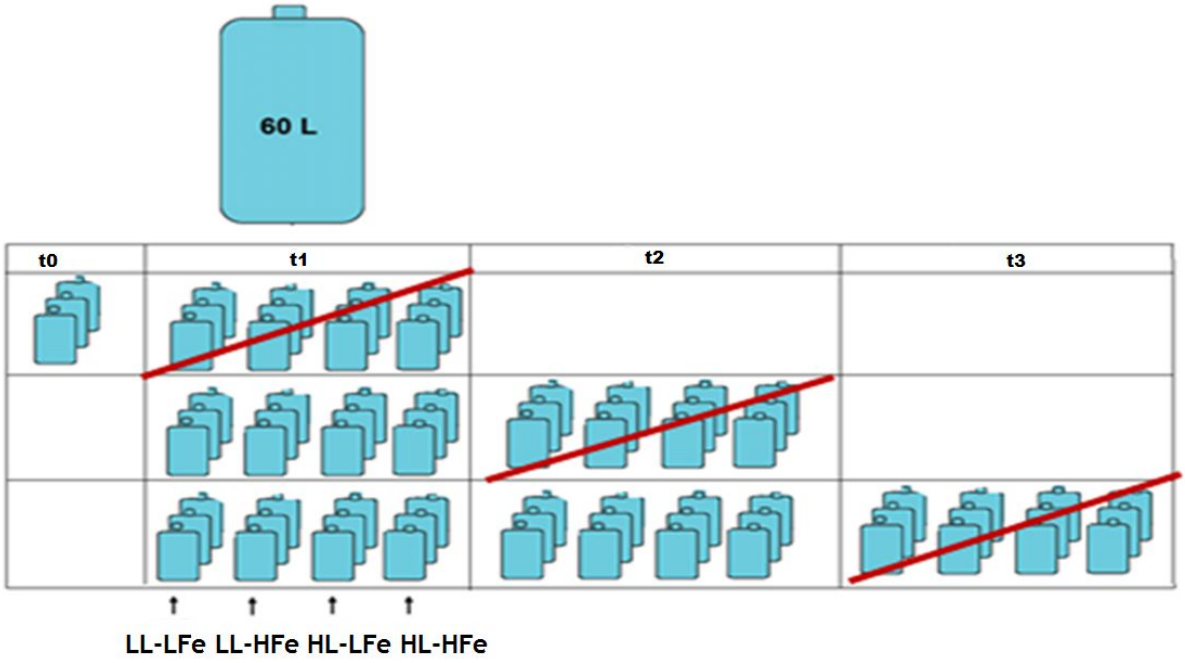

Figure 3.2 Schematic diagram of experimental scheme for Fe/light bioassay experiments. Terminations of incubation samples indicated by t0, t1, t2 and t3. Termination time intervals varied between experiments

Due to insufficient seawater sampled for Experiment 1, the final termination of the HL-HFe treatment was done in duplicate instead of triplicate. Fe enrichment was performed under a laminar flow hood in the trace metal clean container laboratory, using an 89.5µM acidic $FeCl_3$ solution made from a 1000mg/L stock solution (Iron Atomic Spectroscopy Standard, Sigma Aldrich), acidified with ultrapure HCl in a trace metal clean container laboratory and samples were then incubated in specially designed incubators with adjustable LED light strips for HL and LL settings.

Two incubators (Minus40 Specialised Refrigeration) were used for the experiments and were covered with black plastic sheets to prevent outside light interference when opening incubators to mix bottles. Both incubators were equipped with adjustable LED light strips above each shelf and a cooling fan for temperature control. Temperature was set and measured using a handheld thermometer probe (Penta Digital) and light levels were set using a handheld 4π PAR sensor (Biosphere QSL 2100; Biospherical Instruments Inc.).

Table 3.1 SOSCEx experiment sampling information

Parameters	Experiment 1	Experiment 2
Date	01/03/2013	02/03/2013
Latitude (°S)	42.7412	43.4218
Longitude (°E)	8.8111	7.2047
Depth (m)	30 – 20	45 – 35
Seawater temperature (°C)	11.33	10.18
Salinity (PSU)	34.253	34.046
In situ PAR (µmol photon.m^{-2}.s^{-1})	35.00	41.84
HL PAR (µmol photon.m^{-2}.s^{-1})	350	410

Each experiment was run for a total of six days on a night:day cycle of 10:14 hours and was mixed manually, by inverting, every two hours to prevent settling out of particles. Subsamples were taken every two days at sunrise (T_1, T_2 and T_3). The samples terminated were mixed gently but thoroughly, to prevent breaking of cells and to homogenise them, then were filtered for analysis. Each sample was analysed for nutrients (NO_3 + NO_2, PO_4 and SiO_4), PSII photophysiological parameters (F_v/F_m and σ_{PSII}), chl *a*, cell counts and POC to determine the effects of Fe and light amendments on the resident phytoplankton (Table 3.2).

Table 3.2 Variables analysed, volumes filtered and techniques used for SOSCEx experiments

Parameters	Volume filtered (ml)	Analysis technique used
Chl *a*	400	Fluorometry
POC	700	CHN elemental analysis
Cell counts	200	Particle analyser
Photophysiological parameters	10	FRRf
Nutrients	30	FIA and manual spectroscopy

South Atlantic Fe Pool (SAFePool)

During the SAFePool mid-summer cruise, on-board the SA Agulhas II, three bioassay Fe and light incubation experiments were conducted across the SO from the SAZ to the AZ (Figure 3.1(b)). Seawater was collected at the SCM, varying in depth at the separate sampling sites (Table 3.3). During the SAFePool cruise the trace metal clean rosette was equipped with a CTD and Kevlar conductive cable was used to deploy the CTD.

Table 3.3 SAFePool experiment sampling information

Parameters	Experiment 1	Experiment 2	Experiment 3
Date	11/01/2014	05/02/2014	07/02/2014
Latitude (°S)	64.9995	50.0013	44.8707
Longitude (°E)	00.0002	01.3847	06.0277
Depth (m)	40 – 31	50 – 40	61 – 54
Seawater temperature (°C)	-1.4	4.5	8.7
Salinity (PSU)	34.688	33.780	34.390
In situ PAR (µmol photon.m^{-2}.s^{-1})	10	13	15
HL PAR (µmol photon.m^{-2}.s^{-1})	100	130	150

A similar experimental scheme was used during SAFePool as was during SOSCEx (Figure 3.2), with a few alterations. Samples from Experiments 1 and 2 were incubated in triplicate with an added sample for high resolution photophysiology analysis. Due to a shortage of bottles, Experiment 3 samples were incubated in duplicate with an added sample for high resolution photophysiology analysis and T_0 was sampled in triplicate for initial conditions of all three experiments. The acid washed 2.4L bioassay bottles were filled up to 1.6L to allow headspace for gas exchange, which was not considered during the SOSCEx experiments; this did not however seem to affect the results. Spiking with dissolved Fe was done using the same stock solution as was used during SOSCEx and this was done under the same laminar flow hood in the class-100 trace metal clean container laboratory.

Samples were incubated under the same four treatments as was done during SOSCEx and were incubated in the modified incubators previously used (Minus40 Specialised Refrigeration). Light levels were set to in situ PAR and 10 times in situ PAR for LL and HL levels, respectively, and temperature was set to in situ values (Table 3.3). Experiment 1 samples were incubated on a night:day cycle of 4:20 hours for a total of nine days, Experiment 2 samples were incubated on a 9:15 hour cycle for a total of twelve days and Experiment 3 samples were incubated on a 10:14 hour cycle for a total of ten days. Lengths of incubations were varied to determine length of bloom extension within the sample and due to low temperatures a slow response was expected after Experiment 1 incubation results were obtained. All samples were mixed manually, by inverting, every two hours while being incubated and photophysiology analysis was done every 24 hours for the duration of the incubations. A total of three major terminations was done for each experiment; for Experiment 1 terminations were conducted after day 2, day 5 and day 9, Experiment 2 terminations were conducted after day 3, day 6 and day 12 and Experiment 3 terminations were conducted after day 3, day 6 and day 10. Samples were mixed

gently but thoroughly and filtered for analysis, as was done for SOSCEx experiments (Table 3.4).

Table 3.4 Parameters analysed, volumes filtered and techniques used for SAFePool experiments

Parameters	Volume filtered (ml)	Analysis technique used
Chl *a*	400	Fluorometry
POC	600	CHN elemental analysis
Cell counts	200	Particle analyser
Photophysiological parameters	30	FIRe
Nutrients	50	FIA and manual spectroscopy

Subsamples for Fe analysis were taken from incubation samples and were subsequently analysed. Contamination issues encountered, most likely due to bottles used for Fe analysis subsampling or the GoFlo bottles used for initial sampling, did however prevent reporting of any Fe data.

3.2 Biomass analysis

Chl a

400ml of the incubated seawater samples was vacuum filtered through a 25mm Whatmann GF/F glass fibre filter, pore size 0.7µm. Filter papers were then folded, placed in cryovials and stored in a liquid nitrogen storage dewar during the SOSCEx cruise and in a -80°C freezer during the SAFePool cruise, until further analysis on land. Samples were later analysed, by Dr Sandy Thomalla and myself, using the Turner Trilogy laboratory fluorometer, according to the non-acidification fluorometric chlorophyll analysis method as written by Herndon and Cochlan (2012). The fluorometer was calibrated prior to analysis using a Sigma chl *a* standard, according to the Turner Trilogy laboratory fluorometer user manual (Turner Designs 2010).

POC

700ml and 600ml of the incubated sample, for SOSCEx and SAFePool, respectively, was vacuum filtered through a pre-combusted (at ~400°C for 12 – 24 hours) 47mm Whatmann GF/F glass fibre filter, pore size 0.7µm. The filter papers were placed in glass vials, dried and stored in a ziplock bag containing silica gel to be kept dry until further analysis on land. Samples were acid fumed to remove inorganic carbon and oven-dried. The filters containing the samples were subsampled by punching out the sample area,

the sample was then transferred to a tin foil sample cup and subsequently analysed using a Flash EA 1112 series elemental analyser (Thermo Finnigan, Milan, Italy). I did the sample preparation and analysis was done by Mr Ian Newton from the Archeology department at the University of Cape Town. Detection was conducted by a Delta Plus XP IRMS isotope ratio mass spectrometer detector (Thermo electron, Bremen, Germany) via a Conflo III gas control unit (Thermo Finnigan, Bremen, Germany). The instrument was calibrated prior to analysis by making use of a proteinaceous gel (Merck) and *Acacia saligna* leaves (Glencairn, South Africa) as standards.

Cell Count Analysis

200ml of the sample was used to analyse cell counts and size using the Multisizer 4^{TM} particle analyser (Beckman Coulter) on-board the vessel during the SOSCEx and SAFePool cruises. After each run a blank sample was run, seawater filtered through a Whatmann GF/F 0.7µm pore size glass fibre filter. The blank was then subtracted from the samples analysed to subtract small particles. SAFePool Experiment 1 samples were not analysed using the Multisizer 4^{TM} particle analyser. We attempted to use a Scepter^{TM} handheld analyser but it was later determined that the detection limit of the handheld sensor was higher than what was required for the samples analysed. The Multisizer 4^{TM} was calibrated using the beads calibration method according to the user manual (Beckman Coulter 2010) prior to use of the instrument. Cell count analysis was conducted by Dr Sandy Thomalla, Emma Bone and myself.

3.3 Photophysiology analysis

SOSCEx

Photophysiology analysis was done on-board the vessel during the cruise, by Dr Thato Mtshali and myself, using an FRRf instrument (FastAct base unit and FastOcean sensor, 2220-173-PL, Chelsea SMD Telecommunications (Pty) LTD) according to the FRRf user manual. Samples were dark adapted for ~30 minutes and analysed by single turnover to determine the photosynthetic parameters of PSII, F_v/F_m and σ_{PSII}. A blank sample, 0.2µm filtered seawater, was run prior to each sample run following the same procedure used for samples and the instrument was zeroed using MilliQ water before use. The FRRf calibration was conducted by the manufacturer.

The following setup was used for the LEDs of the FRRf instrument:

Protocol A: E_{LED}: 450 = 1	Protocol B: E_{LED}: 450 = 1	Protocol C: E_{LED}: 450 = 1
530 = 0	530 = 0.56	530 = 0.56
624 = 0	624 = 0	624 = 1

These three protocols were run consecutively for the single turnover runs. It was however later determined that the LED settings were too high for resident phytoplankton causing photosynthetic efficiency readings to be very low. LEDs were to be adjusted to insure an $R\sigma_{PSII}$ value (probability of PSII reaction centre being closed during first flashlet) between 0.04 and 0.05 (dimensionless). Although F_v/F_m values were low and did not reflect the true values, the change in efficiency was what was needed and the trend is therefore reported.

Further settings are as follows:

FETS (number of flashlets per sequence) = 100; Pitch (time between flashlets during each sequence) = 2µs

Relaxation phase (Rel): FETS = 20 – 40; Pitch = 50; Increase % = 0

Sequence repetitions: 50; Sequence interval: 120ms

SAFePool

The FRRf was not used during SAFePool due to instrument malfunction and instead high resolution photophysiology analysis was conducted on-board the vessel, by myself, making use of a bench top Satlantic FIRe (Fluorescence Induction and Relaxation) system according to the FIRe user manual. Samples were dark adapted for ~30 minutes and analysed by single turnover to determine the photosynthetic parameters of PSII, F_v/F_m and σ_{PSII}. A blank sample, 0.7µm filtered seawater, was run prior to each sample run following the same procedure used for samples.

The following settings were used for single turnover sample analysis:

1. Gain: to suit sample (typically 2000), sample delay 500

2. Number of runs: 16

3. STF 100, STRP 60, STRI 60, MTF 600, MTRP 60, MTRI 100.

3.4 Nutrient analysis

During the SOSCEx cruise samples were analysed immediately on-board the SA Agulhas. During the SAFePool cruise subsamples were frozen and later analysed on land due to a Flow Injection Analyser (FIA) and spectrophotometer not being available on-board the vessel. All nutrient analyses were done by Mr Craig Attwood.

Nitrate (NO_3) and Silicate (SiO_4)

~50ml of the sample was used for all nutrient analyses. NO_3 and SiO_4 analysis was conducted using the Lachat QuikChem 8500 series 2 FIA. NO_3 analysis was conducted according to the QuickChem® Method, 31-107-04-1-C (Egan 2008) and SiO_4 analysis was conducted according to the QuickChem® Method, 31-114-27-1-D (Wolters 2002). A calibration curve was constructed by running standards made up from a stock standard solution prior to sample analysis.

Phosphate (PO_4) and Nitrite (NO_2)

PO_4 and NO_2 analysis was conducted manually according to the method described by Grasshoff *et al.* (1983). Absorbance of samples and standards was measured using a Spectronic™ Helios™ Epsilon™ spectrophotometer. A calibration curve was constructed by running standards made up from a stock standard solution prior to sample analysis.

3.5 Data processing

All raw data were processed using Microsoft Excel to determine averages and to construct a graphic display of results. Statistics were determined using IBM SPSS Statistics 21 software, running the Kruskal-Wallis test (nonparametric one-way Analysis of Variance) to determine significant differences between treatments. I conducted all data processing and statistical analysis with the guidance of my supervisors.

To determine significant differences between treatments in bioassay experiments the Kruskal-Wallis test was run on all final incubation variable values. The test was run on

the first termination values only in cases where a significant difference was obtained for final values of the treatment, to determine significance of immediate responses. The null hypothesis tested was that the distribution of concentrations is the same across treatments. The null hypothesis was tested at a 90% confidence level. A 90% confidence level was used due to the small sample size. An obtained P value of <0.1 rejects the null hypothesis (detailed statistics shown in Appendix A). In cases where a significant difference was obtained a post hoc pairwise comparison was extracted from the initial test result to determine the specific differences between treatments.

FRRf data with $R\sigma_{PSII}$ values outside the 0.04 – 0.05 (dimensionless) range were excluded and the averages of accepted values were used as valid. FIRe data were processed using a combined Matlab script created from scripts by Brian Hopkinson (Department of Marine Sciences, University of Georgia) and Dr Mark Moore (National Oceanography Centre, Southampton). Due to incorrect saving of data, the initial data for SAFePool Experiment 1, T_0 to T_4, were lost.

Growth/uptake rates and rates of change were taken from the slope of the best fit regression line of the average of replicates analysed *vs.* days of incubation (Figure 3.3).

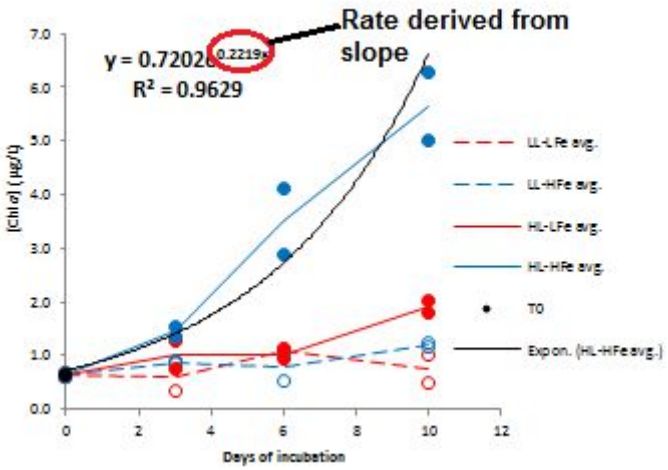

Figure 3.3 Depiction of rate (.day^{-1}) derived from slope of best fit regression (exponential) for parameter *vs.* days of incubation

4. Results

4.1 Site characterisation

SOSCEx

During the SOSCEx late summer cruise two bioassay experiments were conducted in the SAZ region of the SO, as approximated using the method of Orsi *et al.* (1994) (Figure 3.1(a)). The water column nutrient, temperature and % transmission (inverse of biomass) profiles can be seen below (Figure 4.1) for the two sampling sites of Experiment 1 and 2, 42.7°S and 43.4°S, respectively. Macronutrient concentration were relatively low and % transmission relatively high for what is expected in this region, indicative of late bloom decline levels (Klunder *et al.* 2011).

SiO_4 and PO_4 concentrations were ~1µM at sampling depth. SiO_4 is considered limiting at this concentration whereas PO_4 is not. NO_3 concentrations were in the range between 9 – 13µM at the sampling depth, significantly lower than is observed earlier in the season but not considered limiting. The MLD is observed at approximately 50 - 60m depth with nutrient concentrations increasing below 100m and reaching a maximum below 500m, for both sampling sites. The SCM at both sampling sites was above 50m depth and in situ temperature was measured between 10 and 12°C, characteristic of the water mass (Figure 4.1).

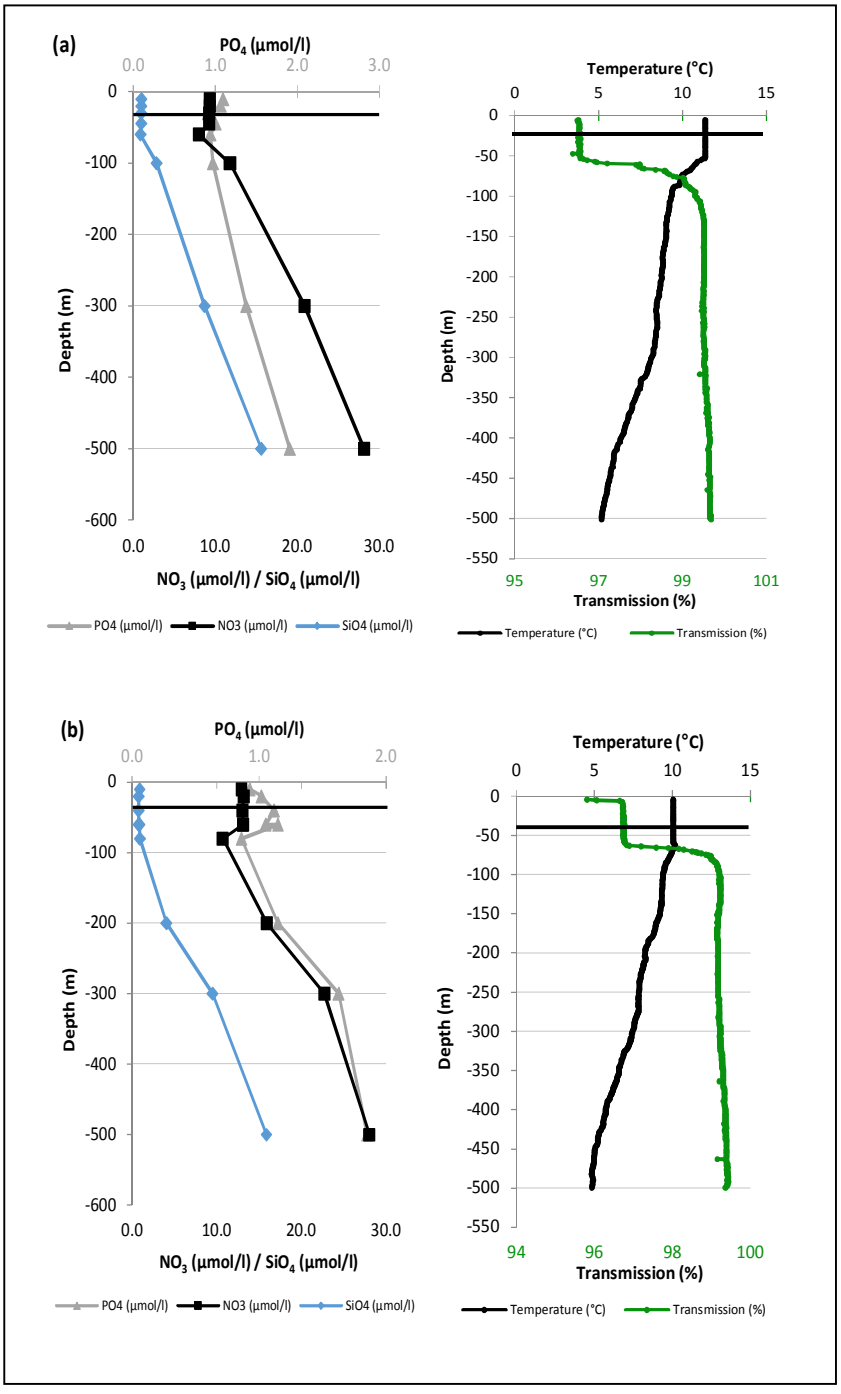

Figure 4.1 Nutrient, temperature and % transmission profiles in the water column at the bioassay sampling sites of Experiment 1 at 42.7°S (a) and Experiment 2 at 43.4°S (b) during the SOSCEx late summer cruise. Solid black line indicates sampling depth.

SAFePool

During the SAFePool mid-summer cruise three bioassay experiments were conducted across the SO, in the SAZ, Polar Frontal Zone (PFZ) and the AZ, as approximated by thee method of Orsi *et al.* (1994) (Figure 3.1(b)). The water column nutrient, temperature and % transmission (inverse of biomass) profiles can be seen below (Figure 4.2) for the

three sampling sites of Experiment 1 at 65°S, Experiment 2 at 50°S and Experiment 3 at 45°S. Macronutrient concentrations were noticeably higher and % transmission lower than that observed during the SOSCEx late summer cruise, which was expected due to the SAFePool experiments being conducted earlier in the season (Klunder *et al.* 2011).

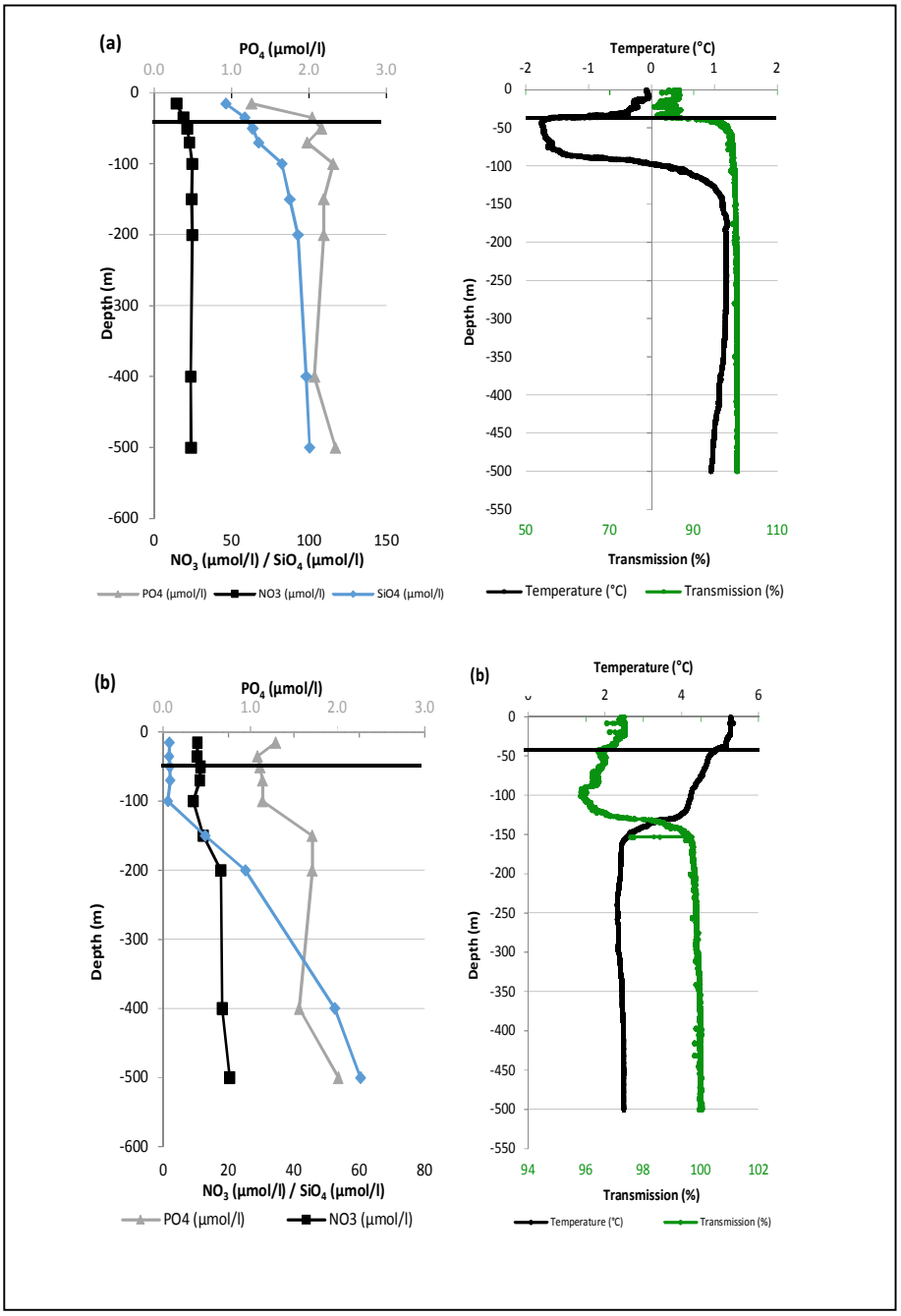

Figure 4.2 Nutrient, temperature and % transmission profiles in the water column at the bioassay sampling sites of Experiment 1 at 65°S (a), Experiment 2 at 50°S (b) during the SAFePool mid-summer cruise. Solid black line indicates sampling depth.

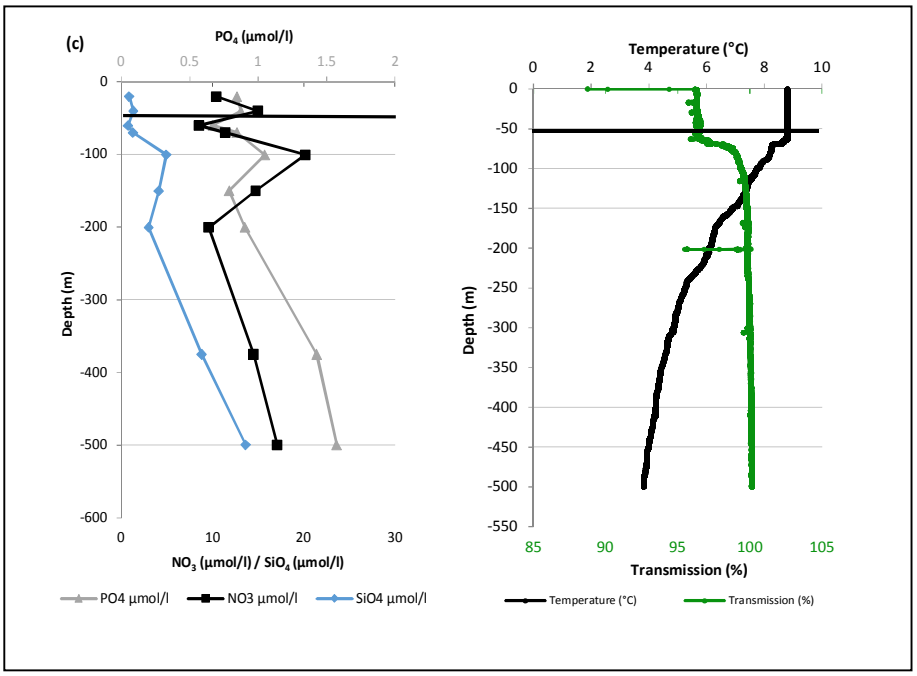

Figure 4.2 (cont.) Nutrient, temperature and % transmission profiles in the water column at the bioassay sampling site of Experiment 3 at 45°S (c) during the SAFePool mid-summer cruise. Solid black line indicates sampling depth.

Macronutrient concentrations at sampling depths increased with increasing latitudes with the highest concentrations measured at the AZ sampling site, as is characteristic of the SO water masses. NO_3 concentrations increased from ~8 - 22µM, PO_4 increased from ~0.9 - 2µM and SiO_4 concentrations increased from ~1µM in the SAZ to ~2µM in the PFZ, and a steep increase to ~60µM in the AZ, similar to previous studies in these areas during early bloom decline and are not considered to be limiting (Klunder *et al.* 2011). The MLD depth increased from ~50 to 200m from the AZ to the SAZ and the sampling depth for the experiments ranged from 30 to 60m from Experiment 1 to 3, following the depth of the SCM. The SCM of the PFZ sampling site was however deeper than sampled, at approximately 100m. In situ sampling temperatures ranged from -2 to 9°C from the AZ to the SAZ, within the expected values of the separate water masses.

4.2 Growth

Five bioassays were conducted within this study. Two were conducted during the SOSCEx cruise in March 2013 and three during the SAFePool cruise in Jan – Feb 2014. The SAFePool sites were chosen along a latitudinal transect, across different water masses (Figure 3.1), while the SOSCEx experiments were conducted within the same water mass (SAZ). In the following I compare the spatial differences along the latitudinal transect during the same season for SAFePool as well as the seasonal difference between SAZ experiments conducted in mid-summer (Feb 2014, SAFePool) and late summer (March 2013, SOSCEx). Growth, photophysiology and nutrient uptake are considered.

4.2.1 Spatial comparison during SAFePool cruise - Chl *a*-derived growth across three SAFePool experiments

A response in chl *a* concentration to Fe enrichment and light variability of three incubation experiments, which were conducted during the SAFePool mid-summer cruise, is displayed in Figure 4.3. An overall significant difference was obtained for final chl *a* concentrations in all three SAFePool incubation experiments, displaying a response of phytoplankton in varying degrees to the separate treatments and therefore rejecting the null hypothesis. The highest increase in chl *a* across all three experiments, from the initial condition, was observed for the HL-HFe treatment, whereas the LL-LFe sample for the three experiments all exhibited no noticeable change in chl *a* concentration.

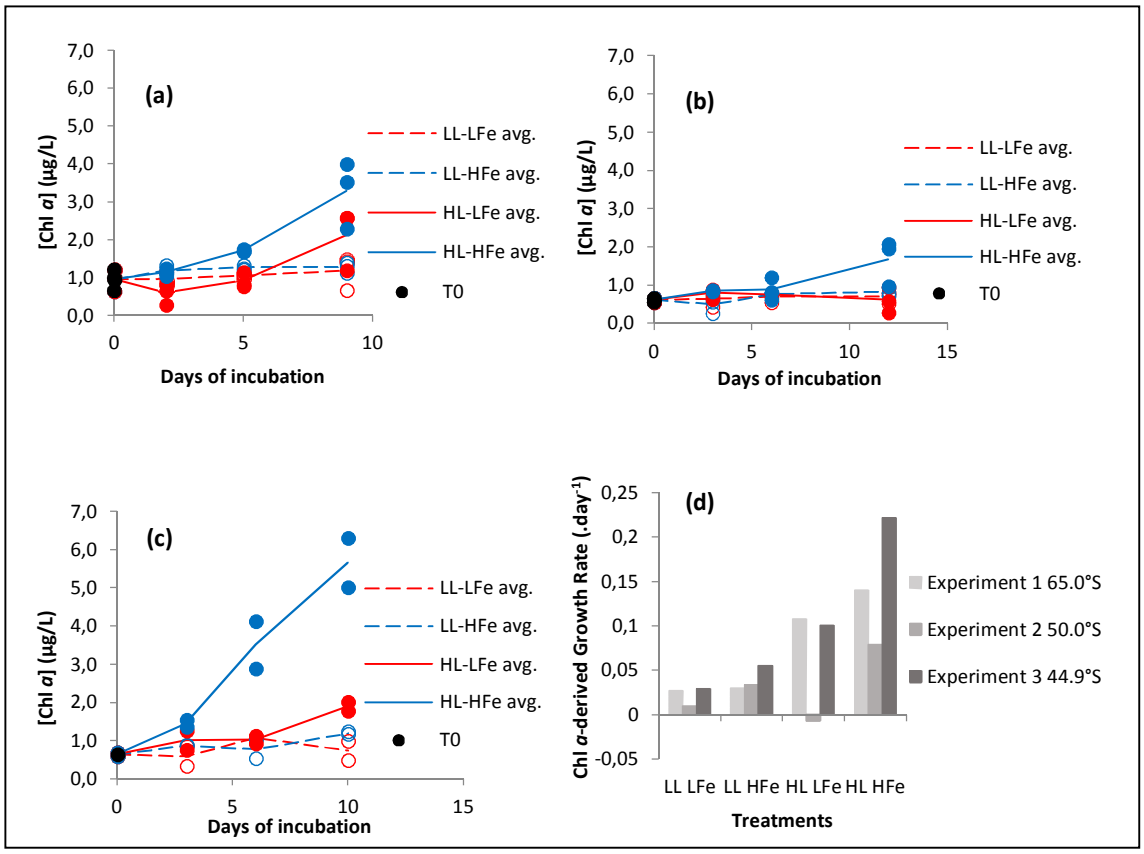

Figure 4.3 Chl *a* *vs.* days of incubation of four treatments for SAFePool Experiment 1 at 65.0°S (a), Experiment 2 at 50.0°S (b) and Experiment 3 at 44.9°S (c); Chl *a*–derived growth rates (derived from slopes of exponential functions) *vs.* treatments of three SAFePool experiments (d). Open red circles – LL-LFe replicates, open blue circles – LL-HFe replicates, filled red cirlces – HL-LFe replicates and filled blue circles – HL-HFe replicates

In Experiment 1 (Figure 4.3(a)) both LL treatments remained relatively constant throughout the incubation. The samples incubated under HL conditions display a noticeable increase in concentration, with or without the addition of Fe. Chl *a* doubled after nine days of incubation under the HL-LFe treatment and displayed a threefold increase for the HL-HFe treatment, therefore displaying the highest increase of the four treatments. Significant differences were observed for final chl *a* concentrations, between the two LL treatments and the HL-HFe treatment at 65.0°S (Appendix A, Table 14).

All treatments in Experiment 2 (Figure 4.3(b)) exhibited very different trends for chl *a* concentrations throughout the incubation, although the LL-HFe treatment gave a slight increase above the initial concentration it was not to a significant degree. The HL-LFe treatment displayed an overall decrease in chl *a* concentration. The decrease may possibly have been due to cells dying due to stress experienced at concurrent exposure to high light and a depletion of nutrients, whereas the HL-HFe treatment displayed a significant increase in chl *a* with a final concentration threefold the initial concentration. Possible grazing in HL-LFe sample could also explain a decrease in biomass. An overall

significant difference for chl *a* between treatments was exhibited in Experiment 2 after twelve days of incubation (Appendix A, Table 23). The final chl *a* concentration of the HL-HFe sample was significantly different to that of the control and HL-LFe samples (Appendix A, Table 24), also displaying the largest chl *a* increase at 50.0°S.

As observed in the previous two experiments the HL treatments, with or without Fe addition, displayed a significant increase in Experiment 3 (Figure 4.3(c)). An overall significant difference between treatments, for Experiment 3, was observed after 10 days of incubation (Appendix A, Table 30). The HL-HFe treatment exhibited the highest increase throughout the incubation; chl *a* increased exponentially and resulted in an overall increase of approximately tenfold the initial concentration, significantly different to both LL treatments. Therefore the highest increase for any treatment experiments was observed at 44.9°S when compared to the experiments at 65°S and 50°S (Appendix A, Table 31). An overall significant difference between treatments, for Experiment 3, was observed after ten days of incubation (Appendix A, Table 30).

A comparison of chl *a*-derived growth rates (derived from the slopes of the exponential function, e.g. Figure 3.3) against Fe enrichment and light variability of three incubation experiments conducted across different water masses, during the SAFePool mid-summer cruise is displayed in Figure 4.3(d). Overall, an increase in chl *a*-derived growth rate is observed for the addition of Fe and an increase in light separately, with the largest increase being observed for the combined addition of the two elements. A substantial increase was observed under HL conditions in all three experiments except for the HL-LFe treatment of Experiment 2 which displayed a negative rate, indicating the overall decrease in chl *a*, as seen in Figure 4.3(b). An increase in the growth rates was observed for HL-HFe in all three experiments, with the highest rate observed for Experiment 3, indicating Fe limitation for growth under HL conditions at all three sampling sites.

4.2.2 POC-derived growth rates across three SAFePool experiments

A comparison of POC-derived growth rates against Fe enrichment and light variability of three incubation experiments conducted across different water masses, during the SAFePool mid-summer cruise is displayed in Figure 4.4. POC-derived growth rates of samples under LL conditions of all three experiments were negative, indicating an overall decrease in POC concentrations whereas samples under HL conditions all displayed a positive growth rate. The LL-HFe treatments did not display a noticeable increase in growth rates, whereas the increase of light exhibited a relatively large increase across the three experiments. The HL-HFe treatment exhibited a relatively large increase in the growth rate of Experiment 3, at 44.9°S. The same response was, however, not seen for

the other two experiments, possibly due to temperature or grazing. In all three experiments phytoplankton responded more strongly to light addition than to Fe addition, with Experiment 2 displaying the lowest rates and Experiment 3 displaying the highest.

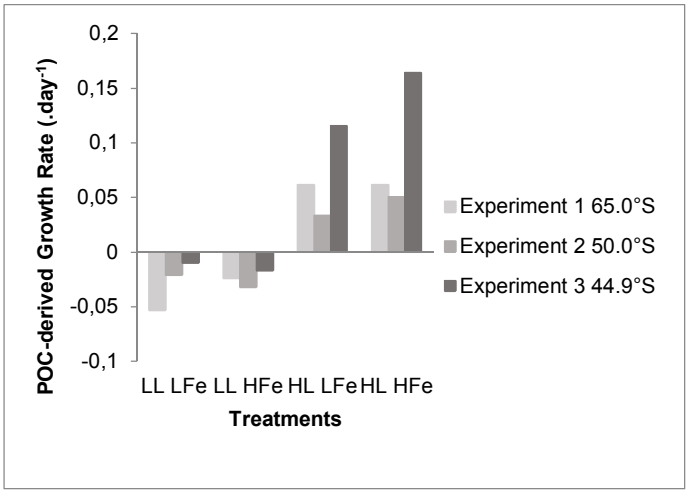

Figure 4.4 POC-derived growth rates (derived from slopes of exponential functions) *vs.* treatments of three SAFePool experiments (detailed growth curves shown in Appendix B)

Significant differences were displayed between treatments for final POC concentrations, for the three experiments (Appendix B, Figure 2). Samples incubated under HL conditions, with or without Fe addition, as seen with the chl *a* concentrations, were significantly different to those incubated under LL conditions for all experiments. A significant difference was obtained in Experiment 2, for the HL-HFe treatment against the LL-HFe treatment (P=0.002). No significant differences were observed for the addition of Fe alone (Appendix A, Table 16, 26 & 32).

The rates of change per day of incubation in chl *a*/POC corresponding to Fe enrichment and light variability, of three SAFePool incubation experiments and coefficients of determination are displayed in Table 4.1. The lowest rates were consistently observed for the HL-LFe treatments, displaying a decline for experiments 2 and 3. This is assumed to be due to depletion of available Fe in the sample. An increase in chl *a*/POC is observed for other treatments of the three experiments, throughout the incubation. A clear trend in response to Fe addition and light variability cannot be seen in rates of change, values ranged from -0.05 to 0.085. The coefficients of determination (R^2) for rates of change in chl *a*/POC against incubation time ranged from very low (0.07 for HL-LFe, Exp. 3) to average (0.51 for LL-HFe, Exp. 2), indicating almost no correlation to a noticeable correlation in ratios against time of incubation.

Table 4.1 Rates of change in Chl *a*/POC per day of incubation (slopes of exponential functions, e.g. Figure 3.3) and coefficients of determination (R^2) for three SAFePool experiments

Experiment	Latitude (°S)	Treatment	Slope = Chl *a*/POC rate of change (.day^{-1})	R^2
SAFePool 1	65	LL-LFe	0.073	0.36
	65	LL-HFe	0.053	0.41
	65	HL-LFe	0.044	0.20
	65	HL-HFe	0.085	0.42
SAFePool 2	50	LL-LFe	0.030	0.24
	50	LL-HFe	0.068	0.51
	50	HL-LFe	-0.050	0.34
	50	HL-HFe	0.023	0.15
SAFePool 3	44.9	LL-LFe	0.036	0.10
	44.9	LL-HFe	0.071	0.38
	44.9	HL-LFe	-0.014	0.07
	44.9	HL-HFe	0.057	0.38

4.2.3 Growth based on cell counts across two SAFePool experiments

Cell count analysis with the Coulter Counter could only be done for Experiment 2 and 3, during SAFePool.

A response in relative cell abundance and size to Fe enrichment and light variability of Experiment 2, conducted during the SAFePool mid-summer cruise at 50.0°S, is displayed in Figure 4.5. The initial (T_0) relative cell abundance displayed a peak at approximately 4µm and 2µm. A varying response in relative cell abundance and size of cells in the sample to the separate treatments was observed in Experiment 2. No increase in cell counts was observed throughout the incubation for the two LL treatments. There was however a decrease observed in the LL-LFe sample (Figure 4.5(a)) at day six (T_6) of the incubation. The LL-HFe treatment (Figure 4.5(b)) gave no overall change in cell counts or size.

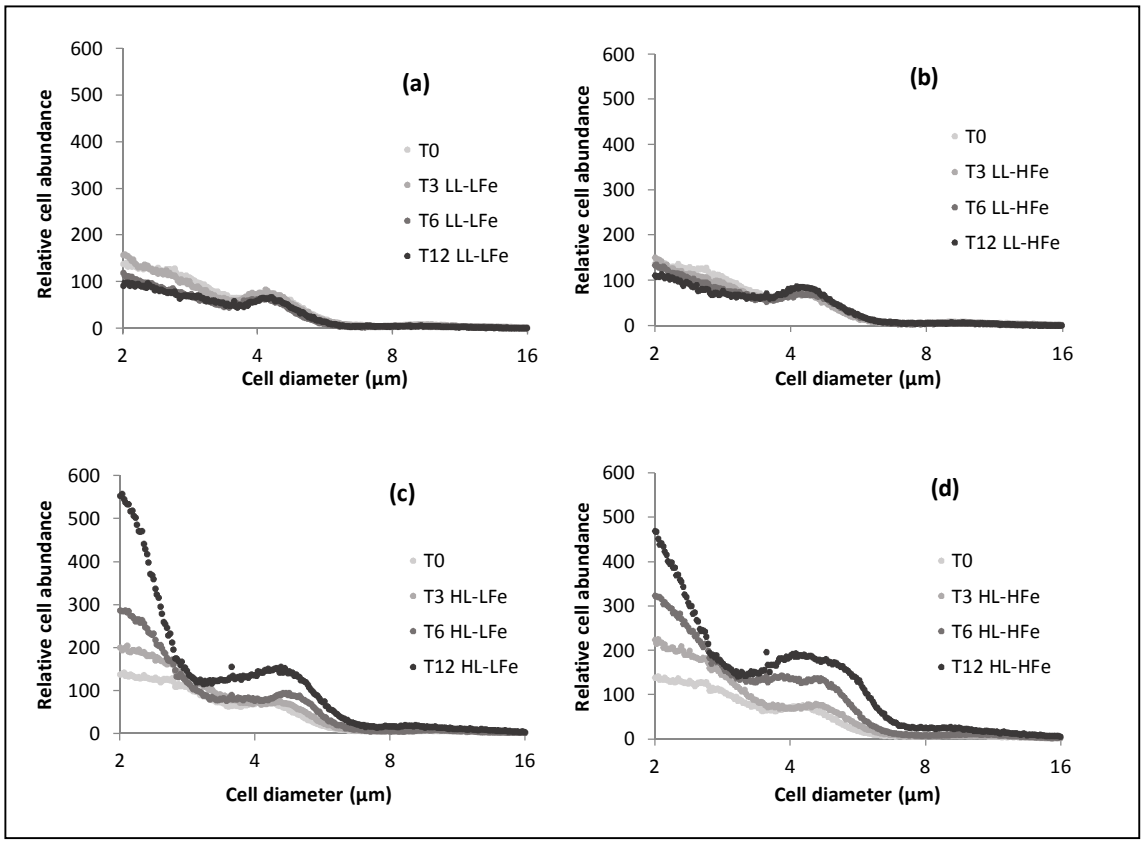

Figure 4.5 Relative cell abundance *vs.* cell diameter of four treatments LL-LFe (a), LL-HFe (b), HL-LFe (c) and HL-HFe (d) for SAFePool Experiment 2 at 50.0°S

Both HL treatments, with or without the addition of Fe, displayed a noticeable increase in cell counts. HL-LFe treatment (Figure 4.5(c)) cell counts increased exponentially throughout the incubation and the initial secondary peak observed at 4µm shifted toward 5µm, indicating an increase in cell sizes. The HL-HFe treatment (Figure 4.5(d)) exhibited a very similar increase in cell counts as observed for the HL-LFe treatment. The increase was, however, less with a more steady increase of approximately 100 units observed at each termination. Fe enrichment under HL displayed an increase in cell size from 4 - 5µm and increased irradiance displayed an increase in relative abundance.

A response in relative cell abundance and size to Fe enrichment and light variability of Experiment 3, conducted during the SAFePool mid-summer cruise at 44.9°S, is displayed in Figure 4.6. The initial (T_0) relative cell abundance displayed a peak at approximately 4µm and 2µm, as observed in Experiment 2. A varying response in relative cell abundance and size of cells in the sample to the separate treatments was also observed in Experiment 3. No increase in cell counts was observed throughout the incubation for the LL-LFe sample (Figure 4.6 (a)) and only a slight increase for the LL-HFe sample (Figure 4.6(b)). HL treatments, with or without the addition of Fe, displayed a noticeable increase in relative cell abundance of peak observed at ~4µm and 2µm. For

both treatments cell counts increased steadily at each termination up to day six (T_6) of incubation. The HL-HFe treatment (Figure 4.6(d)) exhibited an increase in 4µm relative cell abundance and a shift to ~5µm after ten days of incubation (T_{10}).

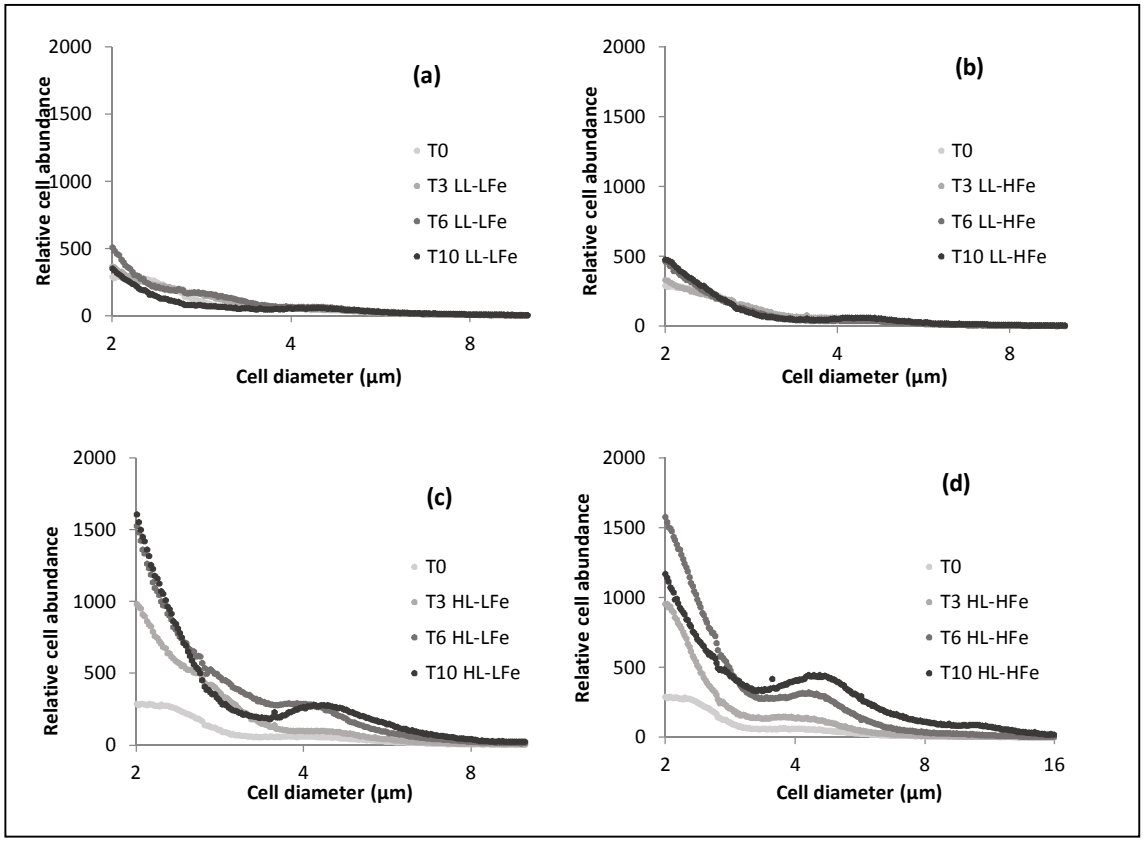

Figure 4.6 Relative cell abundance *vs.* cell diameter of four treatments LL-LFe (a), LL-HFe (b), HL-LFe (c) and HL-HFe (d) for SAFePool Experiment 3 at 44.9°S

4.2.4 Summary – Spatial comparison of growth

Chl *a* and POC concentrations in the initial samples were very similar in magnitude across the three sampling sites. During incubation, the results for biomass measurements display a definite response to the increase in irradiance, with the largest response observed for the HL-HFe treatment, for samples from all three sampling sites. Results indicate an apparent Fe limitation in regions of the ocean with shallower MLDs due to stratification, whereas the addition of Fe did not have a large impact under LL conditions. The sample taken from the SAZ displayed the largest response to HL-HFe treatment, for all analyses done.

The increase of irradiance without Fe addition displayed a slight response in chl *a* in the SAZ and AZ samples. This was however not observed for the PFZ sample. Combined Fe and light addition appears to be the factors that promote the largest chl *a* increase in the SAFePool incubations. The increase of POC was observed for an increase in

irradiance across all three experiments, with only the SAZ sample displaying a noticeable response to the HL-HFe treatment. Increased irradiance gave the largest response for organic carbon fixation. In observation of the cell counts, a noticeable increase in cell size is observed in incubations with Fe addition, with a significantly large response in cell abundance to the increase of light.

4.2.5 Temporal comparison during the SAFePool and SOSCEx cruises - Chl *a*-derived growth across two SOSCEx experiments and SAFePool Experiment 3

A response in chl *a* concentration to Fe enrichment and light variability of two incubation experiments, which were conducted during the SOSCEx late summer cruise, is displayed in Figure 4.7. Comparison of the two SOSCEx experiments with the SAFePool Experiment 3 was done due to the sampling being conducted at similar latitudes, within the SAZ, but at different times of the year. The SOSCEx incubations were conducted during March of 2013 and the SAFePool incubation during February of 2014, therefore we are able to compare the effects of the change of season within the SAZ.

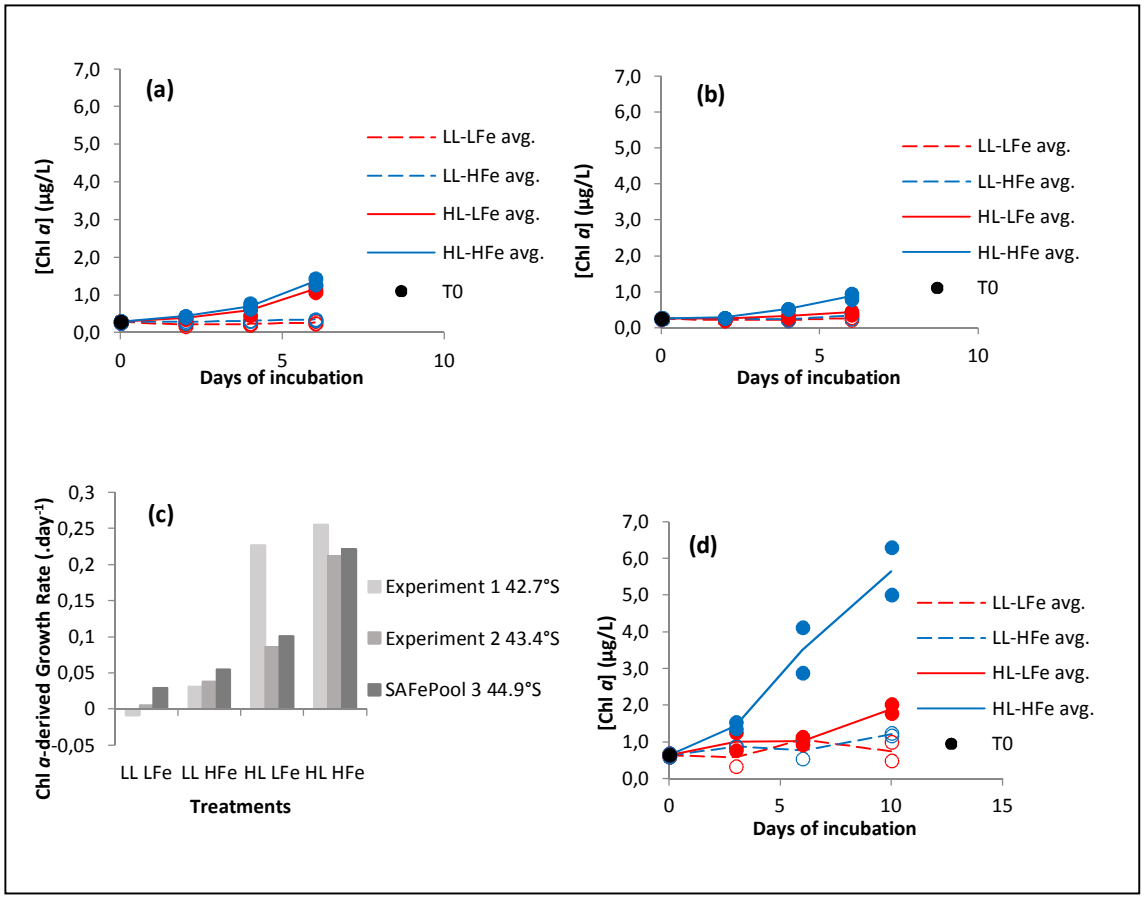

Figure 4.7 Chl *a* concentration *vs.* days of incubation of four treatments for SOSCEx Experiment 1 at 42.7°S (a) and Experiment 2 at 43.4°S (b); Chl a–derived growth rates (derived from slopes of exponential functions) *vs.* treatments across two SOSCEx experiments during March 2013 (c) and SAFePool Experiment 3 at 44.9°S (d). Open red circles – LL-LFe replicates, open blue circles – LL-HFe replicates, filled red cirlces – HL-LFe replicates and filled blue circles – HL-HFe replicates

An overall significant difference was obtained for final chl *a* concentrations in both SOSCEx incubation experiments, displaying a response of phytoplankton in varying degrees to the separate treatments. The highest increase in chl *a* concentration for both experiments, from the initial condition, was observed for the HL-HFe treatment as was

observed in the SAFePool experiments. In SOSCEx Experiment 1 (Figure 4.7(a)) both LL treatments exhibited no significant change in chl *a* concentration from the initial concentration. The samples incubated under HL conditions displayed a significant increase, with or without the addition of Fe, with an immediate response of phytoplankton, displaying a significant difference after only two days of incubation. The HL-HFe treatment displayed a significant difference after day 2 and day 6 of incubation (P=0.005, Appendix A, Table 2 & 3).

After six days of incubation both HL treatments displayed a fourfold increase in chl *a* concentration from the initial condition and the HL-HFe treatment displayed a significant difference to the control sample and to the LL-HFe treatment. The HL-LFe treatment also displayed a significant difference to the control sample. An overall significant difference across the four treatments was observed as soon as 2 days into the incubation and values remained similar through to the end of the incubation (Appendix A, Table 1). The increase of irradiance displayed the largest impact on chl *a* concentration. Fe addition did not however display any significant impact under LL or HL conditions for incubation Experiment 1 at 42.7°S.

For Experiment 2 (Figure 4.7(b)), as seen in Experiment 1, there was no significant increase in chl *a* concentration for the two LL treatments. The HL-LFe treatment did not exhibit the same increase in chl *a* concentration as seen in Experiment 1. There was a slight increase observed in chl *a* but not to a significant degree. The HL-HFe treatment exhibited the largest increase in chl *a*, with a significant difference to the control sample after only two days of incubation (P=0.007, Appendix A, Table 10). After six days of incubation the HL-HFe treatment displayed a threefold increase in chl *a* concentration from the initial condition and displayed a significant difference to both LL treatments, with a significant difference against the control (P=0.005, Appendix A, Table 9). An overall significant difference across the four treatments was observed immediately and values remained similar throughout the incubation, as observed in Experiment 1 (Appendix A, Table 8). The combined addition of Fe and light displayed the largest response in chl *a* concentration, the LL-HFe treatment did not however display any significant impact in Experiment 2 at 43.4°S. SAFePool Experiment 3 chl *a* concentration trends, conducted at 44.9°S, February 2014 (Figure 4.7(d)), were very similar to those observed in SOSCEx Experiment 2, where the HL-HFe treatment had the largest response.

A comparison of chl *a*-derived growth rates against Fe enrichment and light variability of two incubation experiments conducted during the SOSCEx late summer cruise is displayed in Figure 4.7(c). An increase in chl *a*-derived growth rates was observed for

the addition of Fe and the addition of light in both experiments. The largest increase observed in Experiment 1 was displayed for the addition of light with a very slight impact for Fe addition, as observed in the chl *a* concentrations, indicating a lesser in situ Fe limitation than seen in Experiment 2. For Experiment 2 the largest rate increase was observed for the HL-HFe treatment, with the HL-LFe treatment having a lesser impact than observed in Experiment 1. Chl *a*-derived growth rates indicate a previous light limitation for both experiments. The chl *a*-derived growth rates for SOSCEx Experiment 2 and SAFePool Experiment 3 were very similar in response to treatments and values.

4.2.6 POC-derived growth rates across two SOSCEx experiments and compared to SAFePool Experiment 3

A comparison of POC-derived growth rates against Fe enrichment and light variability of two incubation experiments conducted during the SOSCEx late summer cruise is displayed in Figure 4.8. The response of POC-derived growth rates did not correspond with the chl *a*-derived growth rates of the two SOSCEx incubation experiments, which indicates that treatments affected the increase of chl *a* per POC rather than the increase in carbon and likely, rather than the increase in number of cells. Chl *a*-derived growth rates might not only correspond to cell growth, but also to cell restructuring and denser chl *a* packaging. Higher rates were observed for the HL treatments of both experiments. The values were however lower than chl *a* values. In Experiment 1 the addition of Fe under LL and HL displayed a further increase in rates whereas in Experiment 2 the addition of Fe displayed a decrease under the separate light levels. The response of POC-derived growth rates of neither of the experiments corresponded to SAFePool experiment 3, but values were however within a similar range. No overall significant difference, across treatments, was observed for POC concentrations (Appendix B, Figure 1) in both experiments (Appendix A, Table 1 & 8).

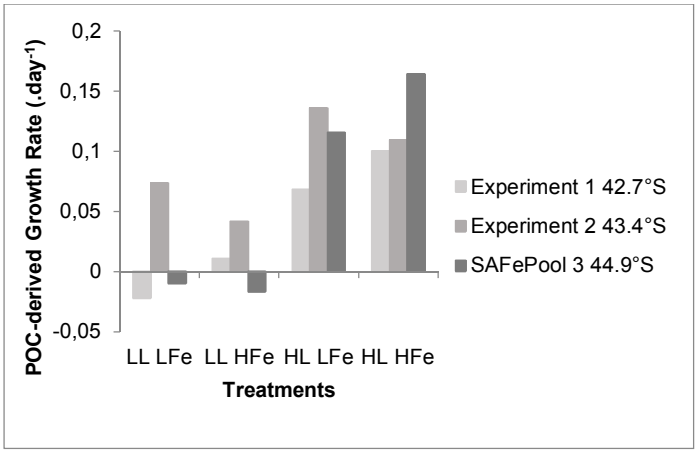

Figure 4.8 POC-derived growth rates (derived from slopes of the exponential functions) *vs.* treatments across two SOSCEx experiments (detailed POC growth curves are shown in Appendix B)

The rates of change per day of incubation in chl *a*/POC corresponding to Fe enrichment and light variability, of two SOSCEx incubation experiments and coefficients of determination are displayed in Table 4.2. The LL-LFe and HL-LFe treatments of Experiment 2 displayed negative rates of change, indicating a decrease in chl *a*/POC, possibly due to extreme Fe limitation in samples as seen in SAFePool experiments. Positive rates of change indicate a general increase in chl *a*/POC for both experiments. In Experiment 1 a clear response can be seen for the two HL treatments. The HL-HFe treatment for Experiment 2 had a substantially higher rate of change relative to other treatments. The coefficients of determination (R^2) for rates of change in chl *a*/POC against incubation time ranged from very low (<0.01 for LL-LFe, Exp. 1) to average (0.55 for HL-HFe, Exp. 1), indicating almost no correlation to a noticeable correlation in ratios over time of incubation, similar to values obtained for the SAFePool experiments.

Table 4.2 Rates of change in Chl *a*/POC per day of incubation (slopes of exponential functions, e.g. Figure 3.2) and coefficients of determination (R^2) for two SOSCEx experiments

Experiment	Latitude (°S)	Treatment	Slope = Chl *a*/POC rate of change (.day^{-1})	R^2
SOSCEx 1	42.7	LL-LFe	0.002	0.00
	42.7	LL-HFe	0.031	0.02
	42.7	HL-LFe	0.151	0.52
	42.7	HL-HFe	0.147	0.55
SOSCEx 2	43.4	LL-LFe	-0.062	0.25
	43.4	LL-HFe	0.019	0.02
	43.4	HL-LFe	-0.047	0.16
	43.4	HL-HFe	0.104	0.52

4.2.7 Cell counts across two SOSCEx experiments and compared to SAFePool Experiment 3

A response in relative cell abundance and size to Fe enrichment and light variability of Experiment 1, conducted during the SOSCEx late summer cruise at 42.7°S, is displayed in Figure 4.9. Response in relative cell abundance and size of phytoplankton in the sample, to varying degrees, was observed in Experiment 1. The initial sample (T_0) cell abundance displayed a peak at 2µm. The control sample (Figure 4.9(a)) exhibited a very slight increase in relative cell abundance after six days of incubation (T_6) and the LL-HFe treatment (Figure 4.9(b)) displayed a slightly higher increase than the control. A noticeably larger response was observed for the addition of light where both HL treatments, with or without the addition of Fe, displayed an exponential increase in relative cell abundance with the peak broadening across cell diameter of up to 4µm. The HL-HFe treatment (Figure 4.9(d)) exhibited a more noticeable broadening in the peak, possibly indicating an increase in larger cells.

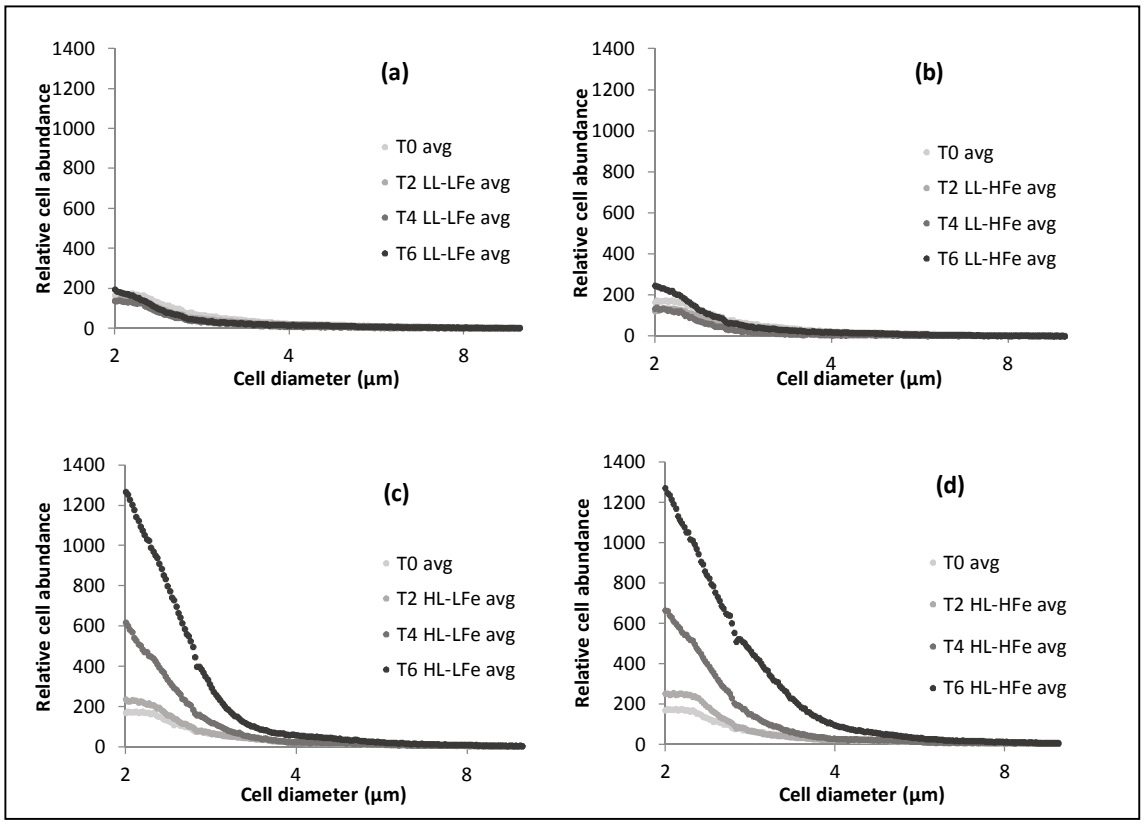

Figure 4.9 Relative cell abundance *vs.* cell diameter of four treatments LL-LFe (a), LL-HFe (b), HL-LFe (c) and HL-HFe (d) for SOSCEx Experiment 1 at 42.7°S

A response in relative cell abundance and size to Fe enrichment and light variability of Experiment 2, conducted during the SOSCEx late summer cruise at 43.4°S, is displayed in Figure 4.10. Response in relative cell abundance and size of phytoplankton in the sample, to varying degrees, was also observed in Experiment 2. The initial sample (T_0) cell abundance displayed a peak at 2µm, as displayed in Experiment 1. The control sample (Figure 4.10(a)) exhibited a slight increase in relative cell abundance after six days of incubation (T_6), whereas the LL-HFe treatment (Figure 4.10 (b)) displayed a slightly lower increase than the control but the formation of a slight peak at 4µm cell diameter was observed. A noticeably larger response was observed for the addition of light. For the HL-LFe treatment (Figure 4.10(c)) an exponential increase was observed in relative cell abundance, throughout the incubation. The HL-HFe treatment (Figure 4.10(d)) displayed a slightly lower increase but, as observed in the LL treatments, a slight peak formed at a higher cell diameter, at approximately 5µm. The addition of Fe under both HL and LL conditions displayed an increase in larger cells.

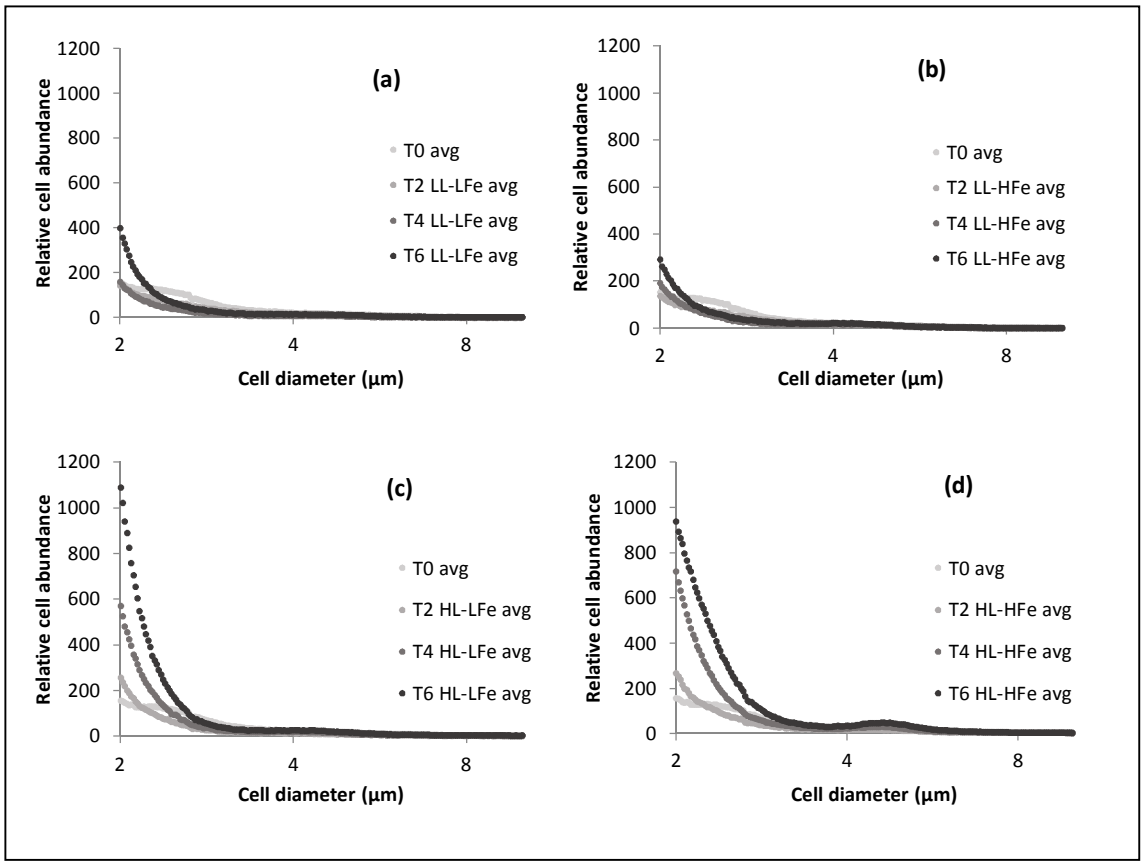

Figure 4.10 Relative cell abundance *vs.* cell diameter of four treatments LL-LFe (a), LL-HFe (b), HL-LFe (c) and HL-HFe (d) for SOSCEx Experiment 2 at 43.4°S

4.2.8 Summary – temporal variability of growth

Initial chl *a* concentrations in SOSCEx incubations were approximately half the concentration obtained in the SAFePool Experiment 3 incubation, which was to be expected due to the SOSCEx experiments being conducted at the end of summer, whereas the initial POC concentrations were very similar. As observed in SAFePool Experiment 3, the largest response in chl *a* was obtained for the HL-HFe treatment, whereas POC concentrations were not significantly impacted by any treatment in particular. A small response to the LL-HFe treatment was also obtained for both chl *a* and POC in SOSCEx experiments, whereas a significantly larger response for the HL-HFe treatment was displayed in SOSCEx Experiment 2 than in Experiment 1, also observed in the SAFePool Experiment 3 incubation. An obvious response to treatments was displayed for chl *a* but was not observed for POC. A response to increased irradiance was observed in relative cell abundance for both experiments, and the addition of Fe displayed an increase in cell size, observed in Experiment 2 as seen in SAFePool Experiment 3, which was not visible in Experiment 1.

4.3 Photophysiology

4.3.1 Spatial comparison during the SAFePool cruise - PSII photochemical efficiency (F_v/F_m) across three SAFePool experiments

A response in F_v/F_m (dimensionless) between treatments to Fe enrichment and light variability, of three incubation experiments, conducted during the SAFePool mid-summer cruise, is displayed in Figure 4.11. A significant difference in F_v/F_m values between treatments, at the end of incubations, was observed for Experiment 1 and Experiment 2 (Appendix A, Table 13 & 23). All three experiments did however display very similar trends in F_v/F_m values. Values were consistently lower for HL treatments than seen in the LL treatments, ranging from ~0.2 to 0.6 (dimensionless). An increase in length of incubation displayed a decrease in F_v/F_m under HL conditions for Experiment 2 and 3, displaying a noticeably faster decline for samples without Fe enrichment. There was however no significant difference observed for the HFe treatments under the two light levels. Overall higher F_v/F_m values were obtained for samples incubated under LL conditions than under HL conditions.

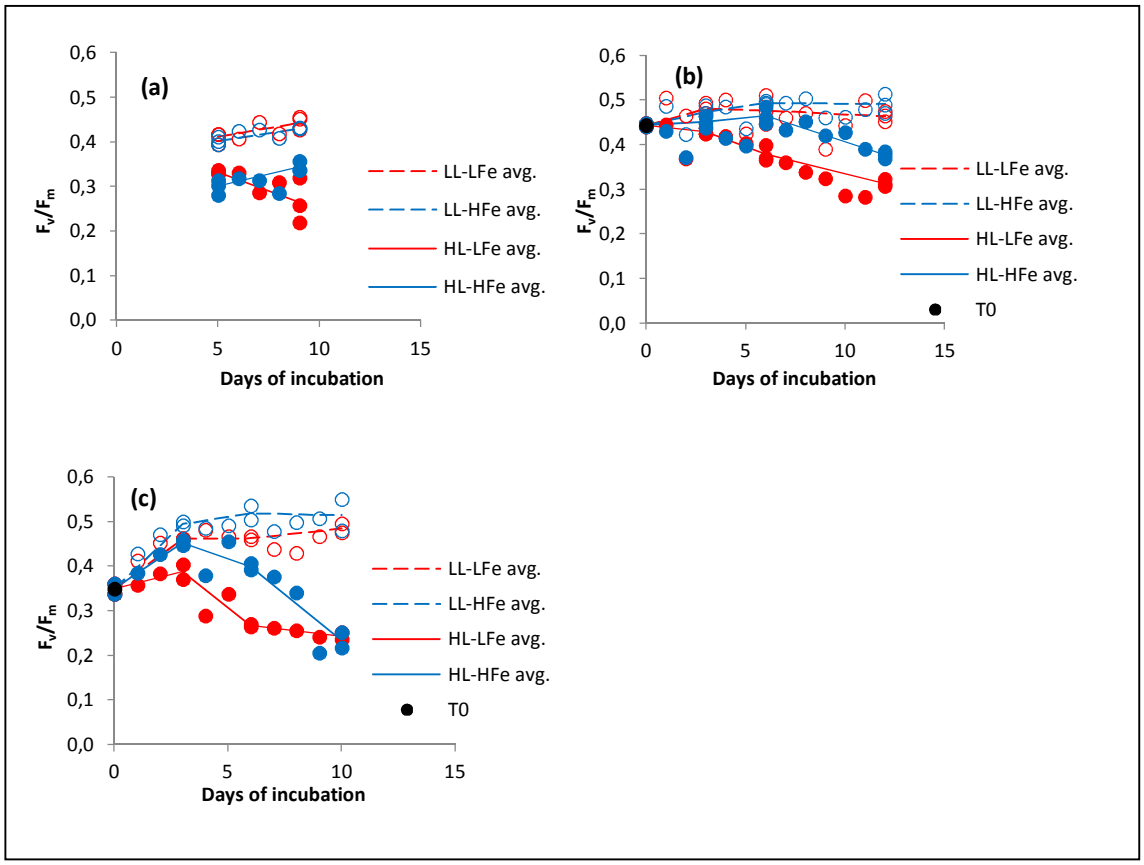

Figure 4.11 F_v/F_m (dimensionless) *vs.* days of incubation of four treatments for SAFePool Experiment 1 at 65.0°S (a), Experiment 2 at 50.0°S (b) and Experiment 3 at 44.9°S (c). Open red circles – LL-LFe replicates, open blue circles – LL-HFe replicates, filled red cirlces – HL-LFe replicates and filled blue circles – HL-HFe replicates

The initial F_v/F_m values for Experiment 1 (Figure 4.11(a)) are unfortunately not known due to the loss of data points up to day 5 of the incubation. Values obtained from day 5 to day 9 of the incubation displayed fluctuation over a range of <0.1, for all treatments. LL treatments fluctuated around ~0.4 (dimensionless), increasing slightly after nine days of incubation and HL treatments were constantly lower, at ~0.3 (dimensionless). For the HL-LFe treatment a decrease in F_v/F_m was observed at the end of incubation, whereas a slight increase was observed for the HL-HFe treatment. A significant difference was displayed between LL and HL treatments, with a significant difference between the LL-LFe and the HL-LFe treatments at the end of the incubation for Experiment 1 (P=0.007, Appendix A, Table 18).

The F_v/F_m values obtained for Experiment 2 (Figure 4.11(b)) were slightly higher than values for Experiment 1, ranging between ~0.4 and 0.5 (dimensionless), with LL treatments only slightly higher than the HL treatments. Initially values also fluctuated over a range of ~0.1 as observed in Experiment 1 and after five days of incubation the HL treatments started to decline, whereas the LL treatments remained relatively constant throughout the incubation. Significant differences were observed at the end of incubation between LL treatments and HL treatments, with a significant difference between the LL-HFe and the HL-LFe treatment (P=0.003, Appendix A, Table 27).

No significant differences were observed in F_v/F_m between treatments for Experiment 3 (Appendix A, Table 30). The lack of significant difference between treatments in Experiment 3 can be due to samples only being incubated in duplicate, therefore sample size was too small for statistical testing at a 90% confidence level. As observed in the previous two experiments LL treatment values were higher than values of HL treatments. Throughout the incubation an increase from an initial value of ~0.35 to 0.5 (dimensionless) was observed for the LL treatments whereas the HL treatment values decreased to ~0.2 (dimensionless). Fe enrichment displayed slightly higher values within separate light levels, indicating a positive impact of Fe on F_v/F_m.

The rates of change per day of incubation in F_v/F_m corresponding to Fe enrichment and light variability, of three SAFePool incubation experiments and P values of regression are displayed in Table 4.3. No clear trend in response to Fe addition and light variability can be seen across treatments and experiments, when looking at rates of change. All rates of change are close to zero, due to F_v/F_m values remaining relatively constant throughout incubation experiments, with only a slight increase or decrease from the initial condition (Figure 4.11).

Table 4.3 Rates of change in F_v/F_m per day of incubation (slopes of regression, e.g. Figure 3.3). Coefficients of determination (R^2), P values of regression, initial and final values (dimensionless) of incubation for three SAFePool experiments

Experiment	Latitude (°S)	Treatment	Average slope = Rate of change (.day^{-1})	R^2	P	T_0	T_{final}
SAFePool 1	65.0	LL-LFe	0.018	0.54	**0.023**	0.412*	0.444
	65.0	LL-HFe	0.010	0.57	**0.019**	0.402*	0.431
	65.0	HL-LFe	-0.051	0.52	**0.029**	0.332*	0.265
	65.0	HL-HFe	0.015	0.43	**0.057**	0.301*	0.343
SAFePool 2	50.0	LL-LFe	-0.004	0.00	**0.793**	0.444	0.463
	50.0	LL-HFe	0.006	0.25	**0.020**	0.444	0.491
	50.0	HL-LFe	-0.037	0.86	**<0.001**	0.444	0.313
	50.0	HL-HFe	-0.005	0.23	**0.029**	0.444	0.377
SAFePool 3	44.9	LL-LFe	0.017	0.72	**<0.001**	0.349	0.485
	44.9	LL-HFe	0.025	0.28	**0.044**	0.349	0.515
	44.9	HL-LFe	-0.050	0.14	**0.175**	0.349	0.243
	44.9	HL-HFe	-0.050	0.10	**0.251**	0.349	0.234

* T_5 values were used for Experiment 1, due to loss of initial data

The coefficients of determination (R^2) obtained for the rates of change (slopes) in F_v/F_m against incubation time ranged from very low (<0.005 for LL-LFe, Exp. 2) to very high (0.86 for HL-LFe, Exp. 2), therefore indicating almost no correlation to very strong correlation in F_v/F_m over the length of incubation for the different treatments. Most of the regression P values obtained indicate a high significance of the rates of change (at a 90% confidence level) with only a few exceptions, such as HL treatments in Experiment 3.

4.3.2 Functional absorption cross-section of PSII (σ_{PSII}) comparison across three SAFePool experiments

A response in σ_{PSII} (Å^2.quanta^{-1}) to Fe enrichment and light variability of three incubation experiments, conducted during the SAFePool mid-summer cruise, is displayed in Figure 4.12. There was no significant differences observed in σ_{PSII} between treatments, across the three incubation experiments (Appendix A, Table 13, 23 & 30). All SAFePool

experiments had very similar values, ~200 – 250 Å^2.quanta^{-1}, which remained relatively constant, with slight fluctuations throughout the incubations and no visible separation between the four treatments. There was no noticeable overall change observed in Experiment 1 and 2, Experiment 3 did however display a slight increase by the end of the incubation. Overall it can be accepted that the σ_{PSII} of the resident phytoplankton present in the SAFePool experiment samples was not affected by Fe enrichment or the increase of irradiance during the incubation experiments.

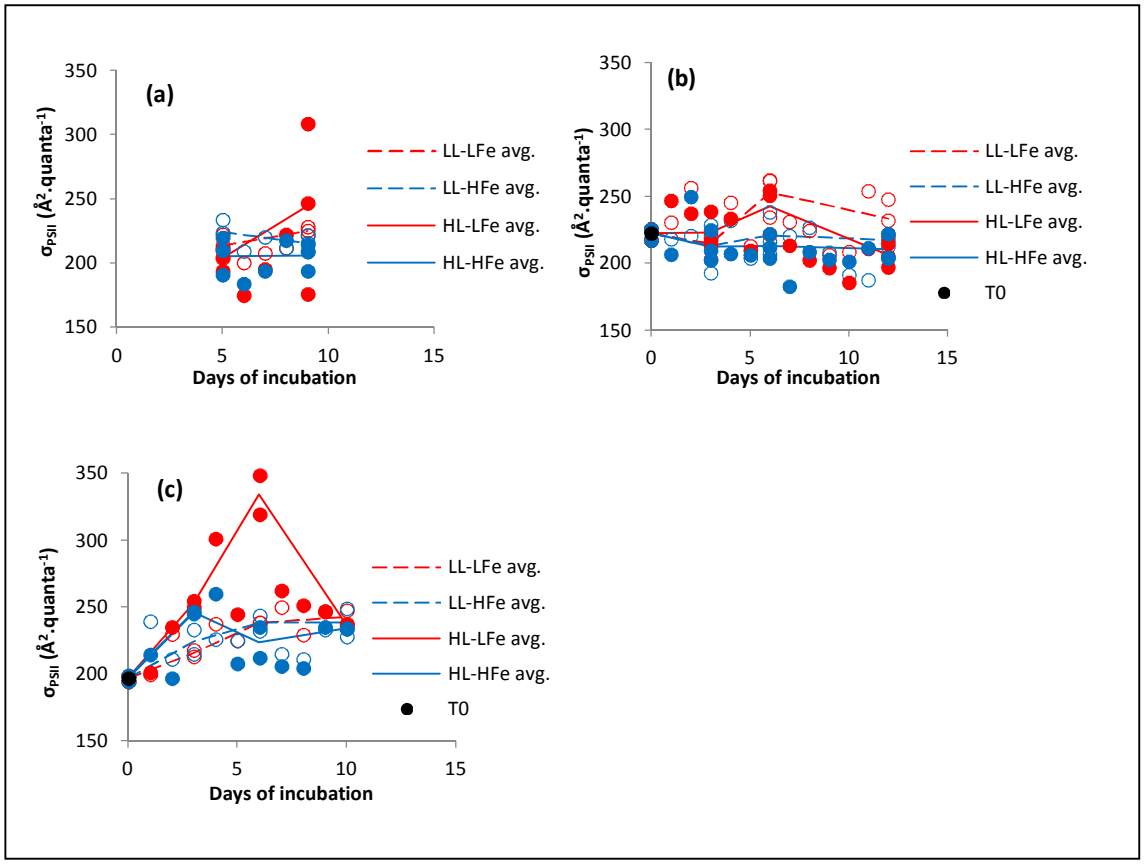

Figure 4.12 σ_{PSII} (Å^2.quanta^{-1}) *vs.* days of incubation of four treatments for SAFePool Experiment 1 at 65.0°S (a), Experiment 2 at 50.0°S (b) and Experiment 3 at 44.9°S (c). Open red circles – LL-LFe replicates, open blue circles – LL-HFe replicates, filled red cirlces – HL-LFe replicates and filled blue circles – HL-HFe replicates

The rates of change per day of incubation in σ_{PSII} (Å^2.quanta^{-1}) corresponding to Fe enrichment and light variability, of three SAFePool incubation experiments, and P values of regression are displayed in Table 4.4. No trend in response to Fe addition and light variability can be seen across treatments and experiments when looking at rates of change, as observed for the F_v/F_m results. All rates of change were very close to zero, due to no overall change in σ_{PSII} at the end of incubation (Figure 4.12). The coefficients of determination (R^2) obtained for the rates of change in σ_{PSII} against incubation time ranged from very low (0.01 for LL-LFe Exp. 2) to high (0.72 for LL-LFe for Exp. 3),

indicating almost no correlation to strong correlation in σ_{PSII} over the length of incubation for the different treatments. Most of the regression P values obtained indicate a low significance of rates of change (at a 90% confidence level) with the exception of the HL-LFe treatment of Experiment 2 and the LL-LFe treatment of Experiment 3.

Table 4.4 Rates of change in σ_{PSII} ($Å^2$.quanta^{-1}) per day of incubation (slopes of regressions, e.g. Figure 3.3). Coefficients of determination (R^2), P values of regression, initial and final values of incubation for three SAFePool experiments

Experiment	Latitude (°S)	Treatment	Average slope = Rate of change (.day^{-1})	R^2	P	T_0 ($Å^2$.quanta^{-1})	T_{final} ($Å^2$.quanta^{-1})
SAFePool 1	65.0	LL-LFe	0.016	0.33	**0.109**	214*	225
	65.0	LL-HFe	-0.006	0.11	**0.374**	224*	216
	65.0	HL-LFe	0.060	0.23	**0.190**	204*	244
	65.0	HL-HFe	0.017	0.02	**0.721**	205*	206
SAFePool 2	50.0	LL-LFe	-0.001	0.01	**0.633**	222	234
	50.0	LL-HFe	0.008	0.11	**0.145**	222	217
	50.0	HL-LFe	-0.016	0.30	**0.010**	222	206
	50.0	HL-HFe	-0.007	0.16	**0.070**	222	210
SAFePool 3	44.9	LL-LFe	0.020	0.72	**<0.001**	197	243
	44.9	LL-HFe	0.008	0.28	**0.044**	197	239
	44.9	HL-LFe	0.019	0.14	**0.175**	197	237
	44.9	HL-HFe	0.008	0.10	**0.251**	197	234

***** T_5 values were used for Experiment 1, due to loss of initial data

4.3.3 Summary – spatial variability of photophysiological response

Very slight overall changes were displayed in photophysiology measurements for samples from the three water masses sampled. Initial F_v/F_m and σ_{PSII} were similar for the three SAFePool incubation samples. Samples incubated under HL conditions displayed a lower F_v/F_m than those incubated under LL conditions, for all three experiments, with very little response to Fe enrichment. Very slight changes were obtained in F_v/F_m for experiments, LL treatments displayed a slight increase and HL treatments a slight decrease. HL-LFe treatments displayed a steeper decline in F_v/F_m relative to the HL-HFe treatments. No noticeable overall change was displayed for σ_{PSII} of resident

phytoplankton in samples by the end of incubations, therefore displaying no significant response to treatments.

4.3.4 Temporal comparison during the SAFePool and SOSCEx cruises - PSII photochemical efficiency (F_v/F_m) across two SOSCEx experiments and SAFePool Experiment 3

A response in F_v/F_m (dimensionless) to Fe enrichment and light variability of two incubation experiments, conducted during the SOSCEx late summer cruise, is displayed in Figure 4.13. Photophysiology measurements were conducted using an FRRf instrument during the SOSCEx cruise whereas a FIRe instrument was used during the SAFePool cruise, due to FRRf instrument malfunction. The LEDs on the FRRf used during the SOSCEx cruise were however not set up optimally, therefore F_v/F_m values were significantly lower than expected. LEDs were set up at a higher intensity than needed for resident phytoplankton in the samples and therefore reaction centres closed too quickly, resulting in fluorescence quenching and F_v/F_m values that were approximately tenfold lower than values obtained during the SAFePool cruise.

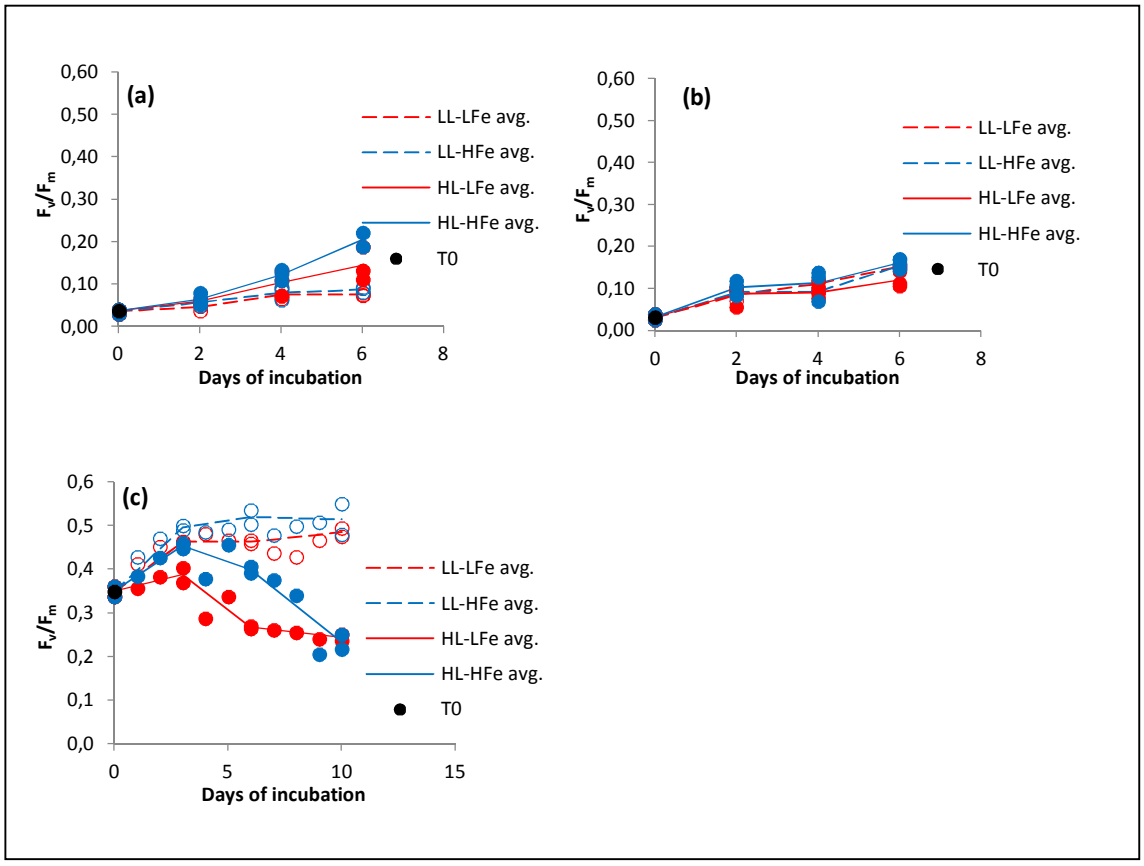

Figure 4.13 F_v/F_m (dimensionless) *vs.* days of incubation of four treatments for SOSCEx Experiment 1 at 42.7°S (a), Experiment 2 at 43.4°S (b) and SAFePool Experiment 3 at 44.9°S (c). Open red circles – LL-LFe replicates, open blue circles – LL-HFe replicates, filled red cirlces – HL-LFe replicates and filled blue circles – HL-HFe replicates

Noticeably different trends were observed in F_v/F_m results of the SOSCEx experiments than that observed in the SAFePool incubations. Values increased significantly throughout the incubation for the SOSCEx experiments whereas there were very slight increases seen in SAFePool results. F_v/F_m obtained at the end of incubations of both SOSCEx experiments exhibited an overall significant difference between treatments (Appendix A, Table 1 & 8). As observed in chl *a* results (Section 4.2.5) the HL-HFe treatment exhibited the highest increase in F_v/F_m for the SOSCEx experiments. In Experiment 1 F_v/F_m values of the samples incubated under HL conditions, with or without Fe addition, displayed a significant difference to the control sample at the end of incubation. The HL-HFe treatment displayed an exceptionally high increase of about tenfold the initial values, exhibiting a significant difference to the control sample ($P=0.008$, Appendix A, Table 4) and to the LL-HFe treatment ($P=0.099$, Appendix A, Table 4). Both HL treatments displayed a much larger increase than the two LL treatments, throughout the incubation experiment.

The F_v/F_m values in SOSCEx Experiment 2 also displayed an overall increase, throughout the experiment, as observed in Experiment 1 but there was however not as much of a separation between the four treatments. Both LL treatments and the HL-HFe treatment were significantly different to the HL-LFe treatment, which in Experiment 2 had the lowest values between the four treatments (Appendix A, Table 11). The HL-HFe treatment displayed an overall increase of four times the initial F_v/F_m values and exhibited the highest final values between treatments for Experiment 2 but was noticeably lower than the values obtained at the end of incubation for Experiment 1.

The rates of change per day of incubation in F_v/F_m (dimensionless) corresponding to Fe enrichment and light variability, of two SOSCEx incubation experiments and P values of regression are displayed in Table 4.5. Rates of change for both SOSCEx experiments were noticeably higher than observed in the SAFePool experiments due to definite positive slopes observed for F_v/F_m *vs.* days of incubation (Figure 4.13). High coefficients of determination were obtained for both experiments, indicating strong correlation in F_v/F_m over the length of incubation for the different treatments. All regression P values obtained were very low (<0.001), indicating a significance of rates.

Table 4.5 Rates of change in F_v/F_m per day of incubation (slopes of regressions, e.g. Figure 3.3). Coefficients of determination (R^2), P values of regression, initial and final values (dimensionless) of incubation for two SOSCEx experiments

Experiment	Latitude (°S)	Treatment	Average slope = Rate of change (.day^{-1})	R^2	P	T_0	T_{final}
SOSCEx 1	42.7	LL-LFe	0.136	0.77	**<0.001**	0.036	0.075
	42.7	LL-HFe	0.151	0.83	**<0.001**	0.036	0.088
	42.7	HL-LFe	0.236	0.80	**<0.001**	0.036	0.143
	42.7	HL-HFe	0.293	0.92	**<0.001**	0.036	0.204
SOSCEx 2	43.4	LL-LFe	0.253	0.95	**<0.001**	0.031	0.152
	43.4	LL-HFe	0.243	0.89	**<0.001**	0.031	0.155
	43.4	HL-LFe	0.206	0.73	**<0.001**	0.031	0.120
	43.4	HL-HFe	0.253	0.81	**<0.001**	0.031	0.161

In Experiment 1 the rates of change for the HL treatments were noticeably larger than for the LL treatments, indicating a steeper increase for HL treatments. No separation between treatments for Experiment 2 was observed, indicating relatively similar rates for all treatments. The addition of Fe and increase in irradiance displayed a clear positive impact on F_v/F_m of resident phytoplankton in the Experiment 1 sample, whereas no clear response is visible due to treatments in Experiment 2.

4.3.5 Functional absorption cross-section of PSII (σ_{PSII}) comparison across two SOSCEx experiments and SAFePool Experiment 3.

A response in σ_{PSII} (Å^2.quanta^{-1}) to Fe enrichment and light variability of two incubation experiments, conducted during the SOSCEx late summer cruise, is displayed in Figure 4.14. As seen for the F_v/F_m results of the SOSCEx experiments, the trend of the σ_{PSII} results was very different to that of the SAFePool results. In both incubations the separation between treatments was not very distinct. Experiment 1 did however have an overall significant difference between treatments at the end of incubation (Appendix A, Table 1) whereas Experiment 2 had no significant difference between treatments. The σ_{PSII} values for both experiments were similar in magnitude and an increase from the initial conditions was observed in both incubations.

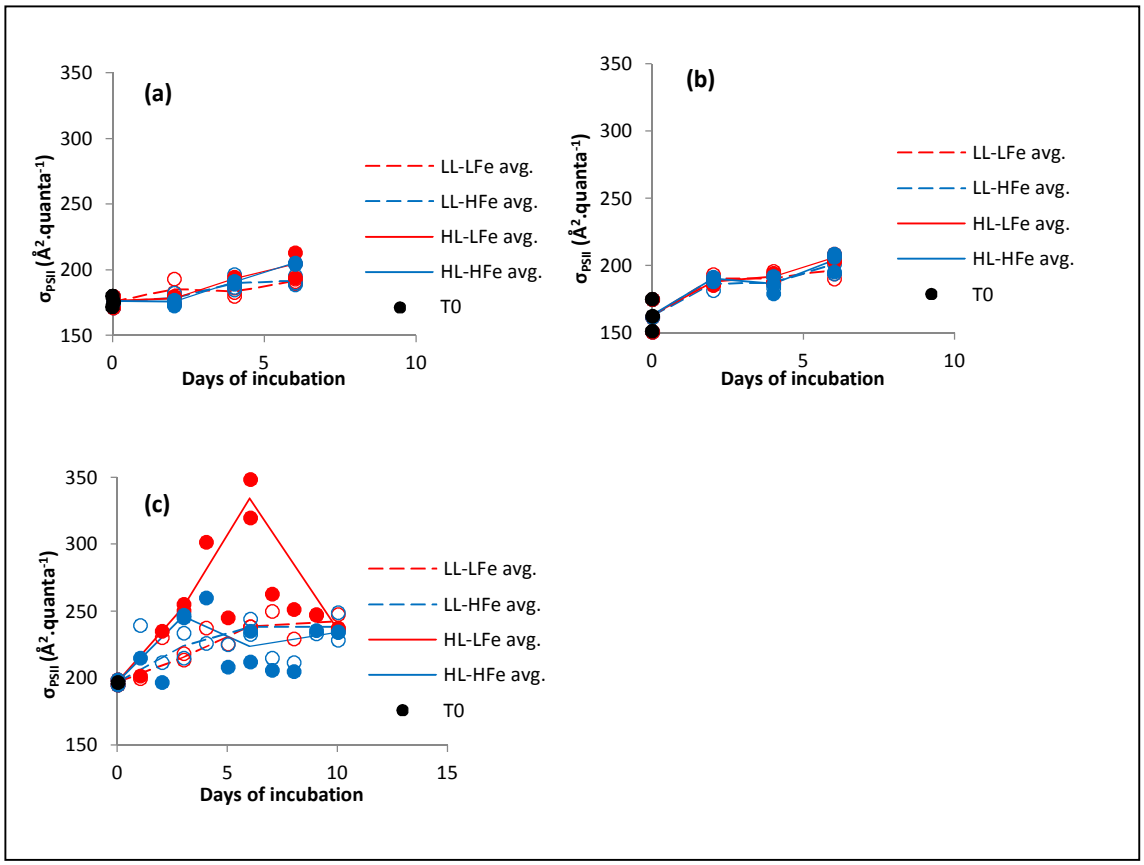

Figure 4.14 σ_{PSII} (Å^2.quanta^{-1}) *vs.* days of incubation of four treatments for SOSCEx Experiment 1 at 42.7°S (a), Experiment 2 at 43.4°S (b) and SAFePool Experiment 3 at 44.9°S (c). Open red circles – LL-LFe replicates, open blue circles – LL-HFe replicates, filled red cirlces – HL-LFe replicates and filled blue circles – HL-HFe replicates

In Experiment 1 a significant difference between treatments was observed at the end of incubation between LL and HL treatments, with or without the addition of Fe (Appendix A, Table 5). Both HL treatments exhibited a steeper increase in σ_{PSII}, of resident phytoplankton throughout the incubation, than that observed for the LL treatments but no impact was displayed for the addition of Fe under the two light conditions, indicating that light was the controlling factor for the σ_{PSII} of the phytoplankton in the Experiment 1 sample. In Experiment 2 a clear increase was observed from the initial condition. There was however no separation between the treatments. The trend observed for Experiment 2 was similar to the corresponding F_v/F_m results, with no visible response to Fe addition or irradiance increase displayed in σ_{PSII} results.

The rates of change per day of incubation in σ_{PSII} (Å^2.quanta^{-1}) corresponding to Fe enrichment and light variability, of two SOSCEx incubation experiments and P values of regression are displayed in Table 4.6. Rates of change were approximately tenfold lower than rates of change for F_v/F_m, but were similar in magnitude to rates obtained in the SAFePool experiments. Coefficients of determination obtained for both experiments

were relatively high when compared to SAFePool values, ranging from 0.56 to 0.84, indicating clear correlation between σ_{PSII} and length of incubation due to Fe enrichment and light variability. Exceptionally low P values were obtained for all samples (<0.01), indicating a high significance of rates of change, as observed for the F_v/F_m results of the SOSCEx experiments. The rates of change for HL treatments in Experiment 1 were noticeably larger than for LL treatments, whereas Experiment 2 displayed no distinct difference between the four treatments. The addition of light had a clear positive effect on σ_{PSII} of resident phytoplankton in the Experiment 1 sample, whereas no clear response was visible for treatments of Experiment 2.

Table 4.6 Rates of change in σ_{PSII} ($Å^2$.quanta^{-1}) per day of incubation (slopes of regressions, e.g. Figure 3.3). Coefficients of determination (R^2), P values of regression, initial and final values of incubation for two SOSCEx experiments

Experiment	Latitude (°S)	Treatment	Average slope = Rate of change (.day^{-1})	R^2	P	T_0 ($Å^2$.quanta^{-1})	T_{final} ($Å^2$.quanta^{-1})
SOSCEx 1	42.7	LL-LFe	0.012	0.56	**0.005**	176	192
	42.7	LL-HFe	0.016	0.70	**<0.001**	176	192
	42.7	HL-LFe	0.027	0.81	**<0.001**	176	204
	42.7	HL-HFe	0.028	0.84	**<0.001**	176	205
SOSCEx 2	43.4	LL-LFe	0.029	0.61	**0.002**	163	197
	43.4	LL-HFe	0.032	0.74	**<0.001**	163	201
	43.4	HL-LFe	0.036	0.82	**<0.001**	163	206
	43.4	HL-HFe	0.033	0.69	**<0.001**	163	204

4.3.6 Summary – temporal variability in photophysiological response

Photophysiology results for SOSCEx incubation experiments were very different to results obtained in SAFePool Experiment 3. A clear increase in F_v/F_m and σ_{PSII} was observed in both SOSCEx incubations, whereas a clear response was not observed in the SAFePool incubation. HL treatments had higher F_v/F_m and slightly larger σ_{PSII} than LL treatments, whereas the LL treatments displayed higher values in the SAFePool experiment. As observed for σ_{PSII} in SAFePool results, there was not much separation between treatments in the SOSCEx experiments. A clear positive response was observed for F_v/F_m of the HL-HFe treatments for both SOSCEx incubations.

4.4 Nutrient uptake

4.4.1 Spatial comparison during the SAFePool cruise - NO_3 + NO_2 uptake across three SAFePool experiments

A comparison of the NO_3 + NO_2 uptake rates between treatments against Fe enrichment and light variability, of three incubation experiments conducted across different water masses, during the SAFePool mid-summer cruise is displayed in Figure 4.15. Relatively low uptake rates were displayed across the three SAFePool incubation experiments, with the exception of the HL-HFe sample for Experiment 3, which had an uptake rate tenfold larger than the other treatments and experiments. The negative rate observed in the LL-LFe treatment of Experiment 3 and the LL-HFe treatment of Experiment 1 indicates release of nitrogen into the water from the phytoplankton during incubation.

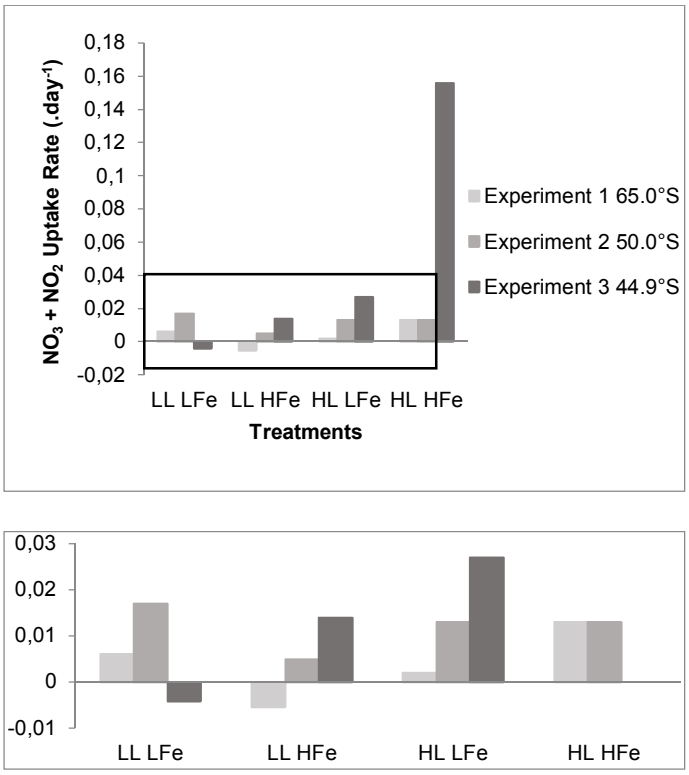

Figure 4.15 NO_3 + NO_2 rates of uptake (slopes of exponential functions) *vs.* treatments for three SAFePool experiments (top), an enlargement of outlined section, containing lower values (bottom) (detailed NO_3 + NO_2 uptake curves are shown in Appendix B)

When comparing N concentrations of treatments in the three experiments (Appendix B, Figure 4), a significant difference is observed at the end of incubations for Experiment 1 and 3, but not in Experiment 2. In Experiment 1 and 2 there is no clear trend in N uptake due to treatments, whereas in Experiment 3 the addition of Fe and increase of irradiance both had a positive impact on the rate of uptake. An overall significant difference is

observed for N uptake between treatments for Experiment 1 (P=0.094, Appendix A, Table 13), the results at the end of incubation displayed a significant difference between the LL-HFe and LL-LFe treatments, and between the LL-HFe and HL-HFe treatments (Appendix A, Table 20). In Experiment 3 an overall significant difference was also obtained between treatments (Appendix A, Table 30). A significant difference was obtained between the HL-HFe and the LL-LFe treatment (Appendix A, Table 35).

4.4.2 PO_4 uptake across three SAFePool experiments

A comparison of the PO_4 uptake rates between treatments against Fe enrichment and light variability, of three incubation experiments conducted across different water masses, during the SAFePool mid-summer cruise is displayed in Figure 4.16. As observed for the uptake of inorganic nitrogen, relatively low rates were also displayed for PO_4 uptake across the three SAFePool incubation experiments, with the exception of the HL-HFe treatment for Experiment 3, which had a PO_4 uptake rate tenfold larger than the other treatments and experiments. A negative rate was observed for the LL-HFe treatment of the Experiment 3 sample, indicating a release of P into the water from the phytoplankton but all other treatments displayed positive rates.

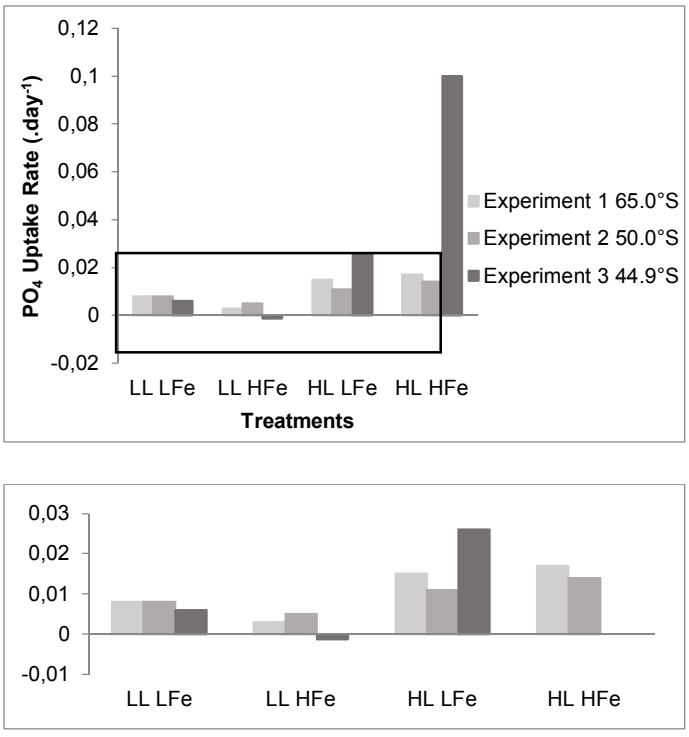

Figure 4.16 PO_4 rates of uptake (slopes of exponential functions) *vs.* treatments for three SAFePool experiments (top), an enlargement of outlined section, containing lower values (bottom) (detailed PO_4 uptake curves are shown in Appendix B)

A comparison of PO_4 concentrations between treatments in experiments (Appendix B, Figure 6) displayed a significant difference at the end of incubations for Experiment 1 and 3, but not for Experiment 2, as was observed for NO_3 uptake. No obvious trend in PO_4 uptake due to treatments was displayed across experiments. Incubation under HL conditions did however display an increase in the rate of uptake and the LL-HFe treatment displayed the lowest rates for all three experiments with a rate lower than that of the control samples. An overall significant difference was observed between treatments for Experiment 1 (Appendix A, Table 13), the results at the end of the incubation displayed a significant difference between the samples incubated under HL conditions, with or without Fe addition, and the LL-HFe treatment (Appendix A, Table 21). In Experiment 3 an overall significant difference was also obtained between treatments (Appendix A, Table 30). A significant difference was observed between the HL-HFe and the LL-LFe treatments (Appendix A, Table 35).

4.4.3 SiO_4 uptake across three SAFePool experiments

A comparison of the SiO_4 uptake rates between treatments against Fe enrichment and light variability, of three incubation experiments conducted across different water masses, during the SAFePool mid-summer cruise is displayed in Figure 4.17. SiO_4 uptake across the three SAFePool incubation experiments was within the same order of magnitude as NO_3 + NO_2 and PO_4 uptake rates, the response of SiO_4 uptake to treatments was however different between experiments. The uptake rates of SiO_4 for Experiment 1 were all low and very similar across the four treatments, with a small negative rate for the LL-HFe treament. In Experiment 2 the HL treatments had a larger uptake rate, with the highest being for the HL-HFe treatment. In Experiment 3 a negative rate, indicating a release of Si, was observed for all treatments except the HL-HFe treatment which exhibited the largest rate of SiO_4 uptake across experiments, approximately four times larger than the rest of the samples.

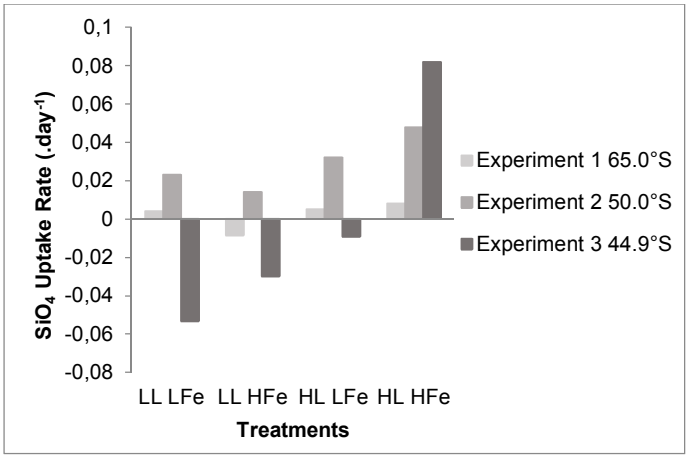

Figure 4.17 SiO_4 rates of uptake (slopes of exponential functions) *vs.* treatments for three SAFePool experiments (detailed SiO_4 uptake curves are shown in Appendix B)

A comparison of SiO_4 concentrations of treatments for the three experiments (Appendix B, Figure 8) displayed a significant difference between treatments at the end of incubation for Experiment 2 and 3, but not for Experiment 1. An overall significant difference was observed between treatments for Experiment 2 (Appendix A, Table 13). The results at the end of incubation displayed a significant difference between the samples incubated under HL conditions, with or without Fe addition, and the LL-HFe treatment. A significant difference was obtained between the LL-HFe and the HL-HFe treatment (P=0.007, Appendix A, Table 29). In Experiment 3 an overall significant difference between treatments was also obtained (Appendix A, Table 30). A significant difference was observed between the HL-HFe treatment and the control sample (Appendix A, Table 36).

4.4.4 Summary – spatial variability of nutrient uptake

Noticeable differences were observed in the concentrations of the three macronutrients analysed. In situ NO_3 + NO_2 and PO_4 concentrations increased across the three water masses sampled, from the SAZ to the AZ. In situ SiO_4 concentration was ~60 times higher in the AZ sample compared to the PFZ and SAZ samples. High NO_3 and low PO_4 concentrations were observed for all samples. SiO_4 was substantially higher in the AZ sample but, similar to PO_4, was low in PFZ and SAZ samples. The largest response in macronutrient uptake was displayed for the HL-HFe treatment of the Experiment 3 sample, which was expected due to relatively higher biomass growth observed in this sample. Relatively low nutrient uptake was observed in the other samples. Low SiO_4 uptake was displayed across treatments in Experiment 1 and a release in all treatments but the HL-HFe treatment for Experiment 3, whereas a positive uptake is displayed in all Experiment 2 treatments. The varied uptake of SiO_4 between incubation samples gives an indication of phytoplankton community variation across the three water masses sampled.

4.4.5 Temporal comparison during the SOSCEx and SAFePool cruises - NO_3 + NO_2 uptake across two SOSCEx experiments and SAFePool Experiment 3

A comparison of the NO_3 + NO_2 uptake rates between treatments against Fe enrichment and light variability, of two incubation experiments conducted during the SOSCEx late summer cruise and SAFePool Experiment 3, is displayed in Figure 4.18. Relatively low NO_3 + NO_2 uptake rates were displayed for both SOSCEx incubation experiments. A small negative rate was obtained for the control sample of Experiment 1 whereas all the other samples had positive rates, indicating NO_3 uptake. The LL-HFe treatment did not have a positive impact on the uptake of NO_3, whereas the HL-LFe and the HL-HFe treatments did display a noticeable positive impact. The largest uptake rate observed in both experiments, displaying a rate that was more than double the rate of uptake observed in the LL treatments, was obtained for the HL-HFe treatment, as observed for SAFePool Experiment 3.

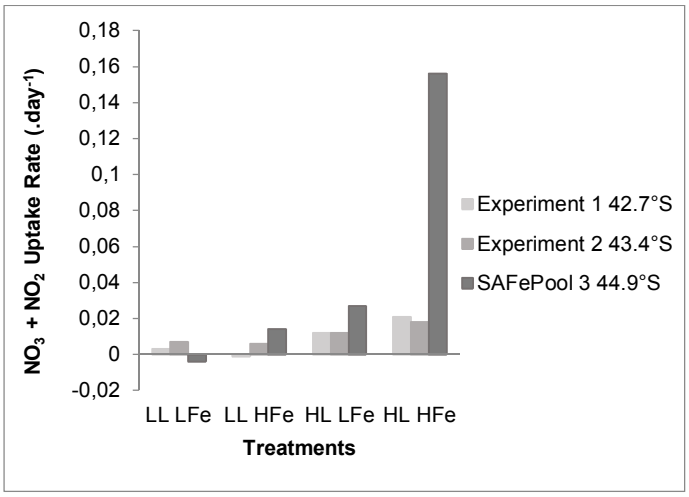

Figure 4.18 NO_3 + NO_2 rates of uptake (slopes of exponential functions) *vs.* treatments for two SOSCEx experiments and SAFePool Experiment 3 (detailed NO_3 + NO_2 uptake curves are shown in Appendix B)

When comparing NO_3 concentrations between treatments for the two SOSCEx incubation experiments (Appendix B, Figure 3), a significant difference is observed between treatments at the end of incubation for both Experiment 1 and 2 (Appendix A, Table 1 & 8). In both experiments the LL treatments were significantly different to the HL treatments, with or without Fe addition, with a significant difference observed between the LL-HFe treatment and the HL-HFe treatment for Experiment 1 ($P=0.007$, Appendix A, Table 6) and Experiment 2 ($P=0.003$, Appendix A, Table 12). NO_3 uptake was noticeably lower in SOSCEx experiments than observed in SAFePool Experiment 3, the response to Fe enrichment and light variability was however similar.

4.4.6 PO_4 uptake across two SOSCEx experiments and SAFePool Experiment 3

A comparison of the PO_4 uptake rates between treatments against Fe enrichment and light variability, of two incubation experiments conducted during the SOSCEx late summer cruise and SAFePool Experiment 3, is displayed in Figure 4.19. PO_4 uptake rates for Experiment 1 were noticeably higher than the rates observed for Experiment 2, showing no clear response to treatments. In Experiment 1 the LL-LFe treatment had the largest rate of uptake, both HL treatments displayed similar rates and the LL-HFe treatment displayed the lowest rate. When comparing the PO_4 concentrations of treatments for the two SOSCEx incubation experiments (Appendix B, Figure 5). A significant difference was displayed between the LL-HFe and LL-LFe treatments and the LL-HFe and HL-HFe treatments (Appendix A, Table 7). No significant difference was displayed between treatments for Experiment 2. PO_4 uptake in SOSCEx experiments was within the same order of magnitude as observed in SAFePool Experiment 3, the response to Fe enrichment and light variability was however very different showing no clear response to treatments for both SOSCEx incubation experiments.

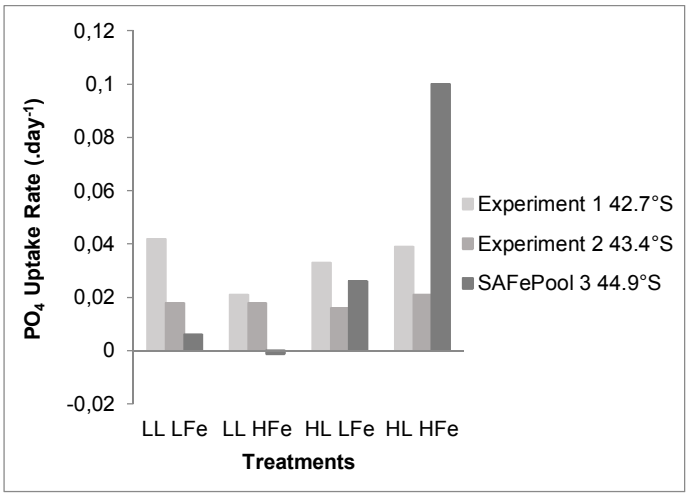

Figure 4.19 PO_4 rates of uptake (slopes of exponential functions) *vs.* treatments for two SOSCEx experiments and SAFePool Experiment 3 (detailed PO_4 uptake curves are shown in Appendix B)

4.4.7 SiO_4 uptake across two SOSCEx experiments and SAFePool Experiment 3

A comparison of the SiO_4 uptake rates between treatments against Fe enrichment and light variability, of two incubation experiments conducted during the SOSCEx late summer cruise and SAFePool Experiment 3, is displayed in Figure 4.20. No significant differences were obtained between treatments for both SOSCEx incubation experiments. The rates for both SOSCEx experiments were negative, indicating a release of Si into the water from the resident phytoplankton. The rates of release of Si

were noticeably larger in Experiment 2 than the rates observed for Experiment 1, with no variation due to treatments. The release of Si into the water could be due to the dying of diatoms as the experiments were conducted at the end of the summer bloom. The release of Si in the SOSCEx experiments did not resemble the results obtained in SAFePool Experiment 3. A definite response to treatments was observed in the SAFePool experiment, displaying a relatively large SiO_4 uptake for the HL-HFe treatment.

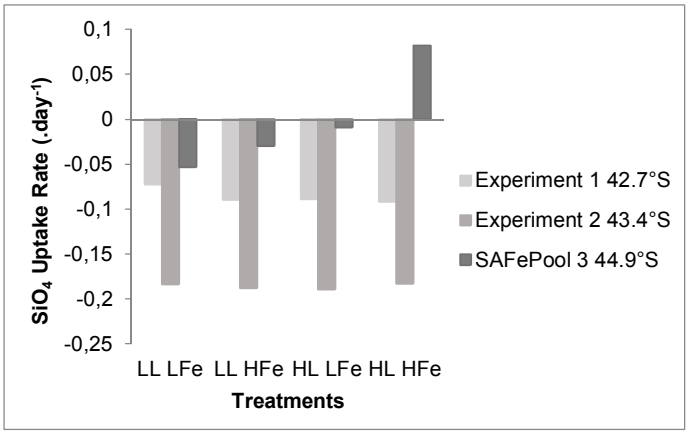

Figure 4.20 SiO_4 rates of uptake (slopes of exponential functions) *vs.* treatments for two SOSCEx experiments and SAFePool Experiment 3 (detailed SiO_4 uptake curves are shown in Appendix B)

4.4.8 Summary – temporal differences in nutrient uptake

In situ NO_3 + NO_2 concentrations for the SOSCEx samples were similar to the SAFePool Experiment 3 sample, there was however a clear response to treatments in uptake for the SOSCEx incubations which was not as noticeable in the SAFePool incubation. HL treatments displayed a larger uptake than observed for the LL treatments, in both incubations, with the HL-HFe treatment exhibiting the largest uptake as was displayed in the SAFePool incubation. In situ PO_4 concentrations were also similar to the SAFePool incubation, Experiment 3, with a clear uptake for all treatments but no clear response to treatments. SOSCEx SiO_4 results, from late summer, were noticeably different to results obtained for SAFePool during mid-summer. In situ SiO_4 concentrations were much lower and no uptake, but rather a release of SiO_4, was displayed in both SOSCEx incubations.

5. Discussion

5.1 Biomass

5.1.1 SAFePool incubations – Spatial comparison

The largest increase in biomass in this study was observed for the increase of chl *a*, for the combined addition of Fe and increase in irradiance (Figure 4.3). This suggests that the phytoplankton, across the three water masses sampled, were limited in both Fe and light, which is consistent with previous studies done across the SO (Boyd *et al.* 1999, 2001, 2010; Feng *et al.* 2010; Hutchins *et al.* 2001, Moore *et al.* 2007; Sosik & Olson 2002). Interactions between Fe and light availability have been shown to influence phytoplankton growth in many other experiments in the SO. Varying levels of limitation are reported as controlling phytoplankton blooms throughout the year, as well as possible Si limitation during summer (Boyd *et al.* 1999, 2001, 2010; Moore *et al.* 2007).

Due to a lack of pigment analysis, community structure determination was not possible. It can however be assumed, based on literature, that diatoms and *P. antarctica* were dominant in the water masses sampled (Alvain *et al.* 2011; Boyd *et al.* 2010; Feng *et al.* 2010) and the response observed due to Fe addition and increases in irradiance, which are characteristic of these phytoplankton groups (Boyd *et al.* 1999, 2001; Feng *et al.* 2010). Based on literature, it is suggested that *P. antarctica* is the dominant species in the sample taken in the AZ (Feng *et al.* 2010). The resident phytoplankton in the AZ sample displayed a stronger response to an increase of irradiance than phytoplankton present in PFZ and SAZ samples (Figure 4.3), possibly due to the higher abundance of *P. antarctica* relative to diatoms in this sample and the better photorecovery ability of *P. antarctica* (Feng *et al.* 2010).

Generally low Chl *a* concentrations (<1µg/L), similar to initial values obtained in this study, are found in these HNLC regions, during summer. Biomass growth is restricted across the majority of the SO due to the intricate web of limiting factors (Boyd *et al.* 1999; Feng *et al.* 2010). The larger response of chl *a* concentrations compared to POC concentrations probably indicates an increase in cellular chl *a* rather than an increase in net growth (Hopkinson *et al.* 2007; Moore *et al.* 2007). The larger increase in chl *a*/POC observed for Fe enrichment and irradiance increase is consistent with cells going from growing under limitation to being relieved of the limitation (Table 4.1) (Berg *et al.* 2011).

The addition of Fe did not have a significant fertilisation effect under LL conditions, which could be an indication that light limitation was the controlling factor and therefore resident phytoplankton were not able to take up available Fe. The samples taken from the SAZ

and PFZ displayed the largest response in chl *a*-derived growth to Fe enrichment under HL conditions, indicative of high diatom abundance due to diatoms being more responsive to Fe addition than is seen for *P. antarctica* (Figure 4.3 (d)) (Feng *et al.* 2010, Hopkinson *et al.* 2007). An increase in irradiance without Fe addition exhibited a slight response in chl *a* in the SAZ and AZ samples. This was however not observed for the PFZ sample, possibly due to stronger Fe limitation in this sample. Combined Fe and light addition appears to be the factors that promote chl *a* increase in the SAFePool incubations.

POC increased due to an increase in irradiance rather than Fe addition across all three experiments, with only the SAZ sample displaying a noticeable response to the HL-HFe treatment (Appendix B, Figure 2). The response in carbon fixation to higher irradiance is to be expected due to the high energy requirement of carbon fixation via the C-B cycle (Bentaleb *et al.* 1998; Falkowski & Raven 2007). A noticeable increase in cell size is observed in incubations with Fe addition and a significantly large response in relative cell abundance due to an increase in irradiance (Figure 4.5 & 4.6). A varied response to Fe addition can be a consequence of different species of phytoplankton and thereby differing degrees of limitation, an increase in larger cells is consistent with previous studies reporting the largest response of diatoms to Fe addition (Hopkinson *et al.* 2007).

Light availability has been shown to be a significant controlling factor in other regions of the SO, playing a significant role in the relative abundance of species (Feng *et al.* 2010) and Fe has been shown to be the limiting nutrient in the Antarctic Circumpolar Current, ultimately restricting phytoplankton growth, in the absence of other limiting factors (Hopkinson *et al.* 2007). Relatively low Si concentrations were detected at the SAZ and PFZ sampling sites (Figure 4.2). Under possible Si limitation in these regions during summer (Klunder *et al.* 2011), the addition of Fe and increased irradiance would lead to an increase in small, lightly silicified diatoms and nonsiliceous pico and nanophytoplankton, therefore creating a shift in community structure (Hutchins *et al.* 2001).

5.1.2 SOSCEx and SAFePool 3 incubations – Temporal comparison of responses observed in the SAZ

Chl *a* and POC concentrations were significantly lower in the SOSCEx incubations than the SAFePool Experiment 3 incubation, which is to be expected due to the SOSCEx experiments being conducted at the end of summer (Figure 4.7), at the later stage of bloom decline, when phytoplankton is assumed to be more limited by Fe, light and Si (Hutchins *et al.* 2001; Moore *et al.* 2007). Decreased cellular chl *a* is characteristic of a

Fe limited system (Hopkinson *et al.* 2007). A higher response in chl *a* compared to POC is indicative of an increase in chl *a*/POC as seen in the mid-summer SAFePool experiment for cells going from nutrient limitation to relief of that limitation after Fe addition and increase in irradiance (Berg *et al.* 2011). A low response with regard to chl *a*/POC was observed for LL treatments, consistent with other experiments in other regions of the SO (Table 4.2) (Feng *et al.* 2010).

It is suggested that Si availability plays a large role in biomass accumulation in the SAZ and can be a limiting factor in the SOSCEx experiments. Despite extremely low SiO_4 concentrations in the SAZ it has been shown that small, lightly silicified diatoms can grow after Fe addition, making use of the Fe to take up the maximum amount of Si available (Hutchins *et al.* 2001). Initial Si concentrations at the SOSCEx sampling sites were <1µM (Figure 4.1). These levels are considered limiting and the community structure is expected to move toward nonsiliceous pico and nanoplankton and small diatoms capable of surviving under low Si and Fe conditions, later in the season. This response is expected for Fe addition to a low Si environment (Hutchins *et al.* 2001). Due to no increase in larger cells, as seen in SAFePool experiments the assumption can be made that chl *a* and POC increases were due to an increase in small cells and the release of Si possibly indicates growth of nonsiliceous plankton rather than diatoms (Figure 4.9 & 4.10).

Increased biomass has been observed for the addition of Fe under HL conditions during bloom decline. Fe limitation has been shown to be evident during early and late stages of bloom decline (Moore *et al.* 2007). As observed in SAFePool, the largest response in chl *a* was obtained for the addition of Fe under HL conditions which was possibly due to diatom abundance (Figure 4.7) (Feng *et al.* 2010). POC concentrations were not significantly impacted by the addition of Fe under LL or HL conditions, possibly due to lower irradiance availability later in the season (Appendix B, Figure 1) (Bentaleb *et al.* 1998; Falkowski & Raven 2007). A low response to Fe addition under LL was also obtained for both chl *a* and POC in SOSCEx experiments. A significantly larger response for Fe addition under HL was observed in SOSCEx Experiment 2 than in Experiment 1, which was also observed in the SAFePool incubation. A clear response to treatments was displayed for chl *a* but was not observed for POC. A large response to an increase in irradiance was observed in cell counts for both experiments, as seen in SAFePool, the addition of Fe also displayed an increase in cell size in Experiment 2 as seen in SAFePool experiments, which was not visible in Experiment 1, possibly due to higher Fe limitation in Experiment 2 (Hopkinson *et al.* 2007). The difference in response between the two SOSCEx experiments is not fully understood, possible contamination

could have played a role. It can be assumed that different degrees of Si limitation between the SOSCEx and SAFePool experiments could have influenced results due to SOSCEx experiments being conducted at a later stage of bloom decline (Boyd *et al.* 2001; Hutchins *et al.* 2001, Moore *et al.* 2007).

5.2 Photophysiology

5.2.1 SAFePool incubations – Spatial comparison

Active fluorescence has been used and has been reported to be an accurate method for the determination of Fe stress, along with genetics analyses, in many SO experiments. Generally, an increase in F_v/F_m has been reported for Fe addition and an increase in irradiance, in response to relief of Fe and light stress, of SO phytoplankton photosynthetic apparatus (Berg *et al.* 2011; Boyd *et al.* 1999; Boyd & Abraham 2001; Feng *et al.* 2010; Hopkinson *et al.* 2007; Moore *et al.* 2007). Supraoptimal irradiance has however shown to induce photoinhibition, in incubation experiments as well as in situ experiments when LL adapted phytoplankton is brought up to the surface by mixing, thereby decreasing photosynthetic efficiency (Boyd & Abraham 2001; Feng *et al.* 2010). Temperature has also been reported to affect the response of phytoplankton to Fe addition, seeing a slower response in lower temperature waters but the relationship is not yet fully understood. (Boyd & Abraham 2001).

The most significant change in F_v/F_m of this study was observed in the sample from the SAZ increasing from ~0.3 to 0.5 (dimensionless) after 3 days of incubation under LL, with or without Fe addition and under HL with Fe addition. F_v/F_m increased for the first three days of incubation and then plateaued out for LL treatments. Initial F_v/F_m values of ~0.3-0.5 (dimensionless) for the three sampling sites were not extremely low indicating that phytoplankton were not severely limited (Figure 4.11). There was not a large response observed for the addition of Fe alone, as observed in many shipboard and in situ Fe enrichment experiments (Berg *et al.* 2011; Boyd & Abraham 2001; Browning *et al.* 2014; Feng *et al.* 2010, Hopkinson *et al.* 2007; Moore *et al.* 2007). Fe enriched samples for SAFePool experiments 2 and 3 did however have slightly higher F_v/F_m values than the controls under both HL and LL conditions.

Samples incubated under HL conditions exhibited lower photosynthetic efficiencies than those incubated under LL conditions in all three experiments (Table 4.3), which is consistent with previous studies indicating that photoinhibition limits photosynthetic efficiency of SO phytoplankton (Boyd & Abraham 2001; Boyd *et al.* 2001; Feng *et al.* 2010; Moore *et al.* 2007). Final F_v/F_m values of LL treatments displayed an overall increase and HL treatments showed an overall decrease in photosynthetic efficiency.

Samples incubated under HL conditions without Fe enrichment displayed a steeper decrease in photosynthetic efficiency indicative of increased Fe stress due to depletion of already low available Fe.

No noticeable change was displayed for σ_{PSII} of phytoplankton in incubated samples from the PFZ and AZ but a slight increase was seen in the SAZ sample (Table 4.4). No separation between treatments was however displayed, therefore displaying no significant response to treatments contrary to previous studies that have reported a decrease in σ_{PSII} upon Fe enrichment (Figure 4.12) (Boyd & Abraham 2001; Hopkinson *et al.* 2007; Moore *et al.* 2007).

5.2.2 SOSCEx incubations – Temporal comparison of responses observed in the SAZ

The most apparent difference between the SOSCEx and SAFePool photophysiology is that in the SOSCEx experiments a large increase was seen for both F_v/F_m and σ_{PSII}, throughout the incubation (Figure 4.13), which can be assumed to be indicative of phytoplankton being severely limited prior to incubation and therefore exhibiting a greater response to relief of the limitation by repairing of non-functional PSII reaction centres (Moore *et al.* 2007). The increases observed in control samples could be due to possible contamination or bottle effects, causing phytoplankton to acclimatise to their new environment. Stronger limitation is to be expected for the time in the season that the experiment was conducted and, as stated previously, Fe, Si and light limitation are presumed to be the controlling factors of the in situ phytoplankton community at this time (Boyd *et al.* 2001, 2010).

Contrary to what was observed in SAFePool, HL treatments in SOSCEx Experiment 1 had higher F_v/F_m and a slightly larger σ_{PSII}, than the LL treatments, indicating that the HL conditions did not cause photoinhibition although light levels were set higher for SOSCEx incubations. This difference in response to the different light levels can be due to a difference in the light history of the in situ phytoplankton, as has been suggested before, that F_v/F_m response can be affected by what the phytoplankton were previously exposed to (Boyd & Abraham 2001). Fe addition under HL conditions in SOSCEx Experiment 1 did show a larger response in F_v/F_m which could be a response to greater Fe stress relief than what was seen in the SAFePool experiment, as a greater Fe limitation is expected at the later stage of bloom decline (Boyd *et al.* 2010). As observed for σ_{PSII} in SAFePool results, there was not much separation between treatments in the SOSCEx results either, indicating no acclimation to treatments (Figure 4.14).

An immediate and rapid response of PSII parameters has been seen in many studies, reaching maximum F_v/F_m quite rapidly (Boyd & Abraham 2001; Boyd *et al.* 1999; Feng *et al.* 2010; Hopkinson *et al.* 2007). F_v/F_m for the SOSCEx incubations did however increase throughout the experiments and due to the shorter duration of the experiments a maximum point was not reached (Table 4.5). Slower responses have been reported in the SO due to low temperature and deep MLDs (Boyd & Abraham 2001; Olson *et al.* 2000). A decrease in F_v/F_m after maximum values are reached due to a return of Fe stress, as seen in previous studies (Boyd *et al.* 1999; Feng *et al.* 2010; Hopkinson *et al.* 2007) and the SAFePool incubations, was not observed in the SOSCEx experiments.

A shift in community due to Fe and Si stress during late summer (Sosik & Olson 2002) will cause a variation in F_v/F_m and σ_{PSII} signals when compared to earlier stages of the season due to the change of dominant species (Behrenfeld & Milligan 2013; Moore *et al.* 2007). Results obtained indicate that this is a possible scenario in the SOSCEx incubations.

5.3 Nutrient uptake

5.3.1 SAFePool incubations – Spatial comparison

In line with the description given to the SO as HNLC, macronutrients are not considered limiting south of the Subtropical Front. Si is however considered a limiting nutrient in the SAZ and PFZ during bloom decline due to high diatom abundance, which was a possible third control in this study (Bentaleb *et al.* 1998; Boyd *et al.* 1999, 2001, 2010; Hutchins *et al.* 2001). Macronutrient concentrations tend to increase with increasing latitude, based on previous studies, which was also observed in this study. PO_4 is considered to be of low significance to phytoplankton growth in the SO and is therefore also considered to be in excess throughout the season (Boyd *et al.* 2010; Klunder *et al.* 2011; Le Moigne *et al.* 2013). The nutrient profiles at sampling sites are similar to previously reported values for water masses sampled (Figure 4.2).

Although NO_3 is not a limiting nutrient in the SO, phytoplankton can become NO_3 stressed under severe Fe limitation, due to Fe being a cofactor in NO_3 and NO_2 reductase enzymes, thereby indirectly causing N stress. As seen in previous studies, Fe concentrations and NO_3 drawdown are intrinsically linked in HNLC waters (Berg *et al.* 2011; Browning *et al.* 2014). NO_3 and NO_2 reductase enzymes cannot be replaced by a non-Fe containing enzyme, as seen in the light harvesting components of phytoplankton, and therefore Fe limitation will negatively impact NO_3 assimilation. The addition of Fe for the relief of indirect NO_3 stress is community specific, as NO_3 uptake mechanisms differ across phytoplankton, and it has been reported that diatoms in particular benefit from

this (Berg *et al.* 2011; Hopkinson *et al.* 2007). Under HL conditions an enhanced NO_3 uptake is observed in the SAZ and PFZ samples but was not observed for the AZ sample (Figure 4.15), possibly due to the AZ sample being dominated by *P. antarctica* relative to diatoms (Schoemann *et al.* 2005). The release of NO_3 observed in the control sample from the SAZ and for the LL-HFe treatment of the AZ sample is indicative of possible cellular membrane loss which can result from cells experiencing Fe limitation and therefore indirect NO_3 limitation (Agustï & Sanchez 2002; Timmermans *et al.* 2007).

The largest macronutrient uptake was displayed for the HL-HFe treatment, of the SAZ incubation sample, which was expected due to high biomass accumulation observed in this sample. The uptake of SiO_4 in this sample indicates that upon the relief of both Fe and light stress diatom growth increased substantially, possibly causing a shift in community structure (Hutchins *et al.* 2001). The release of Si in the SAZ sample, under the other treatments, can be due to diatoms dying in the stressed environment (Figure 4.17). It has been reported that in a Fe limited environment the dissolution of less silicified, Fe limited diatoms is observed (Bucciarelli *et al.* 2010). The Si cycle is primarily controlled by diatom blooms and has been shown to be antagonistically linked to Fe (Boyd *et al.* 2010). It has been observed that Fe limited diatoms take up higher amounts of Si, becoming more silicified than Fe replete diatoms (Boyd *et al.* 1999; Brzezinski *et al.* 2002; Hopkinson *et al.* 2007). It has however also been reported that Fe and light co-limitation or light limitation alone can be the cause of increased silicification of oceanic diatoms (Bucciarelli *et al.* 2010). Low SiO_4 uptake is displayed across all treatments in the AZ sample and due to high concentrations seen in this area (Figure 4.2) it can be assumed that diatoms did not dominate and is probably low in the phytoplankton community relative to *P. antarctica*. The SiO_4 uptake seen in all the PFZ sample treatments indicates that diatoms are probably dominant in this area and a possible extension of bloom due to recycling and balanced nutrient limited growth (Moore *et al.* 2008). The varied uptake of SiO_4 across the three samples gives a good indication of phytoplankton community variation in the absence of taxonomic analyses.

Nutrient uptake varied quite largely across the three water masses sampled. These large differences can be due to a variation in degrees of limitation as well as phytoplankton community structure (Boyd *et al.* 2001; Hutchins *et al.* 2001; Moore *et al.* 2007). Other environmental controls such as temperature can also have a large impact on growth and therefore nutrient uptake which is evident in the fact that growth increased with decreasing latitude and increasing temperature (Browning *et al.* 2014). The combined relief of Fe and light limitation has been reported to have significant interactive effects

on nutrient uptake, which has been observed in this study (Feng *et al.* 2010; Hutchins *et al.* 2001).

5.3.2 SOSCEx incubations – Temporal comparison of responses observed in the SAZ

In March SA waters are probably more characteristic of HNLSiLC, which can be seen in this study as has been observed before (Boyd *et al.* 2001). In situ NO_3 and PO_4 concentrations for SOSCEx samples were similar to concentrations observed for SAFePool Experiment 3 therefore indicating that no limitation of these nutrients was evident at the later stage of bloom decline during the SOSCEx experiments (Figure 4.1). Si was however much lower in the SOSCEx incubations as expected and can be considered a significant limiting factor (Boyd *et al.* 2010). The in situ SiO_4 concentrations are indicative of late summer waters of a once diatom dominated bloom area such as the SAZ, where most Si is taken up throughout the season (Boyd *et al.* 1999, 2001). Si is reported to be a significant control of growth and species composition in these waters (Hutchins *et al.* 2001).

NO_3 uptake was increased by the addition of Fe and increase of irradiance, indicating stress relief of phytoplankton and more efficient NO_3 assimilation (Figure 4.18). It is expected that NO_3 uptake be most influenced by Fe and light addition due to the significance of Fe in NO_3 assimilation as mentioned before (Berg *et al.* 2011, Hopkinson *et al.* 2007). The largest uptake was also seen for the combined relief of Fe and light stress as seen in the SAFePool experiment, indicating the same interactive effects of Fe and light previously reported (Feng *et al.* 2010). No specific response to treatments was seen in the uptake of PO_4 (Figure 4.19) and a significant release of Si was observed for both SOSCEx experiments (Figure 4.20). The high release of Si observed in the SOSCEx incubations is expected due to the significant Si limitation expected at the time of experiments and due to phytoplankton community shift away from diatom dominance upon Fe and light addition (Hutchins *et al.* 2001). The dissolution of large, less silicified diatoms is expected in the Fe limited SA waters at the end of bloom and can explain the high release of Si (Bucciarelli *et al.* 2010). The lack of SiO_4 uptake gave a definite indication that the diatom abundance observed during SAFePool was not present in the SOSCEx samples.

5.4 Discussion summary

The highest increases in biomass accumulation and nutrient uptake were observed for the combined addition of Fe and light, therefore the systems are characteristic of both Fe and light limitation, across three water masses sampled during SAFePool as well as during SOSCEx. The largest response, by far, was observed in the SAZ samples incubated under the HL-HFe treatment, which was expected due to higher biomass in this region and the possible influence of increased temperature. Increases in cellular chl *a* rather than net growth were observed during both early and late stages of bloom decline in response to relief of limitation and an increase of larger cells was observed for Fe addition under both HL and LL conditions in the PFZ and SAZ samples. An overall low response was seen for all LL treatments, indicating the significance of light availability to SO phytoplankton.

NO_3 and PO_4 were not considered limiting in all experiments. Si can however be considered limiting in the SAZ and PFZ samples during SAFePool, and even more so during the SOSCEx experiments. Si limitation is therefore considered to be a significant controlling factor throughout both cruises, north of the Polar Front. Varying degrees of Fe and light limitation were observed across water masses. A larger response to light was observed in the AZ, with or without Fe addition, and a response to both Fe and light interactively, with possible Si limitation for the SAZ and PFZ samples, all influencing growth and nutrient uptake.

Based on literature, it is assumed that diatoms dominated in the SAZ and PFZ samples, whereas *P. antarctica* dominated in the AZ sample. The combined addition of Fe and light is considered to be highly beneficial to diatoms although Si availability is limited. Lower SiO_4 concentrations and biomass during March were characteristic of bloom end and SiO_4 release seen in samples from both SAFePool and SOSCEx is assumed to be due to dying of diatoms under limiting conditions. A possible community shift is expected due to increased limitation at the end of a bloom, either toward or away from diatom dominance, based on Fe and Si availability. Varying nutrient uptake and biomass accumulation can be assumed to be due to community structure and varying limitations across water masses sampled as well as seasonality of limiting factors. Si availability is assumed to be a significant control for both growth and community structure.

F_v/F_m of the SAZ sample increased in all but the HL-LFe treatment up to a threshold of ~0.5. This threshold was seen in all samples. F_v/F_m of phytoplankton was lower in HL treatments than LL treatments and it is assumed to be due to photoinhibition of LL adapted SO phytoplankton. Initial F_v/F_m was not severely low during the SAFePool cruise

and increases seen for Fe addition were not drastic but phytoplankton did respond to Fe addition under HL and LL conditions in the PFZ and SAZ samples. The decrease seen for F_v/F_m in HL treatments toward the end of the incubation indicates re-establishment of Fe stress. σ_{PSII} for SAFePool incubations did not have a noticeable response to treatments and remained relatively unchanged with only a slight increase seen in the SAZ sample. F_v/F_m and σ_{PSII} in SOSCEx incubations did increase significantly throughout the incubations and it is assumed that due to more severe limitation, this response is due to repairing of reaction centres upon stress relief. No photoinhibition was observed in SOSCEx samples, both F_v/F_m and σ_{PSII} were higher in HL treatments, the addition of Fe and light led to a clear increase in F_v/F_m.

6. Conclusion

During this study it has been observed that variations in Fe and light availability significantly impact the photosynthetic efficiency and growth of phytoplankton within the Atlantic sector of the SO, as has been observed in previous studies and other areas of the SO. An increase in chl *a* and POC was observed for amendments in both Fe and light, indicating increased growth due to stress relief. Photosynthetic efficiency is positively influenced by the addition of Fe and light. Supraoptimal light levels do, however, negatively impact the resident phytoplankton photophysiology, causing photoinhibition. Response of resident phytoplankton has been observed to vary considerably due to spatial and temporal variation within the SO, possibly due to varying degrees of limitation and variations in community structure. Other limiting factors are possibly present and therefore can be an influence to the response of phytoplankton, specifically Si in SA waters and possibly temperature in polar waters. The combined addition of Fe and light has by far shown the largest response in biomass accumulation and nutrient uptake, therefore it can be assumed that through the relief of Fe and light co-limitation the biogeochemical cycles within the SO will be significantly influenced and an increase in CO_2 drawdown is expected by increased phytoplankton growth.

Both hypotheses set out to be tested have been validated by our study. Changes in photosynthetic apparatus, as a result of variations in Fe and light availability, led to changes in the photosynthetic efficiency and growth of phytoplankton growth in the SO samples, thereby it can be assumed that biogeochemical cycles within the SO would be affected. Variability was observed in response to Fe and light amendments due to spatial and temporal variation in resident phytoplankton communities.

Shipboard incubations are however flawed due to in situ conditions not being accurately recreated, giving unrealistic results of the whole system. Possible loss of phytoplankton during incubation experiments can alter results, resulting in a possible reduction in photosynthetic results, as well as uncertainty in reproducing the in situ light environment of phytoplankton (Falkowski & Raven 2007). Bottle effects largely influence response as well as the exclusion of grazing and sinking, therefore biomass accumulation increase can be significantly overestimated (Hopkinson *et al.* 2007). These factors could have affected our results and thereby created a limitation to extrapolating our findings to the field.

Recommendations

I recommend that to improve understanding of the results obtained during this study phytoplankton community characterisation analyses be done, such as pigment analysis and flow cytometry. To determine initial Fe limitation, uptake by resident phytoplankton and Fe:C ratios, dissolved Fe analysis should be done. Genetics analysis will also be beneficial to determine Fe limitation and relief of Fe limitation within incubated samples. An increase in replicates of incubated samples will be beneficial to statistical power of results, if logistically possible.

References

Agustï, S., and Sanchez, M.C., 2002, 'Cell viability in natural phytoplankton communities quantified by a membrane permeability probe', Limnology and Oceanography, 47, 818–828, doi:10.4319/lo.2002.47.3.0818.

Alvain, S., Duforêt-Gaurier, L. and Loisel, H., 2011, 'Observation of ocean colour beyond chlorophyll-a', in Handbook of Satellite Remote Sensing Image Interpretation: Applications for Marine Living Resources Conservation and Management, viewed 14 July 2015, from http://www.ioccg.org/handbook/casestudy5_alvain_etal.pdf

Alvain, S., Moulin, C., Dandonneau, Y. and Loisel, H., 2008, 'Seasonal distribution and succession of dominant phytoplankton groups in the global ocean: A satellite view', Global Biogeochemical Cycles, 22, GB3001, doi:10.1029/2007GB003154.

Beckman Coulter, 2010, 'Multisizer™ 4 particle analyzer user's manual', PN A51387AB, Brea, CA, USA.

Behrenfeld, M.J. and Milligan, A.J., 2013, 'Photophysiological expressions of iron stress in phytoplankton', Annual Review of Marine Science, 5, 217–246.

Bentaleb, I., Fontugne, M., Descolas-Gros, C., Girardin, C., Mariotti, A., Pierre, C., Brunet, C. and Poisson, A., 1998, 'Carbon isotopic fractionation by plankton in the Southern Indian Ocean: relationship between δ13C of particulate organic carbon and dissolved carbon dioxide', Journal of Marine Systems, 17, 39–58.

Berg, G.M., Mills, M.M., Long, M.C., Bellerby, R., Strass, V., Savoye, N., Röttgers, R., Croot, P.L., Webb, A. and Arrigo, K.R., 2011, 'Variation in particulate C and N isotope composition following iron fertilization in two successive phytoplankton communities in the Southern Ocean', Global Biogeochemical Cycles 25, GB3013, doi:10.1029/2010GB003824.

Boyd, P., LaRoche, J., Gall, M., Frew, R. and McKay, M.L., 1999, 'Role of iron, light and silicate in controlling algal biomass in subantarctic waters SE of New Zealand', Journal of Geophysical Research, 104(C6), 13,395-13,408.

Boyd, P.W. and Abraham, E.R., 2001, 'Iron-mediated changes in phytoplankton photosynthetic competence during SOIREE', Deep-Sea Research II 48, 2529-2550.

Boyd, P.W., Crossley, A.C., DiTullio, R.G., Griffiths, F.B., Hutchins, D.A., Queguiner, B. Sedwick, P.N. and Trull, T.W., 2001, Control of phytoplankton growth by iron supply

and irradiance in the subantarctic Southern Ocean: Experimental results from the SAZ Project', Journal of Geophysical Research, 106(C12), 31,573-31,583.

Boyd, P.W., Strzepek, R., Fu, F. and Hutchins, D.A., 2010, 'Environmental control of open-ocean phytoplankton groups: Now and in the future', Limnology Oceanography, 55(3), 1353–1376.

British Antarctica Survey, n.d., 'The marine environment', in Discovering Antarctica, viewed 14 July 2015, from http://www.discoveringantarctica.org.uk/alevel_3_3.html

Browning, T.J., Bouman, H.A., Moore, C.M., Schlosser, C., Tarran, G.A., Woodward, E.M.S. and Henderson, G.M., 2014, 'Nutrient regimes control phytoplankton ecophysiology in the South Atlantic', Biogeosciences, 11, 463-479.

Brzenzski, M.A., Pride, C.J., Franck, V.M., Sigman, D.M., Sarmiento, J.L., Matsumoto, K., Gruber, N., Rau, G.H. and Coale, K.H., 2002, 'A switch from $Si(OH)_4$ to NO_3^- depletion in the glacial Southern Ocean', Geophysical Research Letters, 29(12), 10.1029/2001GL014349.

Bucciarelli, E., Pondaven, P. and Sarthou, G., 2010, 'Effects of an iron-light co-limitation on the elemental composition (Si, C, N) of the marine diatoms *Thalassiosira oceanica* and *Ditylum brightwellii*', Biogeosciences, 7, 657-669.

Caldeira, K. and Duffy, P.B., 2000, 'The role of the Southern Ocean in uptake and storage of anthropogenic carbon dioxide', Science, 297, 620–622.

Cassar, N., Laws, E.A., Bidigare, R.R. and Popp, B.N., 2004, 'Bicarbonate uptake by Southern Ocean phytoplankton', Global Biogeochemical Cycles, 18, GB2003, doi:10.1029/2003GB002116.

Cutter, G. and Bruland, K., 2012, 'Rapid and noncontaminating sampling system for trace elements in global ocean surveys', Limnology and Oceanography: Methods, 10, 425–436.

Cutter, G., Andersson, P., Codspoti, L., Croot, P., Francois, R., Lohan, M., Obata, H. and van der Loeff, M.R., 2010, 'Sampling and sample-handling protocols for GEOTRACES cruises', Version 1.0, GEOTRACES Standards and Intercalibration Committee.

DiTullio, G.R., Hutchins, D.A. and Bruland, K.W., 1993, 'Interations of iron and major nutrients control phytoplankton growth and species composition in the tropical North Pacific Ocean', Limnology and Oceanography, 38(3), 495-508.

Egan, L., 2008, 'Nitrate and/or Nitrite in brackish or seawater', QuikChem® Method 31-107-04-1-C, Lachat instruments, Milwaukee, USA.

Falkowski, P.G. and Raven, J.A., 2007, Aquatic photosynthesis, 2nd ed., Princeton University Press, Princeton and Oxford.

Feng, Y., Hare, C.E., Rose, J.M., Handt, S.M., DiTullio, G.R., Lee, P.A., Smith Jr., W.O., Peloquin, J., Tozzi, S., Sun, J., Zhang, Y., Dunbar, R.B., Long, M.C., Sohst, B., Lohan, M. and Hutchins, D.A., 2010, 'Interactive effects of iron, irradiance and CO_2 on Ross Sea phytoplankton', Deep-Sea Research I, 57, 368–383.

Grasshoff, K., Ehrhardt, M. and Kremling, K., 1983, 'Methods of seawater analysis', Verlag Chemie, Weinheim, Germany.

Herndon, H. and Cochlan, W.P., 2012, 'Fluorometric chlorophyll analysis', Cochlan Phytoplankton Ecophysiology Laboratory, San Francisco State University, California, USA.

Hopkinson, B.M., Mitchell, B.G., Reynolds, R.A., Wang, H., Selph, K.E., Measures, C.I., Hewes, C.D., Holm-Hansen, O. and Barbeau, K.A., 2007, 'Iron limitation across chlorophyll gradients in the southern Drake Passage: Phytoplankton responses to iron addition and photosynthetic indicators of iron stress', Limnology and Oceanography, 52(6), 2540-2554.

Hutchins, D.A. and Bruland, K.W., 1998, 'Iron-limited diatom growth and Si : N uptake ratios in a coastal upwelling regime', Nature, 393, 561–564, doi:10.1038/31203.

Hutchins, D.A., Sedwick, P.A., DiTullio, G.R., Boyd, P.W., Quéguiner, B., Griffiths, F.B. and Crossley, C., 2001, 'Control of phytoplankton growth by iron and silicic acid availability in the subantarctic Southern Ocean: Experimental results from the SAZ Project', Journal of Geophysical Research, 106(C12), 31,559-31,572.

Klunder, M.B., Laan, P., De Baar, H.J.W., Neven, I., Middag, R. and Van Ooijen, J., 2013, 'Dissolved Fe across the Weddell Sea and Drake Passage: impact of DFe on nutrients uptake in the Weddell Sea', Biogeosciences Discussions, 10, 7433–7489.

Klunder, M.B., Laan, P., Middag, R., De Baar, H.J.W. and Van Ooijen, J.C., 2011, 'Dissolved iron in the Southern Ocean (Atlantic sector)', Deep-Sea Research II, 58, 2678–2694.

Lagzi, I., Mészáros, R., Gelybó, G. and Leelőssy, Á., 2013, Atmospheric chemistry, viewed 14 July 2015, from

http://elte.prompt.hu/sites/default/files/tananyagok/AtmosphericChemistry/index.html.

Le Moigne, F.A.C., Boye, M., Masson, A., Corvaisier, R., Grossteffan, E., Guéneugues, A. and Pondaven, P., 2013, 'Description of the biogeochemical features of the subtropical southeastern Atlantic and the Southern Ocean south of South Africa during the austral summer of the International Polar Year', Biogeosciences, 10, 281–295.

Maldonado, M., Boyd, P.W., Price, N.M. and Harrison, P.J., 1999, 'Co-limitation of phytoplankton by light and Fe during winter in the NE subarctic Pacific Ocean', Deep-Sea Research II, 46, 2475–2486.

Moore, C.M., Mills, M.M., Langlois, R., Milne, A., Achterberg, E.P., La Roche, J. and Geider, R. J., 2008, 'Relative influence of nitrogen and phosphorus availability on phytoplankton physiology and productivity in the oligotrophic sub-tropical North Atlantic Ocean', Limnology and Oceanography, 53, 291–305.

Moore, C.M., Seeyave, S., Hickman, A.E., Allen, J.T., Lucas, M.I., Planquette, H., Pollard, R.T. and Poulton, A.J., 2007, 'Iron–light interactions during the CROZet natural iron bloom and EXport experiment (CROZEX) I: Phytoplankton growth and photophysiology', Deep-Sea Research II, 54, 2045–2065.

Muller, M., 2010, 'Processes of cellular and organismic function: cell structure, respiration, photosynthesis, molecular genetics and development, structure, and physiology of plants and animals', in BIOS 100 Summer 2010, viewed 14 July 2015, from http://www.uic.edu/classes/bios/bios100/lectures/ps01.htm

Olson, R.J., Sosik, H.M., Chekalyuk, A.M. and Shalapyonok, A., 2000, 'Effects of iron enrichment on phytoplankton in the Southern Ocean during late summer: active fluorescence and flow cytometric analyses', Deep-Sea Research II, 47, 3181-3200.

Orsi, A.H., Whitworth III, T. and Nowlin Jr., W.D., 1994, 'On the meridional extent and fronts of the Antarctic Circumpolar Current', Deep-Sea Research I, 42(5), 641-673.

Oxborough, K., 2012, 'FastPro8 GUI and FRRf3 systems documentation', 2230-801-HB-E, © Chelsea Technologies Group Ltd, West Molesey, UK.

Price, N.M., Andersen, L.F. and Morel, F.M.M., 1991, 'Iron and nitrogen nutrition of Equatorial Pacific plankton', Deep-Sea Research, 38, 1361–1378.

Riebeek, H. and Simmon, R., 2006, 'Paleoclimatology: Explaining the evidence', in NASA Earth Observatory, viewed 14 July 2015, from http://earthobservatory.nasa.gov/Features/Paleoclimatology_Evidence/paleoclimatology_evidence_2.php

Rose, J.M., Feng, Y., DiTullio, G.R., Dunbar, R.B., Hare, C.E., Lee, P.A., Lohan, M., Long, M., Smith Jr., W.O., Sohst, B., Tozzi, S., Zhang, Y. and Hutchins, D.A., 2009, 'Synergistic effects of iron and temperature on Antarctic phytoplankton and microzooplankton assemblages', Biogeosciences, 6, 3131–3147.

Sarmiento, J.L. and Gruber, N., 2006, Ocean biogeochemical dynamics, Princeton University Press, Princeton and Oxford.

Satlantic LP, 2012, 'Operation manual for the FIRe fluorometer system', SAT-DN-00265, revision D, Halifax, Nova Scotia, Canada.

Schlitzer, R., 2015, 'Ocean Data View', viewed 28 July 2015 from http://odv.awi.de.

Schoemann, S., Becquevort, S., Stefels, J., Rousseau, V. and Lancelot, C., 2005, 'Phaeocystis blooms in the global ocean and their controlling mechanisms: A review', Journal of Sea Research, 53, 43–66, doi:10.1016/j.seares.2004.01.008.

Sigman, D.M., Altabet, M.A., Francois, R., McCorkle, D.C. and Gaillard J.F., 1999, 'The isotopic composition of diatom-bound nitrogen in Southern Ocean sediments', Paleoceanography, 14(2), 118–134, doi:10.1029/1998PA900018.

Sosik, H.M. and Olson, R.J., 2002, 'Phytoplankton and iron limitation of photosynthetic efficiency in the Southern Ocean during late summer', Deep-Sea Research I, 49, 1195–1216.

Sunda, W.G. and Huntsman, S.A., 1997, 'Interrelated influence of iron, light and cell size on marine phytoplankton growth', Nature, 390, 389-392, doi:10.1038/37093.

Tagliabue, A., Sallée, J., Bowie, A.R., Lévy, M., Swart, S. and Boyd, P.W., 2014, 'Surface-water iron supplies in the Southern Ocean sustained by deep winter mixing', Nature Geoscience, 7, 314-350.

Timmermans, K.R., Veldhuis, M.J.W. and Brussard, C.P.D., 2007, 'Cell death in three marine diatom species in response to different irradiance levels, silicate or iron concentrations', Aquatic Microbial Ecology, 46, 253–261, doi:10.3354/ame046253.

Turner Designs, 2010, 'Trilogy laboratory fluorometer user's manual', version 1.2, Sunnyvale, CA, USA.

Wolters, M., 2002, 'Silicate in Brackish or Seawater', QuikChem® Method 31-114-27-1-D, Lachat instruments, Milwaukee, USA.

Appendix A

Kruskal-Wallis Statistics, as determined using IBM SPSS Statistics 21 software, for SOSCEx and SAFePool cruise data, are displayed in Appendix A. Overall values indicate statistical analysis on final incubation variable values and only in cases where a significant difference was obtained, further statistical analysis was conducted on first termination values (e.g. Day 2, Day 3, etc.).

Box and whisker plots are representative of the sample mean and standard error of distribution. Where sample size was less than three standard error was not calculated. Pairwise comparison values are the post hoc statistical analyses extracted from initial Kruskal-Wallis analyses, indicating specific differences between samples.

Statistical Results for SOSCEx Experiment 1

Table 1 Overall P values, test statistic and sample size (N) for variables of Day 2, with significant differences, and final concentrations of SOSCEx Experiment 1

	Final			Day 2		
Parameter	**P value**	**Test statistic**	**Total N**	**P value**	**Test statistic**	**Total N**
Chl *a*	0.024	9.409	11	0.023	9.549	12
POC	0.203	4.606	11			
F_v/F_m	0.029	9.030	11			
σ_{PSII}	0.088	6.545	11			
NO_3+NO_2	0.039	8.379	11			
PO_4	0.103	6.181	11			
SiO_4	0.369	3.152	11			

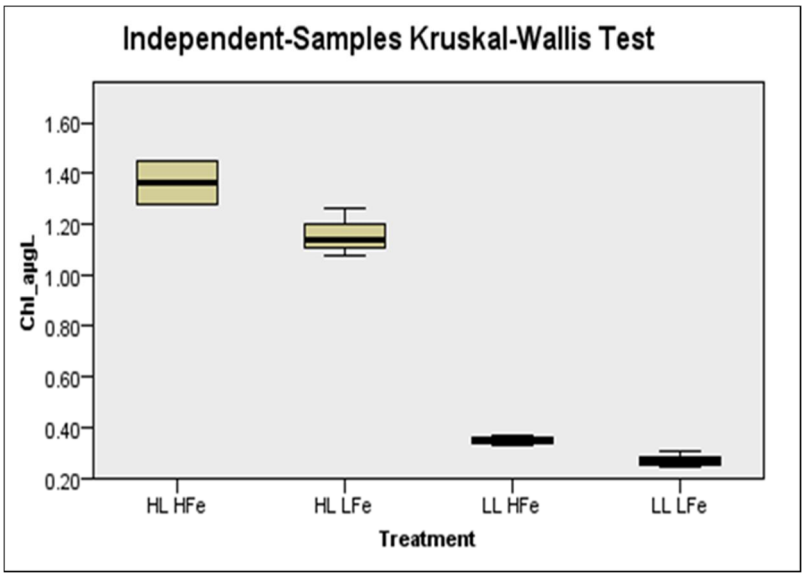

Figure 1 Box and whisker plot representing mean and standard error of final Chl *a* for treatments of SOSCEx Experiment 1

Table 2 P values, test statistic and sample size (N) for pairwise comparison of final Chl *a* for treatments of SOSCEx Experiment 1

Treatment vs. Treatment	P-value	Test statistic	Total N
LL-LFe – LL-HFe	0.268	3.000	6
LL-LFe – HL-LFe	0.027	6.000	6
LL-LFe – HL-HFe	0.005	8.500	5
LL-HFe – HL-LFe	0.268	3.000	6
LL-HFe – HL-HFe	0.069	5.500	5
HL-LFe – HL-HFe	0.409	2.500	5

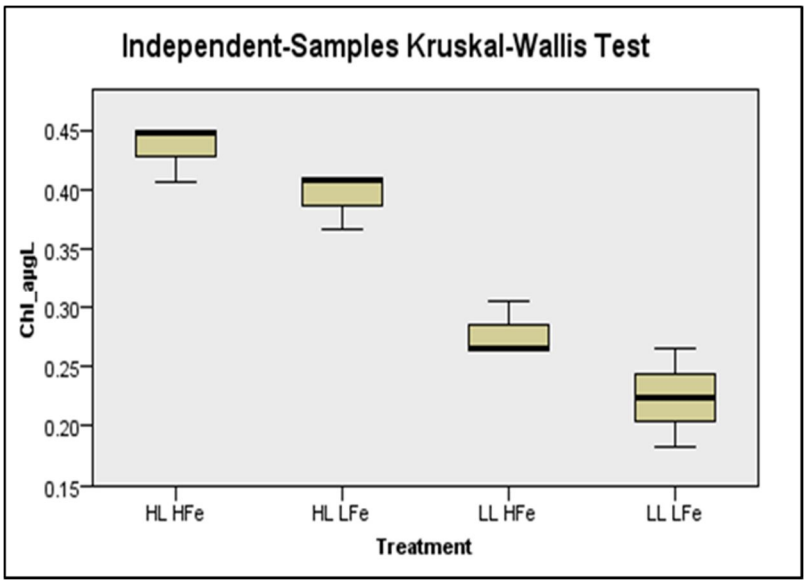

Figure 2 Box and whisker plot representing mean and standard error of Day 2 Chl *a* for treatments of SOSCEx Experiment 1

Table 3 P values, test statistic and sample size (N) for pairwise comparison of day 2 Chl *a* for treatments of SOSCEx Experiment 1

Treatment vs. Treatment	P-value	Test statistic	Total N
LL-LFe – LL-HFe	0.363	2.667	6
LL-LFe – HL-LFe	0.026	6.500	6
LL-LFe – HL-HFe	0.005	8.167	6
LL-HFe – HL-LFe	0.191	3.833	6
LL-HFe – HL-HFe	0.060	5.500	6
HL-LFe – HL-HFe	0.569	1.667	6

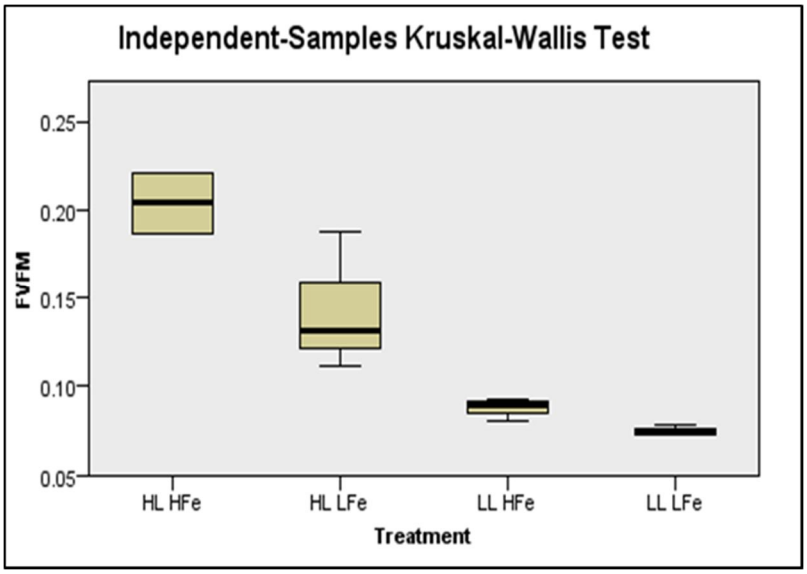

Figure 3 Box and whisker plot representing mean and standard error of final F_v/F_m for treatments of SOSCEx Experiment 1

Table 4 P values, test statistic and sample size (N) for pairwise comparison of final F_v/F_m for treatments of SOSCEx Experiment 1

Treatment vs. Treatment	P-value	Test statistic	Total N
LL-LFe – LL-HFe	0.268	3.000	6
LL-LFe – HL-LFe	0.019	6.333	6
LL-LFe – HL-HFe	0.008	8.000	5
LL-HFe – HL-LFe	0.218	3.333	6
LL-HFe – HL-HFe	0.099	5.000	5
HL-LFe – HL-HFe	0.582	1.667	5

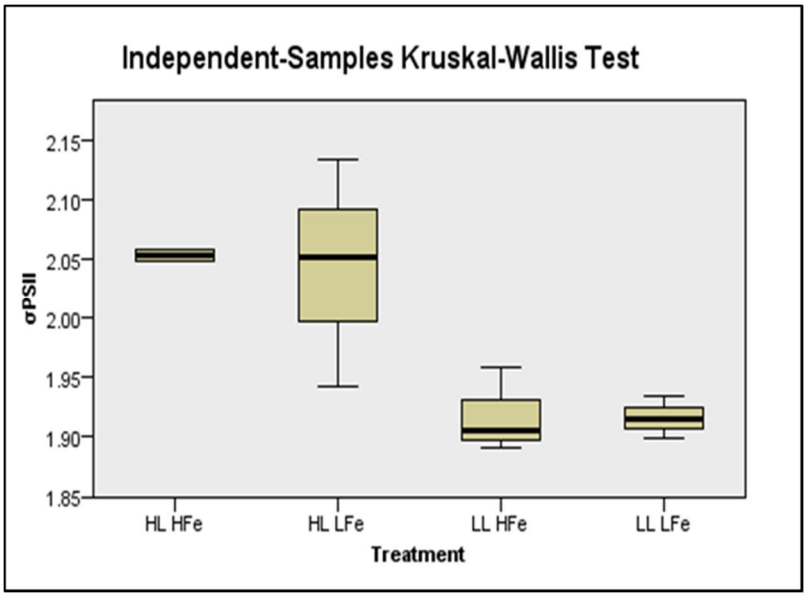

Figure 4 Box and whisker plot representing mean and standard error of final σ_{PSII} for treatments of SOSCEx Experiment 1

Table 5 P values, test statistic and sample size (N) for pairwise comparison of final σ_{PSII} for treatments of SOSCEx Experiment 1

Treatment vs. Treatment	P-value	Test statistic	Total N
LL-LFe – LL-HFe	1.000	0.000	6
LL-LFe – HL-LFe	0.065	5.000	6
LL-LFe – HL-HFe	0.078	5.333	5
LL-HFe – HL-LFe	0.065	5.000	6
LL-HFe – HL-HFe	0.078	5.333	5
HL-LFe – HL-HFe	0.912	0.333	5

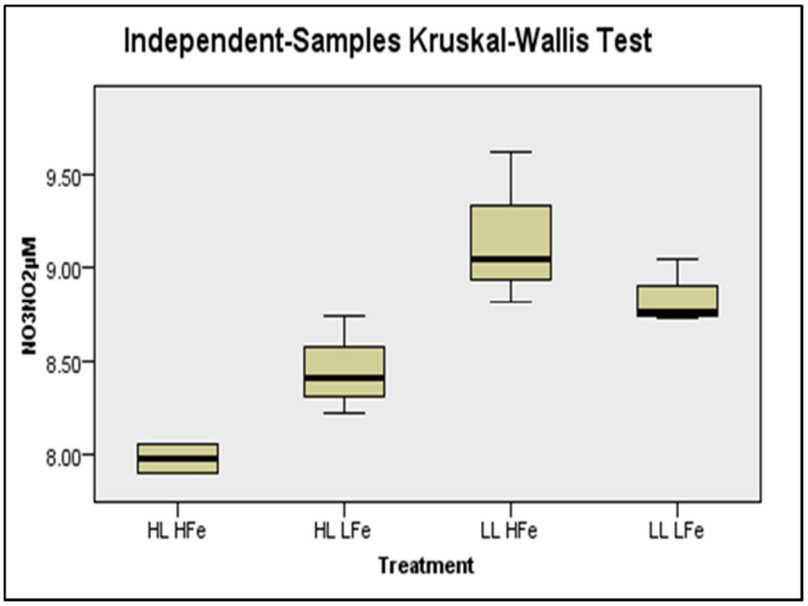

Figure 5 Box and whisker plot representing mean and standard error of final NO_3 + NO_2 for treatments of SOSCEx Experiment 1

Table 6 P values, test statistic and sample size (N) for pairwise comparison of final NO_3 + NO_2 for treatments of SOSCEx Experiment 1

Treatment vs. Treatment	P-value	Test statistic	Total N
LL-LFe – LL-HFe	0.325	2.667	6
LL-LFe – HL-LFe	0.325	2.667	6
LL-LFe – HL-HFe	0.069	5.500	5
LL-HFe – HL-LFe	0.049	5.333	6
LL-HFe – HL-HFe	0.007	8.167	5
HL-LFe – HL-HFe	0.349	2.833	5

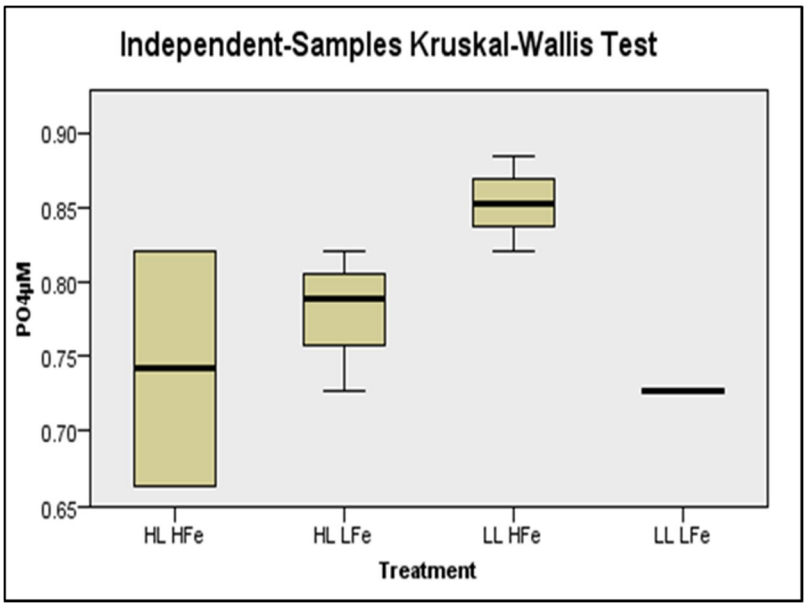

Figure 6 Box and whisker plot representing mean and standard error of final PO_4 for treatments of SOSCEx Experiment 1

Table 7 P values, test statistic and sample size (N) for pairwise comparison of final PO_4 for treatments of SOSCEx Experiment 1

Treatment vs.Treatment	P-value	Test statistic	Total N
LL-LFe – LL-HFe	0.019	6.167	6
LL-LFe – HL-LFe	0.373	2.333	6
LL-LFe – HL-HFe	0.733	1.000	5
LL-HFe – HL-LFe	0.144	3.833	6
LL-HFe – HL-HFe	0.078	5.167	5
HL-LFe – HL-HFe	0.649	1.333	5

Statistical Results for SOSCEx Experiment 2

Table 8 Overall P values, test statistic and sample size (N) for variables of Day 2, with significant differences, and final concentrations of SOSCEx Experiment 2

	Final			Day 2		
Parameter	**P-value**	**Test statistic**	**Total N**	**P-value**	**Test statistic**	**Total N**
Chl *a*	0.032	8.774	12	0.039	8.383	12
POC	0.424	2.795	12			
F_v/F_m	0.082	6.692	12			
σ_{PSII}	0.408	2.897	12			
NO_3+NO_2	0.019	9.974	12			
PO_4	0.970	0.244	12			
SiO_4	0.238	4.231	12			

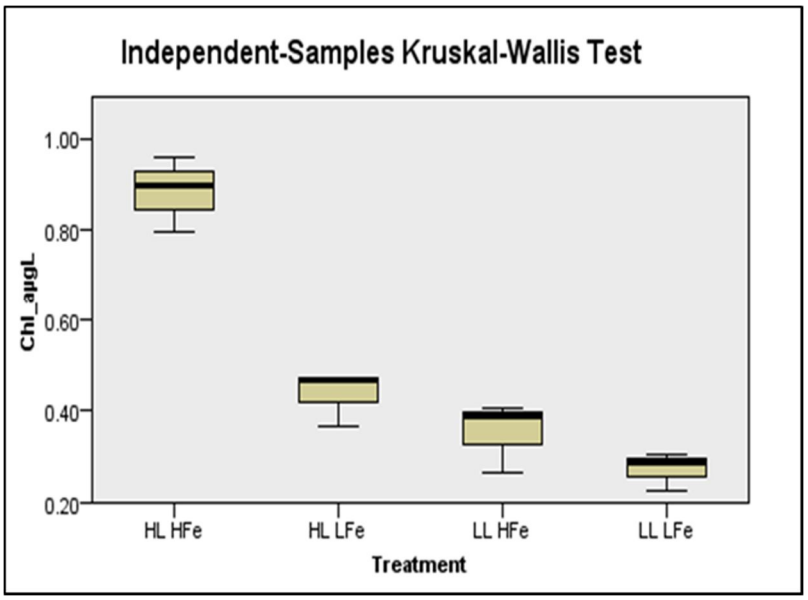

Figure 7 Box and whisker plot representing mean and standard error of final Chl *a* for treatments of SOSCEx Experiment 2

Table 9 P values, test statistic and sample size (N) for pairwise comparison of final Chl *a* for treatments of SOSCEx Experiment 2

Treatment vs. Treatment	P-value	Test statistic	Total N
LL-LFe – LL-HFe	0.427	2.333	6
LL-LFe – HL-LFe	0.112	4.667	6
LL-LFe – HL-HFe	0.005	8.333	6
LL-HFe – HL-LFe	0.427	2.333	6
LL-HFe – HL-HFe	0.041	6.000	6
HL-LFe – HL-HFe	0.212	3.667	6

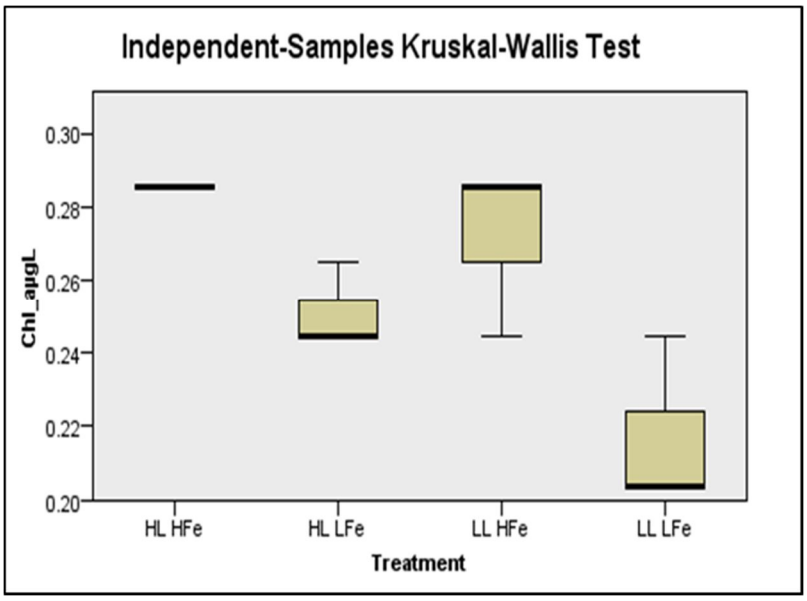

Figure 8 Box and whisker plot representing mean and standard error of Day 2 Chl *a* for treatments of SOSCEx Experiment 2

Table 10 P values, test statistic and sample size (N) for pairwise comparison of Day 2 Chl *a* for treatments of SOSCEx Experiment 2

Treatment vs. Treatment	P-value	Test statistic	Total N
LL-LFe – LL-HFe	0.041	5.667	6
LL-LFe – HL-LFe	0.308	2.833	6
LL-LFe – HL-HFe	0.007	7.500	6
LL-HFe – HL-LFe	0.308	2.833	6
LL-HFe – HL-HFe	0.510	1.833	6
HL-LFe – HL-HFe	0.093	4.667	6

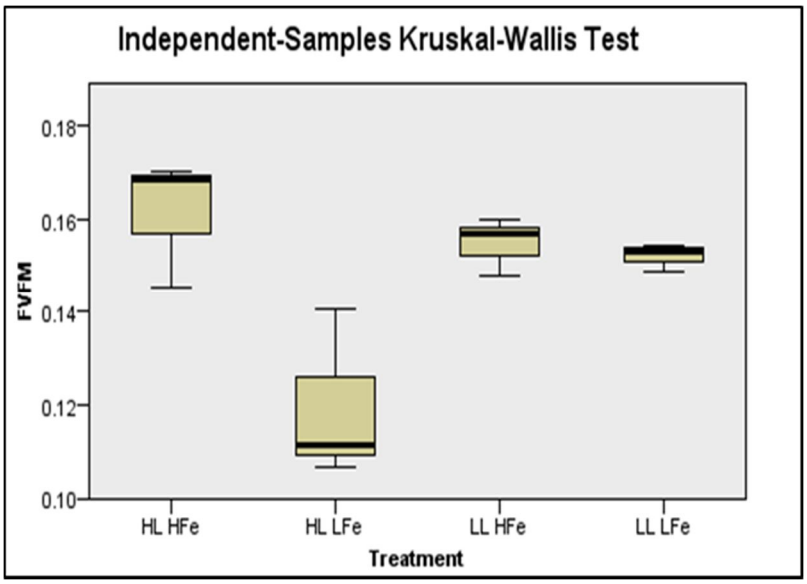

Figure 9 Box and whisker plot representing mean and standard error of final F_v/F_m for treatments of SOSCEx Experiment 2

Table 11 P values, test statistic and sample size (N) for pairwise comparison of final F_v/F_m for treatments of SOSCEx Experiment 2

Treatment vs. Treatment	P-value	Test statistic	Total N
LL-LFe – LL-HFe	0.734	1.000	6
LL-LFe – HL-LFe	0.089	5.000	6
LL-LFe – HL-HFe	0.497	2.000	6
LL-HFe – HL-LFe	0.042	6.000	6
LL-HFe – HL-HFe	0.734	1.000	6
HL-LFe – HL-HFe	0.017	7.000	6

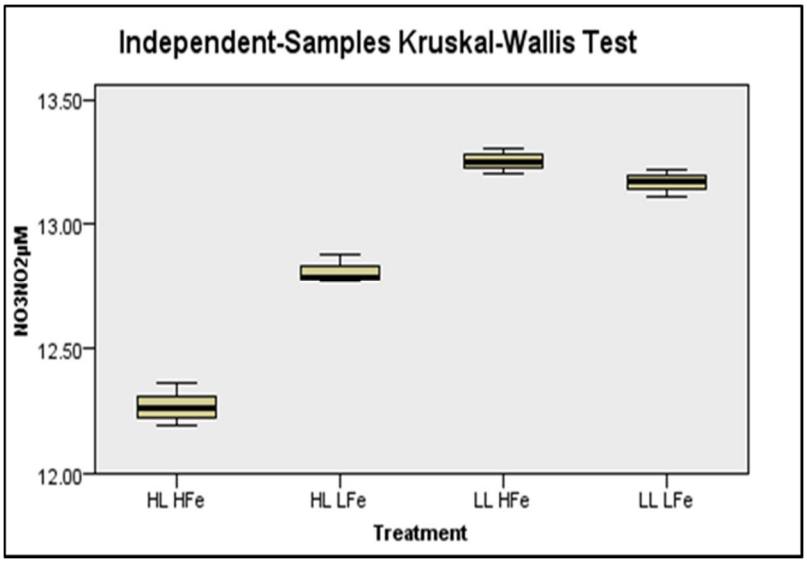

Figure 10 Box and whisker plot representing mean and standard error of final NO_3 + NO_2 for treatments of SOSCEx Experiment 2

Table 12 P values, test statistic and sample size (N) for pairwise comparison of final NO_3 + NO_2 for treatments of SOSCEx Experiment 2

Treatment vs. Treatment	P-value	Test statistic	Total N
LL-LFe – LL-HFe	0.428	2.333	6
LL-LFe – HL-LFe	0.258	3.333	6
LL-LFe – HL-HFe	0.031	6.333	6
LL-HFe – HL-LFe	0.054	5.667	6
LL-HFe – HL-HFe	0.003	8.667	6
HL-LFe – HL-HFe	0.308	3.000	6

Statistical Results for SAFePool Experiment 1

Table 13 Overall P values, test statistic and sample size (N) for variables of Day 2 and Day 5, with significant differences, and final concentrations of SAFePool Experiment 1

	Final		Day 5		Day 2		
Parameter	**P-value**	**Test statistic**	**P-value**	**Test statistic**	**P-value**	**Test statistic**	**Total N**
Chl *a*	0.103	6.179			0.066	7.205	12
POC	0.034	8.684					12
F_v/F_m	0.024	9.462	0.021			9.701	12
σ_{PSII}	0.218	4.436					12
NO_3+NO_2	0.094	6.385					12
PO_4	0.088	6.535			0.065	7.229	12
SiO_4	0.203	4.606					12

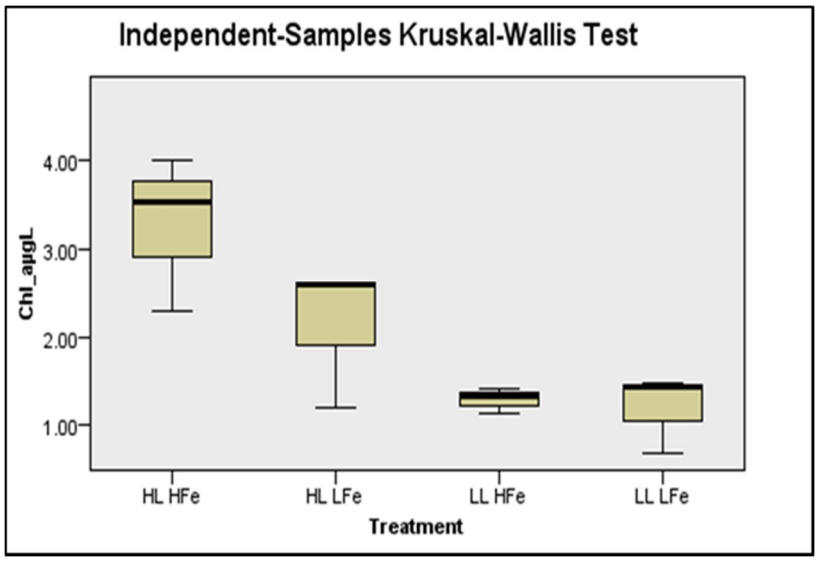

Figure 11 Box and whisker plot representing mean and standard error of final Chl *a* for treatments of SAFePool Experiment 1

Table 14 P values, test statistic and sample size (N) for pairwise comparison of final Chl *a* for treatments of SAFePool Experiment 1

Treatment vs. Treatment	P-value	Test statistic	Total N
LL-LFe – LL-HFe	0.734	1.000	6
LL-LFe – HL-LFe	0.365	2.667	6
LL-LFe – HL-HFe	0.054	5.667	6
LL-HFe – HL-LFe	0.213	3.667	6
LL-HFe – HL-HFe	0.024	6.667	6
HL-LFe – HL-HFe	0.308	3.000	6

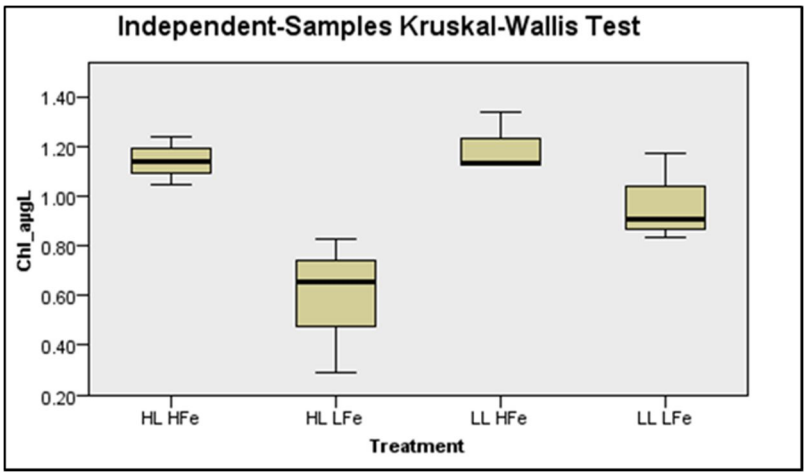

Figure 12 Box and whisker plot representing mean and standard error of Day 2 Chl *a* for treatments of SAFePool Experiment 1

Table 15 P values, test statistic and sample size (N) for pairwise comparison of Day 2 Chl *a* for treatments of SAFePool Experiment 1

Treatment vs. Treatment	P-value	Test statistic	Total N
LL-LFe – LL-HFe	0.365	2.667	6
LL-LFe – HL-LFe	0.141	4.333	6
LL-LFe – HL-HFe	0.428	2.333	6
LL-HFe – HL-LFe	0.017	7.000	6
LL-HFe – HL-HFe	0.910	0.333	6
HL-LFe – HL-HFe	0.024	6.667	6

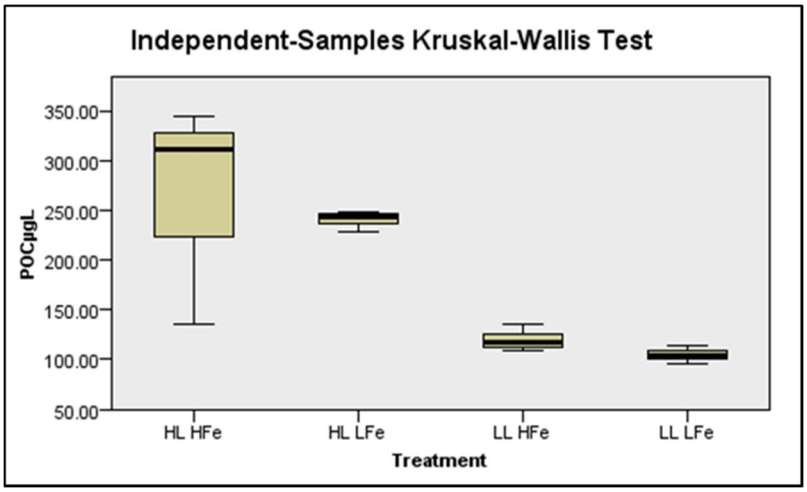

Figure 13 Box and whisker plot representing mean and standard error of final POC for treatments of SAFePool Experiment 1

Table 16 P values, test statistic and sample size (N) for pairwise comparison of final POC for treatments of SAFePool Experiment 1

Treatment vs. Treatment	P-value	Test statistic	Total N
LL-LFe – LL-HFe	0.395	2.500	6
LL-LFe – HL-LFe	0.023	6.667	6
LL-LFe – HL-HFe	0.011	7.500	6
LL-HFe – HL-LFe	0.156	4.167	6
LL-HFe – HL-HFe	0.089	5.000	6
HL-LFe – HL-HFe	0.777	0.833	6

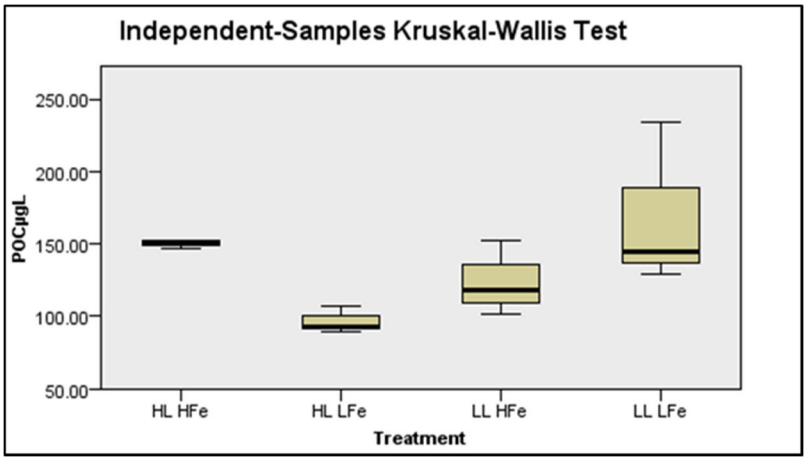

Figure 14 Box and whisker plot representing mean and standard error of Day 2 POC for treatments of SAFePool Experiment 1

Table 17 P values, test statistic and sample size (N) for pairwise comparison of Day 2 POC for treatments of SAFePool Experiment 1

Treatment vs. Treatment	P-value	Test statistic	Total N
LL-LFe – LL-HFe	0.497	2.000	6
LL-LFe – HL-LFe	0.042	6.000	6
LL-LFe – HL-HFe	0.821	0.667	6
LL-HFe – HL-LFe	0.174	4.000	6
LL-HFe – HL-HFe	0.365	2.667	6
HL-LFe – HL-HFe	0.024	6.667	6

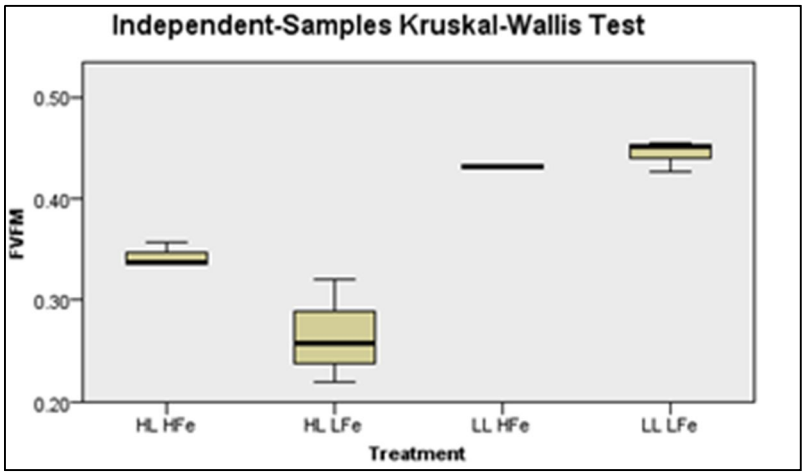

Figure 15 Box and whisker plot representing mean and standard error of final F_v/F_m for treatments of SAFePool Experiment 1

Table 18 P values, test statistic and sample size (N) for pairwise comparison of final F_v/F_m for treatments of SAFePool Experiment 1

Treatment vs. Treatment	P-value	Test statistic	Total N
LL-LFe – LL-HFe	0.734	1.000	6
LL-LFe – HL-LFe	0.007	8.000	6
LL-LFe – HL-HFe	0.089	5.000	6
LL-HFe – HL-LFe	0.017	7.000	6
LL-HFe – HL-HFe	0.174	4.000	6
HL-LFe – HL-HFe	0.308	3.000	6

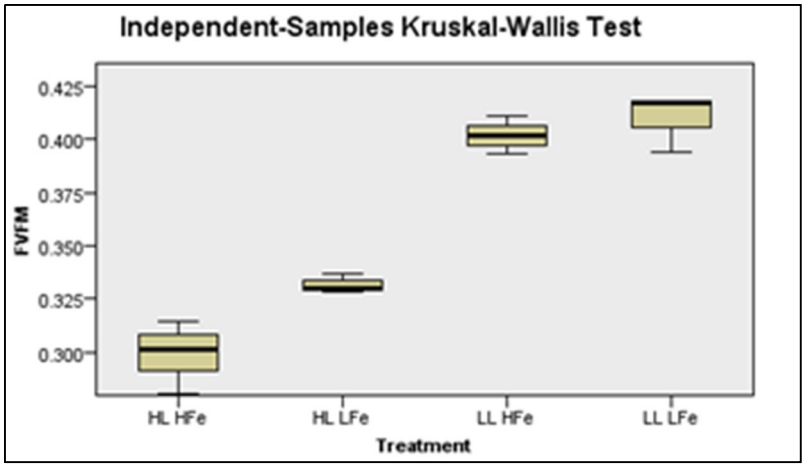

Figure 16 Box and whisker plot representing mean and standard error of Day 5 F_v/F_m for treatments of SAFePool Experiment 1

Table 19 P values, test statistic and sample size (N) for pairwise comparison of Day 5 F_v/F_m for treatments of SAFePool Experiment 1

Treatment vs. Treatment	P-value	Test statistic	Total N
LL-LFe – LL-HFe	0.571	1.667	6
LL-LFe – HL-LFe	0.070	5.333	6
LL-LFe – HL-HFe	0.005	8.333	6
LL-HFe – HL-LFe	0.212	3.667	6
LL-HFe – HL-HFe	0.023	6.667	6
HL-LFe – HL-HFe	0.307	3.000	6

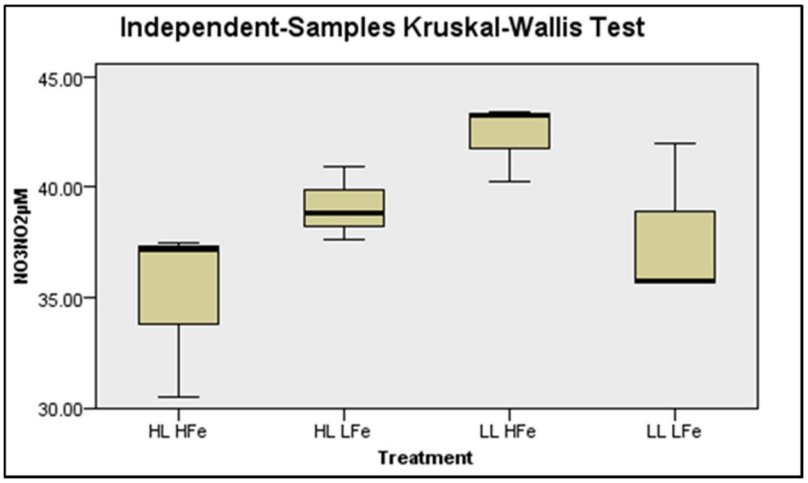

Figure 17 Box and whisker plot representing mean and standard error of final NO_3 + NO_2 for treatments of SAFePool Experiment 1

Table 20 P values, test statistic and sample size (N) for pairwise comparison of final NO_3 + NO_2 for treatments of SAFePool Experiment 1

Treatment vs. Treatment	P-value	Test statistic	Total N
LL-LFe – LL-HFe	0.070	5.333	6
LL-LFe – HL-LFe	0.428	2.333	6
LL-LFe – HL-HFe	0.571	1.667	6
LL-HFe – HL-LFe	0.308	3.000	6
LL-HFe – HL-HFe	0.017	7.000	6
HL-LFe – HL-HFe	0.174	4.000	6

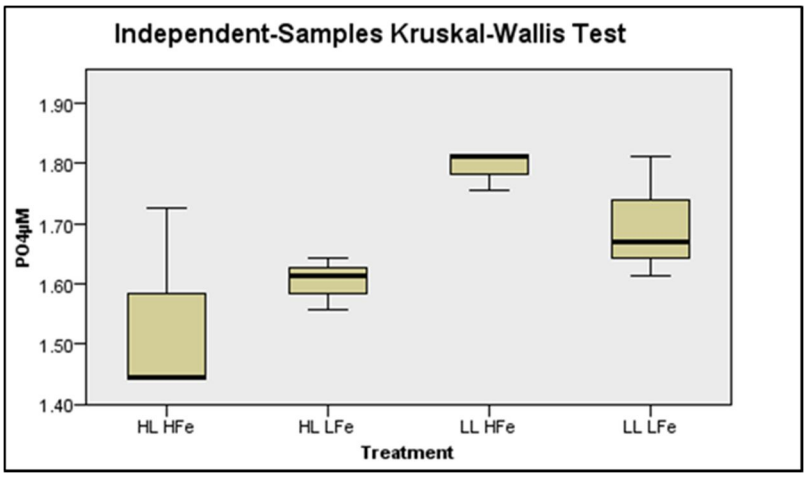

Figure 18 Box and whisker plot representing mean and standard error of final PO_4 for treatments of SAFePool Experiment 1

Table 21 P values, test statistic and sample size (N) for pairwise comparison of final PO_4 for treatments of SAFePool Experiment 1

Treatment vs. Treatment	P-value	Test statistic	Total N
LL-LFe – LL-HFe	0.331	2.833	6
LL-LFe – HL-LFe	0.303	3.000	6
LL-LFe – HL-HFe	0.188	3.833	6
LL-HFe – HL-LFe	0.045	5.833	6
LL-HFe – HL-HFe	0.022	6.667	6
HL-LFe – HL-HFe	0.775	0.833	6

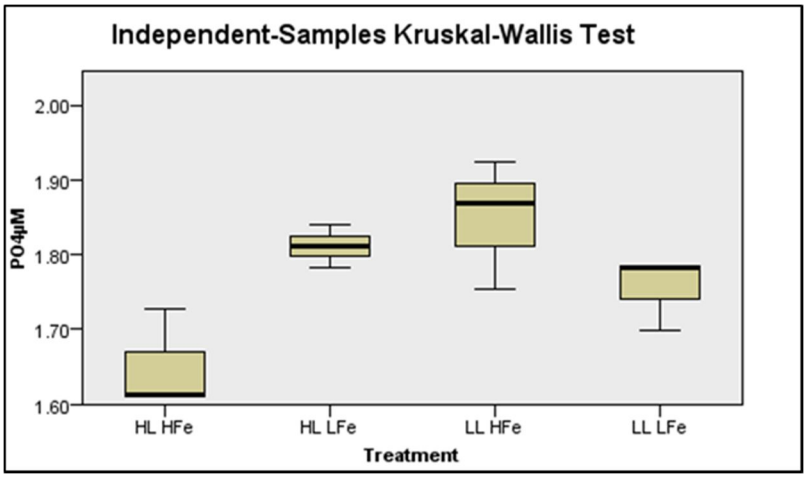

Figure 19 Box and whisker plot representing mean and standard error of Day 2 PO_4 for treatments of SAFePool Experiment 1

Table 22 P values, test statistic and sample size (N) for pairwise comparison of Day 2 PO_4 for treatments of SAFePool Experiment 1

Treatment vs. Treatment	P-value	Test statistic	Total N
LL-LFe – LL-HFe	0.209	3.667	6
LL-LFe – HL-LFe	0.304	3.000	6
LL-LFe – HL-HFe	0.253	3.333	6
LL-HFe – HL-LFe	0.819	0.667	6
LL-HFe – HL-HFe	0.016	7.000	6
HL-LFe – HL-HFe	0.030	6.333	6

Statistical Results for SAFePool Experiment 2

Table 23 Overall P values, test statistic and sample size (N) for variables of Day 3, with significant differences, and final concentrations of SAFePool Experiment 2

	Final			Day 3		
Parameter	**P-value**	**Test statistic**	**Total N**	**P-value**	**Test statistic**	**Total N**
Chl a	0.077	6.846	12	0.063	7.308	12
POC	0.016	10.385	12			
F_v/F_m	0.019	9.974	12	0.022	9.667	12
σ_{PSII}	0.121	5.821	12			
NO_3+NO_2	0.392	3.000	12			
PO_4	0.730	1.296	12			
SiO_4	0.055	7.615	12			

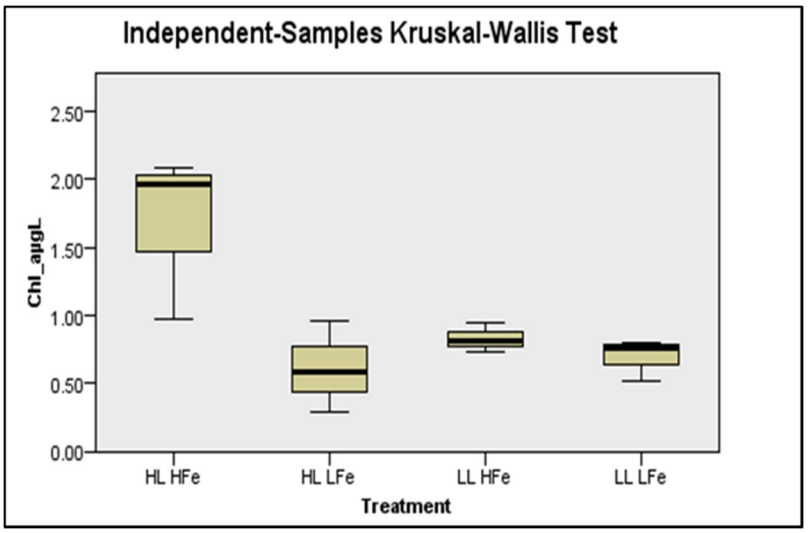

Figure 20 Box and whisker plot representing mean and standard error of final Chl *a* for treatments of SAFePool Experiment 2

Table 24 P values, test statistic and sample size (N) for pairwise comparison of final Chl *a* for treatments of SAFePool Experiment 2

Treatment vs. Treatment	P-value	Test statistic	Total N
LL-LFe – LL-HFe	0.497	2.000	12
LL-LFe – HL-LFe	1.000	0.000	12
LL-LFe – HL-HFe	0.024	6.667	12
LL-HFe – HL-LFe	0.497	2.000	12
LL-HFe – HL-HFe	0.113	4.667	12
HL-LFe – HL-HFe	0.024	6.667	12

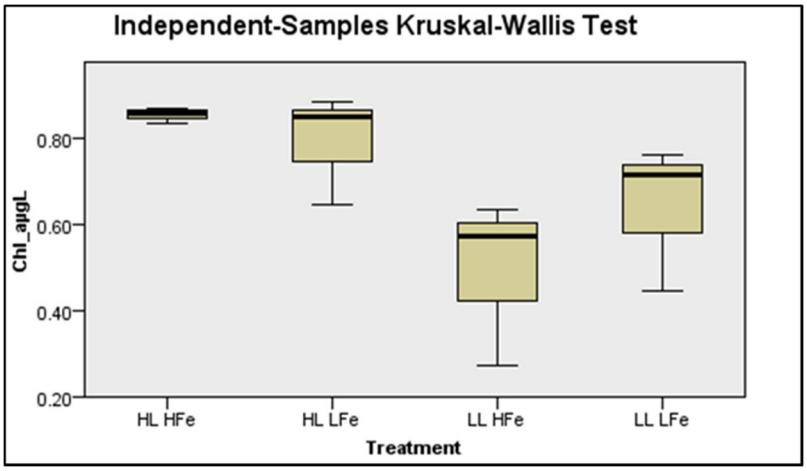

Figure 21 Box and whisker plot representing mean and standard error of Day 3 Chl *a* for treatments of SAFePool Experiment 2

Table 25 P values, test statistic and sample size (N) for pairwise comparison of Day 3 Chl *a* for treatments of SAFePool Experiment 2

Treatment vs. Treatment	P-value	Test statistic	Total N
LL-LFe – LL-HFe	0.428	2.333	6
LL-LFe – HL-LFe	0.213	3.667	6
LL-LFe – HL-HFe	0.113	4.667	6
LL-HFe – HL-LFe	0.042	6.000	6
LL-HFe – HL-HFe	0.017	7.000	6
HL-LFe – HL-HFe	0.734	1.000	6

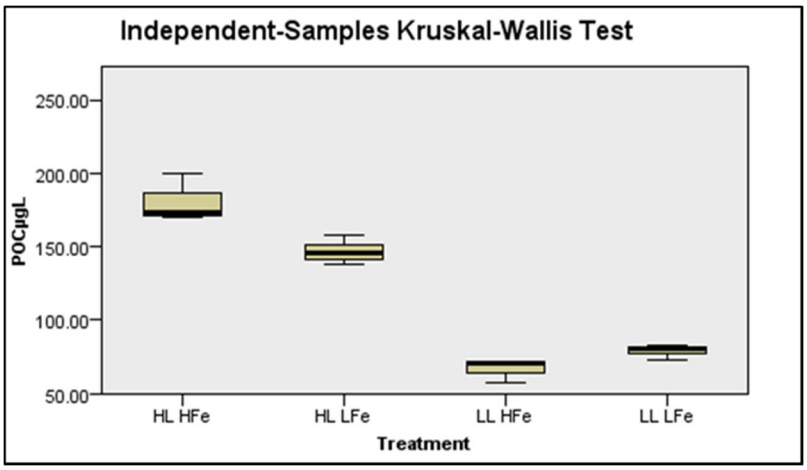

Figure 22 Box and whisker plot representing mean and standard error of final POC for treatments of SAFePool Experiment 2

Table 26 P values, test statistic and sample size (N) for pairwise comparison of final POC for treatments of SAFePool Experiment 2

Treatment vs. Treatment	P-value	Test statistic	Total N
LL-LFe – LL-HFe	0.308	3.000	6
LL-LFe – HL-LFe	0.308	3.000	6
LL-LFe – HL-HFe	0.042	6.000	6
LL-HFe – HL-LFe	0.042	6.000	6
LL-HFe – HL-HFe	0.002	9.000	6
HL-LFe – HL-HFe	0.308	3.000	6

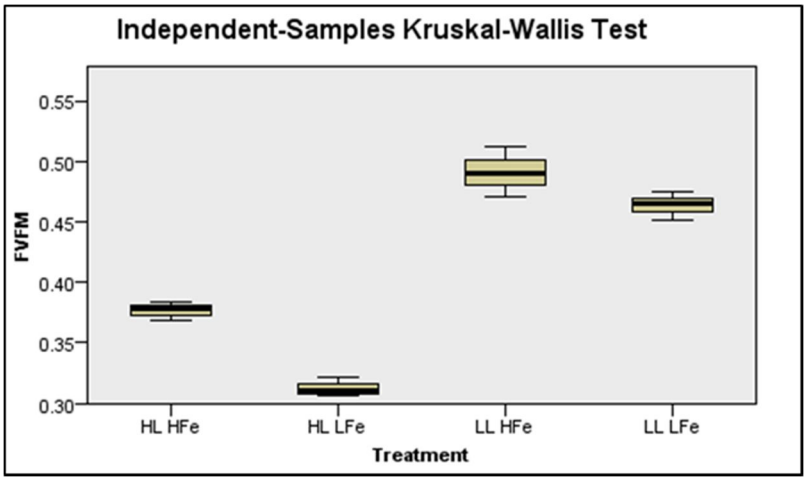

Figure 23 Box and whisker plot representing mean and standard error of final F_v/F_m for treatments of SAFePool Experiment 2

Table 27 P values, test statistic and sample size (N) for pairwise comparison of final F_v/F_m for treatments of SAFePool Experiment 2

Treatment vs. Treatment	P-value	Test statistic	Total N
LL-LFe – LL-HFe	0.428	2.333	6
LL-LFe – HL-LFe	0.031	6.333	6
LL-LFe – HL-HFe	0.258	3.333	6
LL-HFe – HL-LFe	0.003	8.667	6
LL-HFe – HL-HFe	0.054	5.667	6
HL-LFe – HL-HFe	0.308	3.000	6

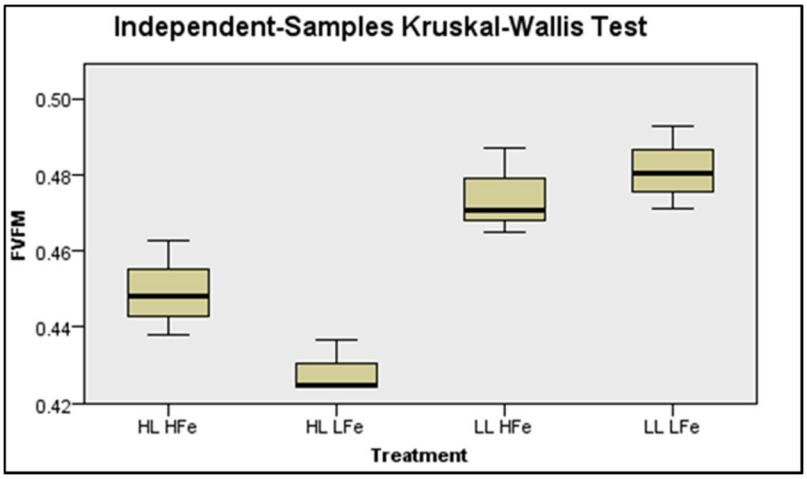

Figure 24 Box and whisker plot representing mean and standard error of Day 3 F_v/F_m for treatments of SAFePool Experiment 2

Table 28 P values, test statistic and sample size (N) for pairwise comparison of Day 3 F_v/F_m for treatments of SAFePool Experiment 2

Treatment vs. Treatment	P-value	Test statistic	Total N
LL-LFe – LL-HFe	0.571	1.667	6
LL-LFe – HL-LFe	0.005	8.333	6
LL-LFe – HL-HFe	0.070	5.333	6
LL-HFe – HL-LFe	0.024	6.667	6
LL-HFe – HL-HFe	0.213	3.667	6
HL-LFe – HL-HFe	0.308	3.000	6

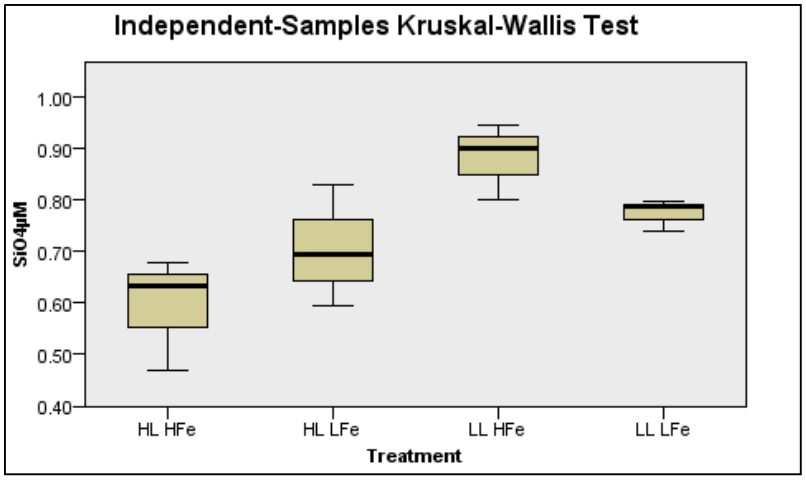

Figure 25 Box and whisker plot representing mean and standard error of final for treatments of SAFePool Experiment 2

Table 29 P values, test statistic and sample size (N) for pairwise comparison of final SiO_4 for treatments of SAFePool Experiment 2

Treatment vs. Treatment	P-value	Test statistic	Total N
LL-LFe – LL-HFe	0.213	3.667	6
LL-LFe – HL-LFe	0.651	1.333	6
LL-LFe – HL-HFe	0.141	4.333	6
LL-HFe – HL-LFe	0.089	5.000	6
LL-HFe – HL-HFe	0.007	8.000	6
HL-LFe – HL-HFe	0.308	3.000	6

Statistical Results for SAFePool Experiment 3

Table 30 Overall P values, test statistic and sample size (N) for variables of Day 3, with significant differences, and final concentrations of SAFePool Experiment 3

	Final			Day 3		
Parameter	**P-value**	**Test statistic**	**Total N**	**P-value**	**Test statistic**	**Total N**
Chl a	0.083	6.667	8			
POC	0.104	6.167	8			
F_v/F_m	0.139	5.500	8	0.083	6.667	8
σ_{PSII}	0.446	2.667	8			
NO_3+NO_2	0.083	6.667	8			
PO_4	0.083	6.667	8			
SiO_4	0.083	6.667	8			

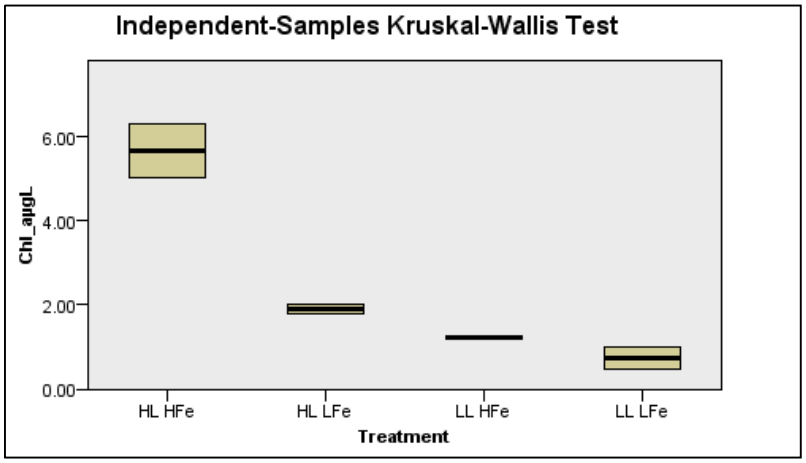

Figure 26 Box plot representing mean of final Chl *a* for treatments of SAFePool Experiment 3

Table 31 P values, test statistic and sample size (N) for pairwise comparison of final Chl *a* for treatments of SAFePool Experiment 3

Treatment vs. Treatment	P-value	Test statistic	Total N
LL-LFe – LL-HFe	0.414	2.000	4
LL-LFe – HL-LFe	0.102	4.000	4
LL-LFe – HL-HFe	0.014	6.000	4
LL-HFe – HL-LFe	0.414	2.000	4
LL-HFe – HL-HFe	0.102	4.000	4
HL-LFe – HL-HFe	0.414	2.000	4

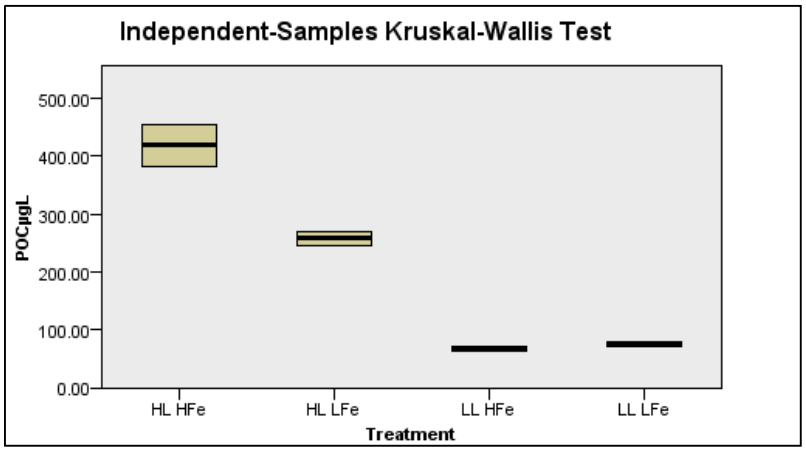

Figure 27 Box plot representing mean of final POC for treatments of SAFePool Experiment 3

Table 32 P values, test statistic and sample size (N) for pairwise comparison of final POC for treatments of SAFePool Experiment 3

Treatment vs. Treatment	P-value	Test statistic	Total N
LL-LFe – LL-HFe	0.683	1.000	4
LL-LFe – HL-LFe	0.307	2.500	4
LL-LFe – HL-HFe	0.066	4.500	4
LL-HFe – HL-LFe	0.153	3.500	4
LL-HFe – HL-HFe	0.025	5.500	4
HL-LFe – HL-HFe	0.414	2.000	4

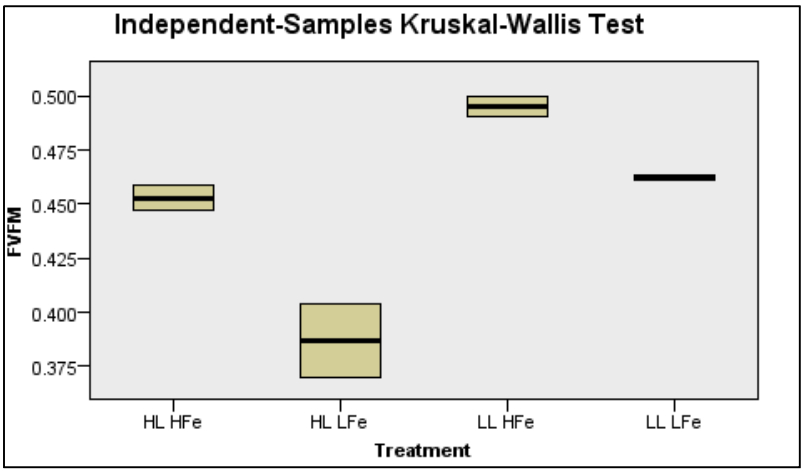

Figure 28 Box plot representing mean of Day 3 F_v/F_m for treatments of SAFePool Experiment 3

Table 33 P values, test statistic and sample size (N) for pairwise comparison of Day 3 F_v/F_m for treatments of SAFePool Experiment 3

Treatment vs. Treatment	P-value	Test statistic	Total N
LL-LFe – LL-HFe	0.414	2.000	4
LL-LFe – HL-LFe	0.102	4.000	4
LL-LFe – HL-HFe	0.414	2.000	4
LL-HFe – HL-LFe	0.014	6.000	4
LL-HFe – HL-HFe	0.102	4.000	4
HL-LFe – HL-HFe	0.414	2.000	4

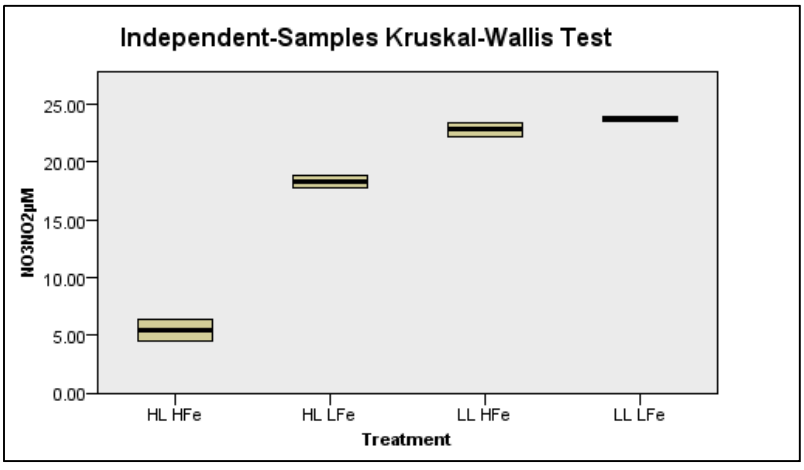

Figure 29 Box plot representing mean of final NO_3 + NO_2 for treatments of SAFePool Experiment 3

Table 34 P values, test statistic and sample size (N) for pairwise comparison of final NO_3 + NO_2 for treatments of SAFePool Experiment 3

Treatment vs. Treatment	P-value	Test statistic	Total N
LL-LFe – LL-HFe	0.414	2.000	4
LL-LFe – HL-LFe	0.102	4.000	4
LL-LFe – HL-HFe	0.014	6.000	4
LL-HFe – HL-LFe	0.414	2.000	4
LL-HFe – HL-HFe	0.102	4.000	4
HL-LFe – HL-HFe	0.414	2.000	4

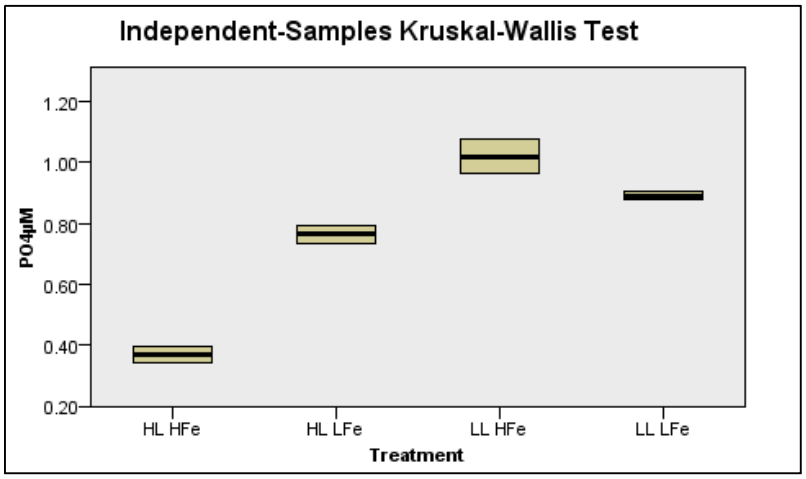

Figure 30 Box plot representing mean of final PO_4 for treatments of SAFePool Experiment 3

Table 35 P values, test statistic and sample size (N) for pairwise comparison of final PO_4 for treatments of SAFePool Experiment 3

Treatment vs. Treatment	P-value	Test statistic	Total N
LL-LFe – LL-HFe	0.414	2.000	4
LL-LFe – HL-LFe	0.414	2.000	4
LL-LFe – HL-HFe	0.102	4.000	4
LL-HFe – HL-LFe	0.102	4.000	4
LL-HFe – HL-HFe	0.014	6.000	4
HL-LFe – HL-HFe	0.414	2.000	4

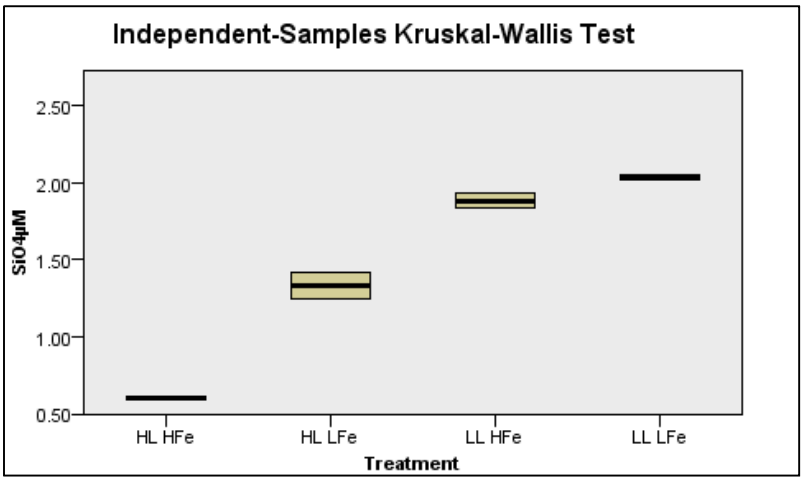

Figure 31 Box plot representing mean of final SiO_4 for treatments of SAFePool Experiment 3

Table 36 P values, test statistic and sample size (N) for pairwise comparison of final SiO_4 for treatments of SAFePool Experiment 3

Treatment vs. Treatment	P-value	Test statistic	Total N
LL-LFe – LL-HFe	0.414	2.000	4
LL-LFe – HL-LFe	0.102	4.000	4
LL-LFe – HL-HFe	0.014	6.000	4
LL-HFe – HL-LFe	0.414	2.000	4
LL-HFe – HL-HFe	0.102	4.000	4
HL-LFe – HL-HFe	0.414	2.000	4

Appendix B

Graphical representation of POC and macronutrient data of SOSCEx and SAFePool cruises

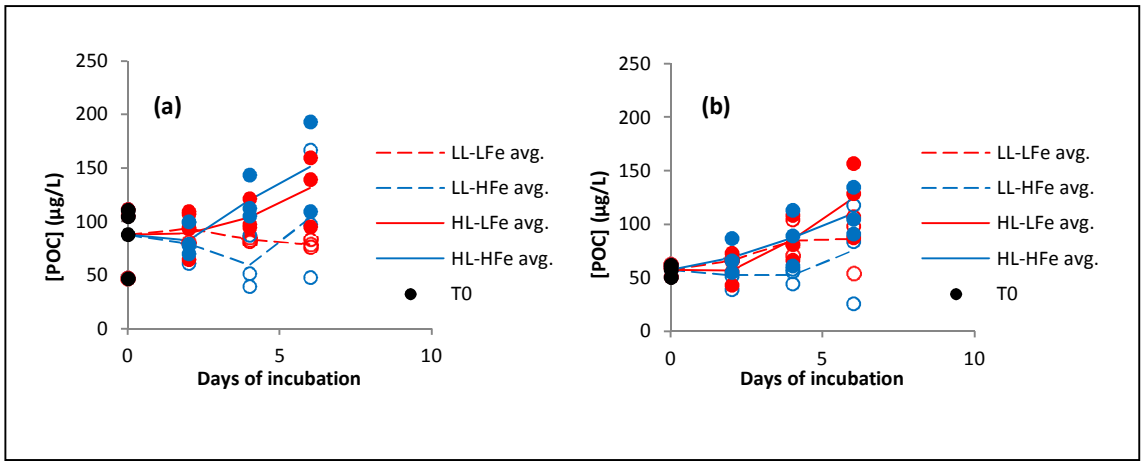

Figure 1 POC concentration vs. days of incubation of four treatments for SOSCEx Experiment 1 at 42.7°S (a) and Experiment 2 at 43.4°S (b), March 2013. Open red circles – LL-LFe replicates, open blue circles – LL-HFe replicates, filled red cirlces – HL-LFe replicates and filled blue circles – HL-HFe replicates

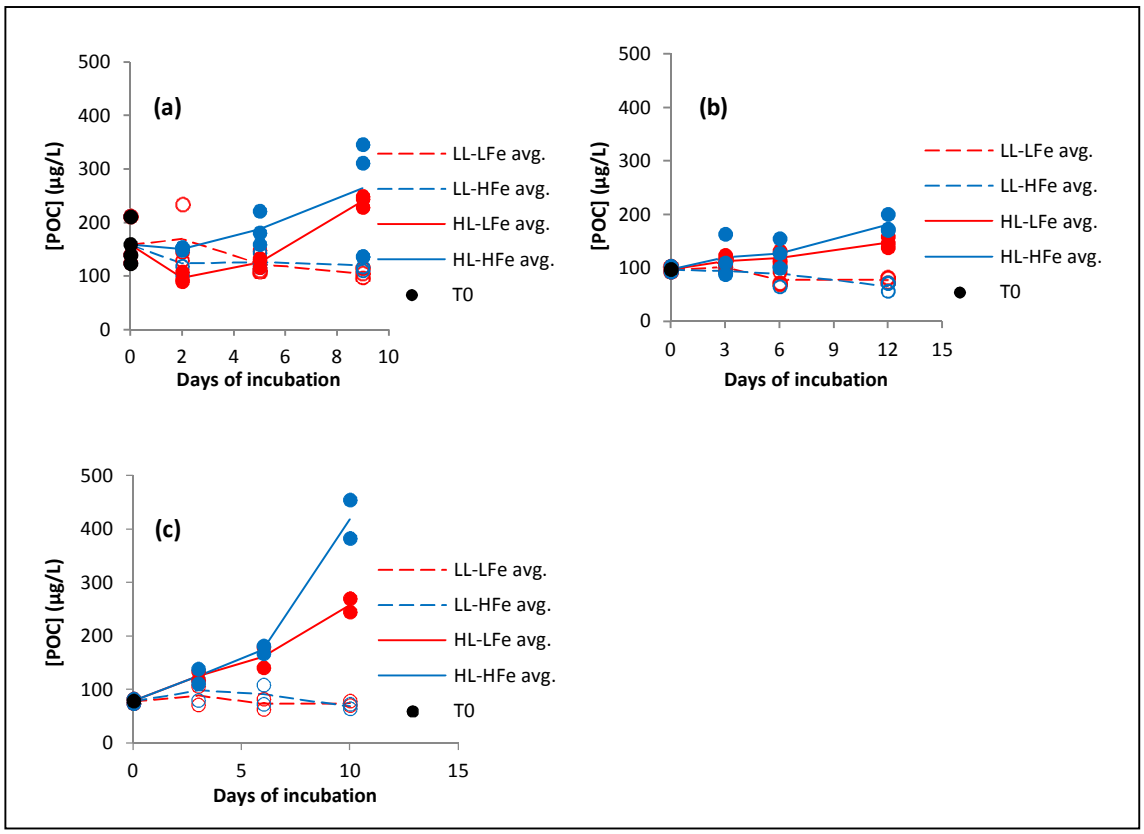

Figure 2 POC vs. days of incubation of four treatments for SAFePool Experiment 1 at 65.0°S (a), Experiment 2 at 50.0°S (b) and Experiment 3 at 44.9°S (c). Open red circles – LL-LFe replicates, open blue circles – LL-HFe replicates, filled red cirlces – HL-LFe replicates and filled blue circles – HL-HFe replicates

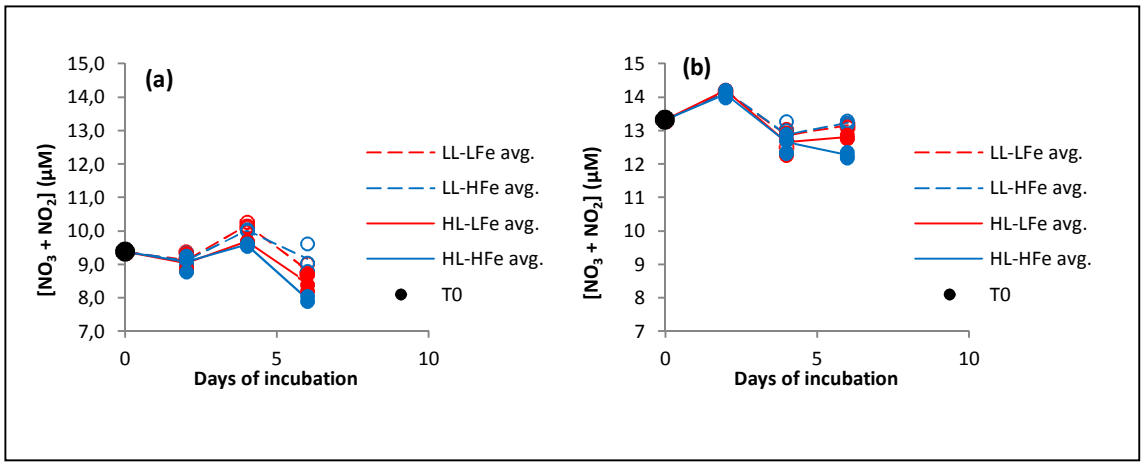

Figure 3 NO_3 + NO_2 concentration vs. days of incubation of four treatments for SOSCEx Experiment 1 at 42.7°S (a) and Experiment 2 at 43.4°S (b), March 2013. Open red circles – LL-LFe replicates, open blue circles – LL-HFe replicates, filled red cirlces – HL-LFe replicates and filled blue circles – HL-HFe replicates

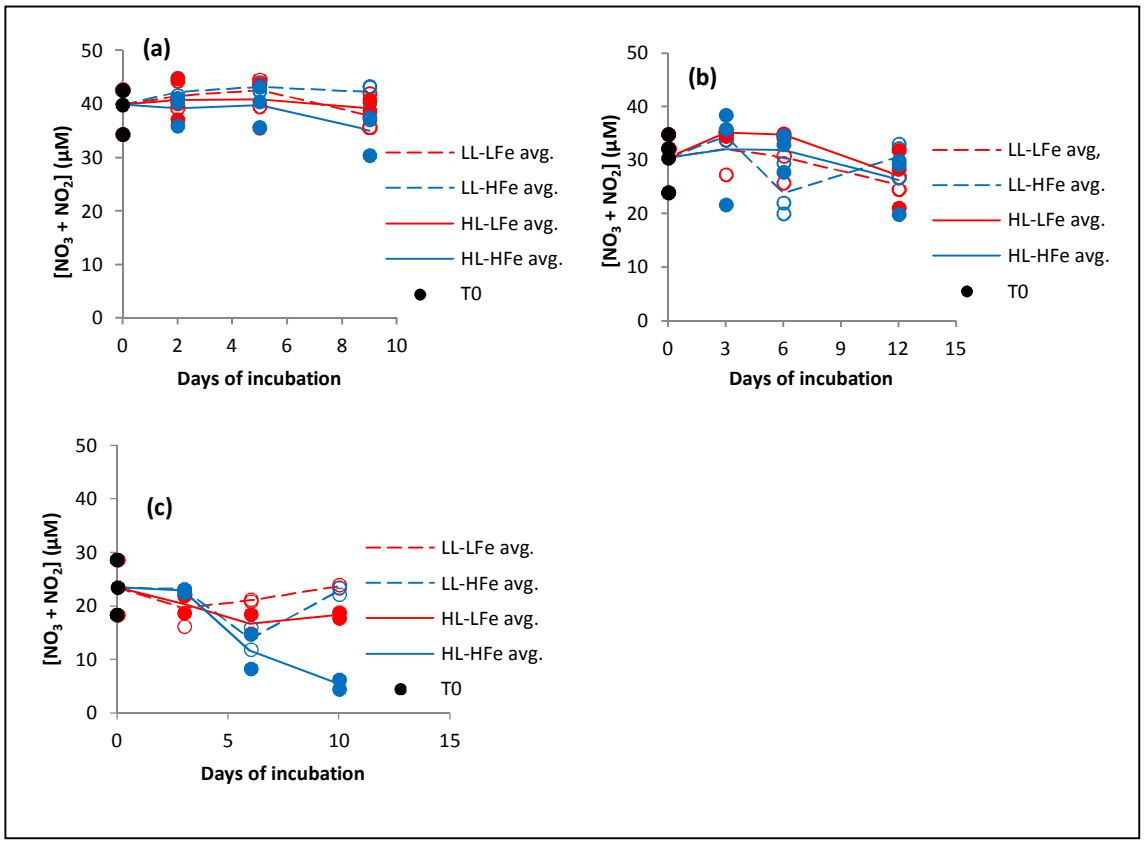

Figure 4 NO_3 + NO_2 vs. days of incubation of four treatments for SAFePool Experiment 1 at 65.0°S (a), Experiment 2 at 50.0°S (b) and Experiment 3 at 44.9°S (c). Open red circles – LL-LFe replicates, open blue circles – LL-HFe replicates, filled red cirlces – HL-LFe replicates and filled blue circles – HL-HFe replicates

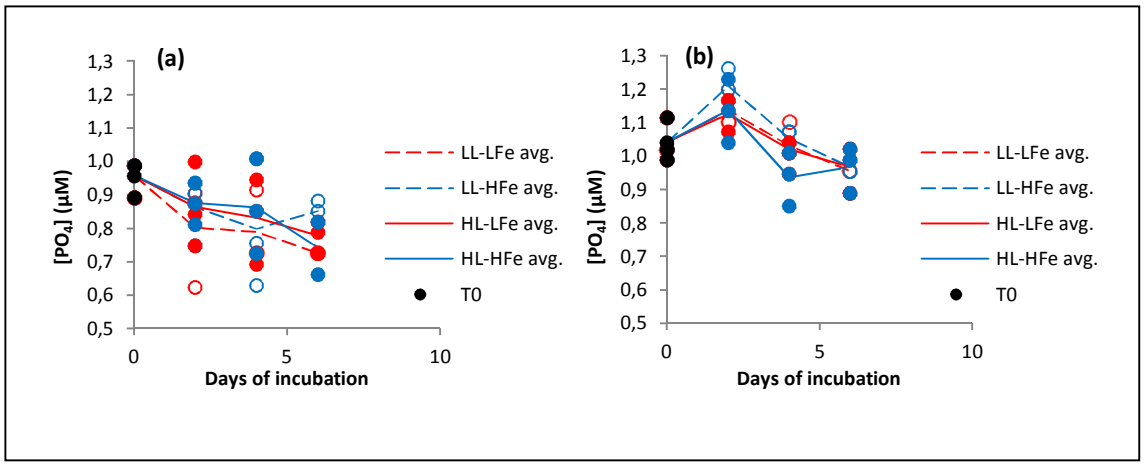

Figure 5 PO_4 concentration vs. days of incubation of four treatments for SOSCEx Experiment 1 at 42.7°S (a) and Experiment 2 at 43.4°S (b), March 2013. Open red circles – LL-LFe replicates, open blue circles – LL-HFe replicates, filled red cirlces – HL-LFe replicates and filled blue circles – HL-HFe replicates

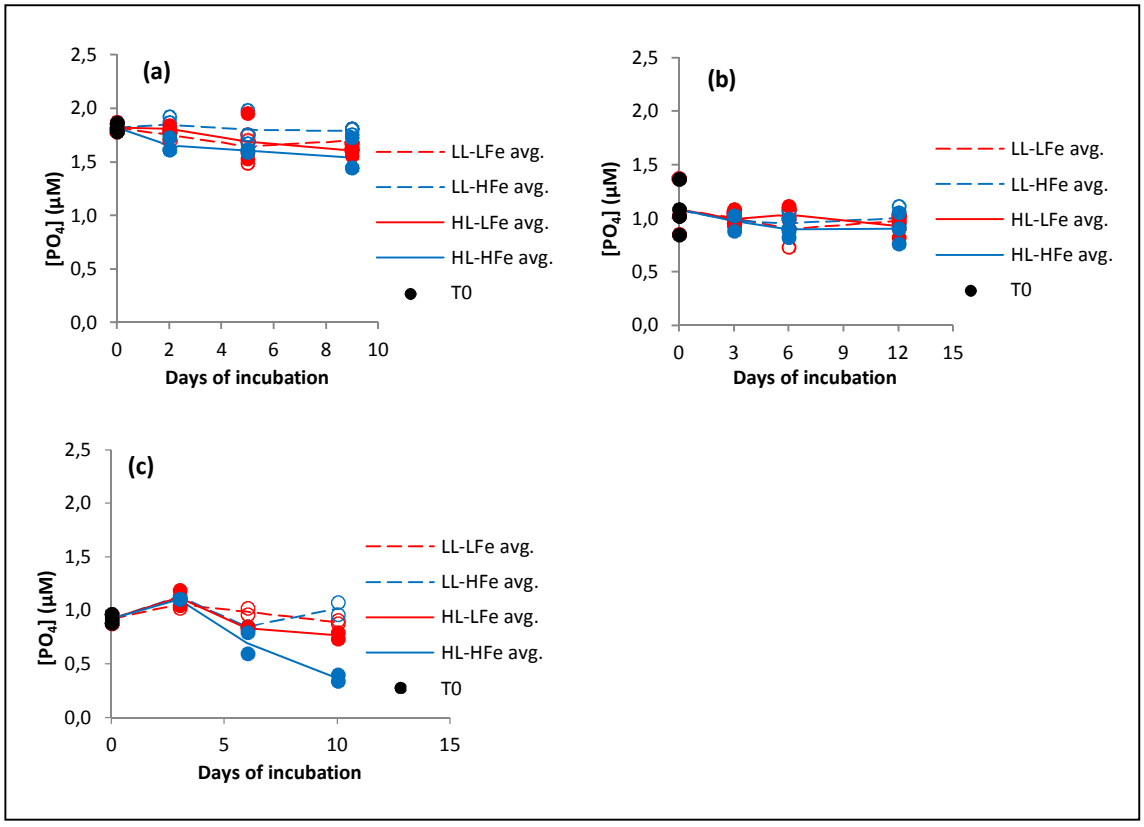

Figure 6 PO_4 vs. days of incubation of four treatments for SAFePool Experiment 1 at 65.0°S (a), Experiment 2 at 50.0°S (b) and Experiment 3 at 44.9°S (c). Open red circles – LL-LFe replicates, open blue circles – LL-HFe replicates, filled red cirlces – HL-LFe replicates and filled blue circles – HL-HFe replicates

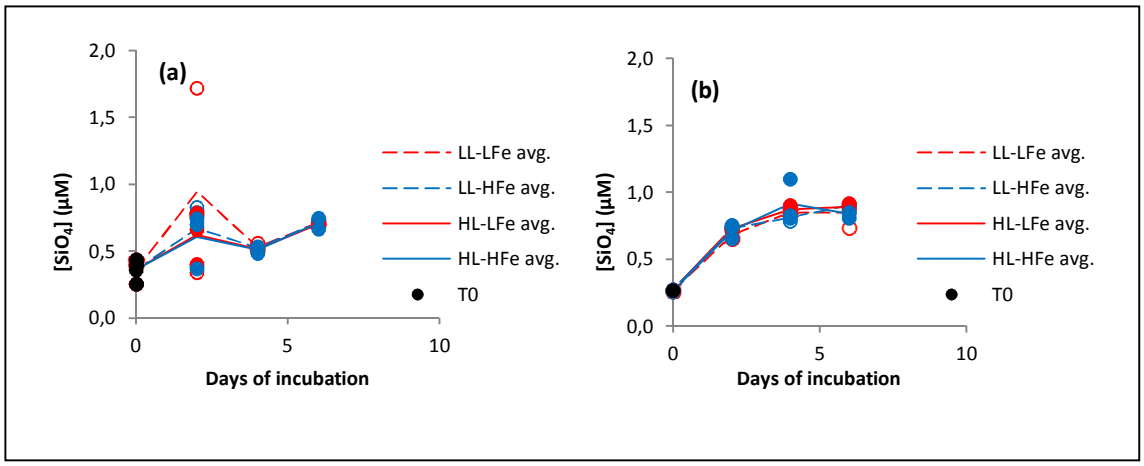

Figure 7 SiO_4 concentration vs. days of incubation of four treatments for SOSCEx Experiment 1 at 42.7°S (a) and Experiment 2 at 43.4°S (b), March 2013. Open red circles – LL-LFe replicates, open blue circles – LL-HFe replicates, filled red cirlces – HL-LFe replicates and filled blue circles – HL-HFe replicates

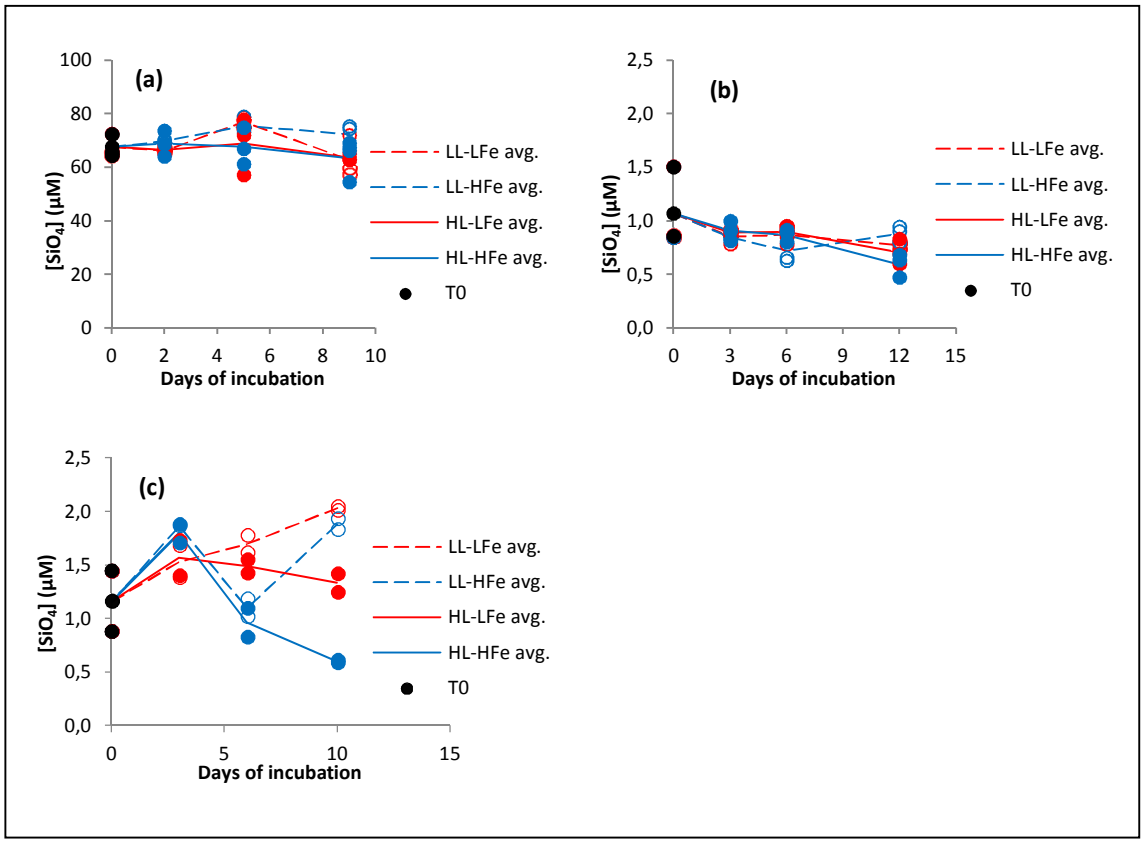

Figure 8 SiO_4 vs. days of incubation of four treatments for SAFePool Experiment 1 at 65.0°S (a), Experiment 2 at 50.0°S (b) and Experiment 3 at 44.9°S (c). Open red circles – LL-LFe replicates, open blue circles – LL-HFe replicates, filled red cirlces – HL-LFe replicates and filled blue circles – HL-HFe replicates

Appendix C

Data

Table 1 Chl *a* data for SOSCEx Experiment 1

Experiment 1	Chl *a* (µg/L)			
Days of incubation	0	2	4	6
LL-LFe avg.	0.292	0.224	0.231	0.272
LL-LFe A	0.306	0.265	0.204	0.265
LL-LFe B	0.265	0.183	0.244	0.244
LL-LFe C	0.306	0.224	0.244	0.306
LL-HFe avg.	0.292	0.278	0.312	0.346
LL-HFe A	0.306	0.306	0.326	0.367
LL-HFe B	0.265	0.265	0.306	0.326
LL-HFe C	0.306	0.265	0.306	0.346
HL-LFe avg.	0.292	0.394	0.591	1.161
HL-LFe A	0.306	0.367	0.672	1.141
HL-LFe B	0.265	0.407	0.631	1.080
HL-LFe C	0.306	0.407	0.468	1.263
HL-HFe avg.	0.292	0.434	0.699	1.365
HL-HFe A	0.306	0.448	0.672	1.283
HL-HFe B	0.265	0.448	0.631	1.446
HL-HFe C	0.306	0.407	0.794	

Table 2 Chl *a* data for SOSCEx Experiment 2

Experiment 2	Chl *a* (µg/L)			
Days of incubation	0	2	4	6
LL-LFe avg.	0.265	0.217	0.224	0.272
LL-LFe A	0.244	0.204	0.224	0.306
LL-LFe B	0.285	0.244	0.224	0.224
LL-LFe C	0.265	0.204	0.224	0.285
LL-HFe avg.	0.265	0.272	0.244	0.353
LL-HFe A	0.244	0.285	0.204	0.387
LL-HFe B	0.285	0.285	0.265	0.407
LL-HFe C	0.265	0.244	0.265	0.265
HL-LFe avg.	0.265	0.251	0.319	0.435
HL-LFe A	0.244	0.265	0.285	0.468
HL-LFe B	0.285	0.244	0.306	0.468
HL-LFe C	0.265	0.244	0.367	0.367
HL-HFe avg.	0.265	0.285	0.530	0.883
HL-HFe A	0.244	0.285	0.530	0.957
HL-HFe B	0.285	0.285	0.530	0.794
HL-HFe C	0.265	0.285	0.530	0.896

Table 3 POC data for SOSCEx Experiment 1

Experiment 1	POC (µg/L)			
Days of incubation	0	2	4	6
LL-LFe avg.	87.74	93.83	83.25	78.72
LL-LFe A	104.97	94.41	81.32	75.77
LL-LFe B	111.23	106.56	83.03	82.60
LL-LFe C	47.02	80.53	85.39	77.79
LL-HFe avg.	87.74	79.33	59.30	103.88
LL-HFe A	104.97	98.89	39.19	97.37
LL-HFe B	111.23	60.66	87.27	166.47
LL-HFe C	47.02	78.46	51.45	47.78
HL-LFe avg.	87.74	88.88	104.08	131.03
HL-LFe A	104.97	109.07	93.97	159.13
HL-LFe B	111.23	93.21	97.00	139.01
HL-LFe C	47.02	64.36	121.27	94.96
HL-HFe avg.	87.74	82.40	120.15	151.02
HL-HFe A	104.97	77.75	143.48	109.20
HL-HFe B	111.23	99.48	111.87	192.83
HL-HFe C	47.02	69.98	105.09	

Table 4 POC data for SOSCEx Experiment 2

Experiment 2	POC (µg/L)			
Days of incubation	0	2	4	6
LL-LFe avg.	57.40	66.07	84.82	86.29
LL-LFe A	50.94	66.53	103.71	106.73
LL-LFe B	59.45		80.29	97.78
LL-LFe C	61.82	65.61	70.44	54.37
LL-HFe avg.	57.40	52.24	52.48	75.62
LL-HFe A	50.94	51.12	55.54	83.58
LL-HFe B	59.45	66.97	44.27	117.57
LL-HFe C	61.82	38.64	57.63	25.71
HL-LFe avg.	57.40	56.83	85.24	124.13
HL-LFe A	50.94	42.61	66.34	87.44
HL-LFe B	59.45	72.56	107.94	128.38
HL-LFe C	61.82	55.31	81.44	156.57
HL-HFe avg.	57.40	68.87	87.41	109.86
HL-HFe A	50.94	65.64	88.92	104.68
HL-HFe B	59.45	86.25	112.70	134.18
HL-HFe C	61.82	54.73	60.61	90.72

Cell counts

Table 5 Condensed cell count data for SOSCEx Experiment 1

Experiment 1		T_1				T_2				T_3			
Cell diameter (µm)	T_0	LL-LFe	LL-HFe	HL-LFe	HL-HFe	LL-LFe	LL-HFe	HL-LFe	HL-HFe	LL-LFe	LL-HFe	HL-LFe	HL-HFe
2.00	167.78	140.70	122.57	234.65	249.40	137.36	135.60	618.29	663.42	194.71	247.53	1265.45	1269.83
2.14	174.97	154.68	135.17	223.36	250.19	129.76	122.20	483.82	556.44	165.62	222.67	1074.36	1095.33
2.29	151.02	127.35	113.68	193.10	227.87	101.58	92.73	394.33	464.20	123.80	166.80	910.71	942.37
2.45	114.47	90.35	85.57	137.19	154.35	69.22	64.71	281.71	338.36	81.09	109.49	694.91	752.83
2.63	82.42	65.82	68.82	95.48	103.24	51.13	44.69	184.27	227.58	58.11	79.78	495.98	599.20
2.81	67.38	49.87	55.60	69.10	68.11	32.93	23.71	123.71	150.36	41.78	56.38	313.33	477.77
3.01	53.50	39.45	46.10	55.90	49.45	29.04	19.62	85.09	106.71	29.69	43.56	190.27	370.40
3.22	46.48	31.92	38.30	44.04	40.69	21.60	14.33	58.96	75.02	28.20	36.20	124.20	280.03
3.45	38.12	28.92	30.90	37.67	32.32	15.31	10.38	42.87	53.38	23.58	30.00	85.78	197.20
3.69	31.42	22.53	22.97	27.76	25.28	11.69	9.38	29.51	37.47	16.91	22.04	67.33	140.13
3.95	25.38	21.00	18.67	24.05	24.00	8.18	6.29	21.69	26.13	16.67	20.13	60.58	100.23
4.23	21.55	21.07	19.40	23.07	23.81	6.80	5.80	20.80	20.51	15.09	18.69	50.98	77.30
4.52	19.73	17.78	16.77	18.74	22.48	7.09	7.69	19.76	23.56	14.22	16.38	44.47	60.83
4.84	19.33	15.98	14.72	18.04	19.72	9.02	8.67	19.31	21.64	13.47	14.22	36.87	51.80
5.18	15.63	13.57	12.60	17.34	17.85	5.18	5.11	14.51	17.02	11.56	12.31	30.11	41.80
5.55	13.68	11.25	10.32	14.11	13.22	5.18	3.11	11.87	11.51	8.67	9.89	26.42	32.63
5.94	12.07	8.32	7.97	10.08	10.81	3.78	3.40	9.71	8.36	8.44	8.56	19.42	25.10
6.36	11.05	7.32	7.40	8.91	10.12	4.42	2.96	7.93	6.98	7.47	6.84	14.44	18.00
6.80	8.48	7.15	6.42	7.81	7.87	4.42	3.33	8.91	7.02	6.33	6.27	13.67	17.27
7.28	6.52	5.80	5.63	6.60	8.00	4.64	2.71	7.44	8.09	4.69	5.22	11.84	14.43
7.80	6.72	5.65	4.43	6.17	6.95	3.40	2.20	5.96	6.02	5.40	4.47	11.04	12.47
8.34	5.72	4.57	4.48	5.10	5.94	3.07	2.04	5.04	4.69	4.07	4.02	7.62	10.70
8.93	4.75	3.92	3.83	4.28	4.85	2.69	1.76	4.44	4.96	3.31	3.76	6.47	10.40
9.56	4.18	3.45	2.88	3.54	4.17	2.24	2.07	3.60	4.09	2.62	2.18	5.31	6.23
10.23	3.73	2.70	2.95	2.67	2.90	1.38	1.56	2.58	2.27	1.76	1.82	4.84	5.53
10.95	3.15	2.35	2.23	2.08	2.43	2.02	1.18	2.53	2.27	1.91	2.00	3.82	4.57

Table 6 Condensed cell count data for SOSCEx Experiment 2

Experiment 2		T_1				T_2				T_3			
Cell diameter (µm)	T_0	LL-LFe	LL-HFe	HL-LFe	HL-HFe	LL-LFe	LL-HFe	HL-LFe	HL-HFe	LL-LFe	LL-HFe	HL-LFe	HL-HFe
2.00	155.75	144.04	138.22	256.49	268.33	159.66	192.71	569.75	718.22	401.69	292.82	1089.15	938.60
2.14	128.15	103.29	102.49	143.29	158.69	92.23	117.97	314.17	436.83	194.89	169.67	604.80	679.04
2.29	129.63	85.84	85.84	95.62	116.67	58.03	79.75	179.39	265.59	110.18	97.89	332.00	475.31
2.45	117.83	67.29	74.53	63.96	80.02	41.48	55.94	97.67	157.54	71.33	70.07	186.84	308.20
2.63	102.20	57.98	65.40	42.84	60.84	30.04	38.24	58.33	94.64	49.93	51.67	97.98	186.64
2.81	71.28	44.56	48.07	27.69	38.49	21.93	29.36	36.83	60.07	35.56	37.89	57.09	112.56
3.01	50.48	32.84	38.04	21.18	28.13	17.94	21.33	25.82	41.27	23.84	29.38	38.22	67.13
3.22	39.22	26.87	29.62	18.93	23.13	12.32	20.03	20.88	30.39	21.42	26.18	30.40	48.11
3.45	30.53	21.24	23.56	15.49	19.47	11.04	19.22	18.88	26.97	16.49	23.40	26.44	36.64
3.69	27.82	19.02	21.82	14.29	16.87	9.17	17.72	18.26	21.81	16.27	20.71	24.13	30.47
3.95	23.57	16.87	19.40	14.82	17.22	9.78	21.23	21.63	23.92	16.64	21.53	26.33	31.22
4.23	21.15	13.24	16.58	12.71	17.51	10.27	19.20	18.51	27.09	15.11	21.49	24.93	40.33
4.52	20.30	12.38	15.78	10.38	18.13	11.12	19.32	16.98	30.36	15.69	19.73	22.53	45.07
4.84	18.08	12.11	13.93	9.44	15.93	7.82	14.19	12.64	26.71	13.51	17.09	18.58	43.33
5.18	14.58	9.24	11.42	7.98	12.44	5.67	11.24	9.48	19.42	11.33	11.96	14.20	33.24
5.55	13.25	7.27	8.69	6.11	8.96	4.77	6.80	5.91	11.60	7.82	8.96	10.60	22.02
5.94	10.15	6.18	6.76	5.02	7.44	4.03	5.94	5.43	8.63	5.82	7.96	6.62	14.80
6.36	9.03	5.31	5.80	4.93	5.84	4.02	5.59	5.82	7.46	5.76	6.47	6.64	10.31
6.80	5.87	3.84	4.07	3.93	4.31	3.79	4.26	4.39	6.64	3.47	4.69	6.09	7.76
7.28	4.55	3.07	2.33	2.04	3.16	2.57	3.31	4.07	4.80	2.67	3.29	4.56	6.11
7.80	4.62	3.44	3.31	3.18	3.11	1.87	2.33	3.37	3.95	3.00	3.38	4.29	4.53
8.34	4.62	2.93	3.24	2.84	2.49	2.81	2.52	2.98	4.01	2.98	2.93	3.67	3.93
8.93	4.23	3.00	2.76	3.20	2.82	2.35	2.26	2.63	3.06	2.56	2.84	3.60	4.16
9.56	3.37	2.51	1.98	1.98	2.64	2.05	1.61	2.68	2.81	2.51	2.80	2.71	3.33
10.23	2.97	2.31	2.29	1.49	1.96	1.68	2.05	2.05	3.01	1.96	2.07	2.62	2.62
10.95	2.60	2.56	2.16	1.73	1.38	1.75	1.86	2.75	2.22	2.42	1.91	2.31	2.89

Table 7 F_v/F_m data for SOSCEx Experiment 1

Experiment 1	F_v/F_m			
Days of incubation	0	2	4	6
LL-LFe avg.	0.036	0.046	0.075	0.075
LL-LFe A	0.040	0.037	0.089	0.074
LL-LFe B	0.039	0.047	0.065	0.078
LL-LFe C	0.029	0.055	0.071	0.073
LL-HFe avg.	0.036	0.057	0.080	0.088
LL-HFe A	0.040	0.067	0.092	0.093
LL-HFe B	0.039	0.049	0.085	0.089
LL-HFe C	0.029	0.054	0.062	0.080
HL-LFe avg.	0.036	0.059	0.104	0.143
HL-LFe A	0.040	0.059	0.109	0.188
HL-LFe B	0.039	0.061	0.073	0.111
HL-LFe C	0.029	0.055	0.130	0.131
HL-HFe avg.	0.036	0.064	0.122	0.204
HL-HFe A	0.040	0.060	0.134	0.221
HL-HFe B	0.039	0.051	0.107	0.187
HL-HFe C	0.029	0.079	0.124	

Table 8 F_v/F_m data for SOSCEx Experiment 2

Experiment 2	F_v/F_m			
Days of incubation	0	2	4	6
LL-LFe avg.	0.031	0.086	0.111	0.152
LL-LFe A	0.025	0.092	0.118	0.149
LL-LFe B	0.029	0.094	0.097	0.154
LL-LFe C	0.039	0.071	0.120	0.153
LL-HFe avg.	0.031	0.092	0.094	0.155
LL-HFe A	0.025	0.084	0.093	0.160
LL-HFe B	0.029	0.104	0.092	0.148
LL-HFe C	0.039	0.088	0.096	0.157
HL-LFe avg.	0.031	0.086	0.090	0.120
HL-LFe A	0.025	0.055	0.089	0.107
HL-LFe B	0.029	0.104	0.077	0.112
HL-LFe C	0.039	0.098	0.104	0.141
HL-HFe avg.	0.031	0.102	0.112	0.161
HL-HFe A	0.025	0.119	0.138	0.145
HL-HFe B	0.029	0.084	0.127	0.169
HL-HFe C	0.039	0.104	0.069	0.170

Table 9 σ_{PSII} data for SOSCEx Experiment 1

Experiment 1	σ_{PSII} (Å^2/quanta)			
Days of incubation	0	2	4	6
LL-LFe avg.	176	186	183	192
LL-LFe A	175	183	187	192
LL-LFe B	180	194	180	193
LL-LFe C	172	180	183	190
LL-HFe avg.	176	179	190	192
LL-HFe A	175	179	187	191
LL-HFe B	180	183	197	189
LL-HFe C	172	174	185	196
HL-LFe avg.	176	178	193	204
HL-LFe A	175	180	195	213
HL-LFe B	180	174	193	205
HL-LFe C	172	179	191	194
HL-HFe avg.	176	175	191	205
HL-HFe A	175	177	190	205
HL-HFe B	180	173	191	206
HL-HFe C	172	175	191	

Table 10 σ_{PSII} data for SOSCEx Experiment 2

Experiment 2	σ_{PSII} (Å^2/quanta)			
Days of incubation	0	2	4	6
LL-LFe avg.	163	190	191	197
LL-LFe A	162	186	188	205
LL-LFe B	151	194	188	191
LL-LFe C	175	191	196	194
LL-HFe avg.	163	186	188	201
LL-HFe A	162	188	184	207
LL-HFe B	151	182	187	194
LL-HFe C	175	189	192	201
HL-LFe avg.	163	188	192	206
HL-LFe A	162	189	195	203
HL-LFe B	151	187	188	204
HL-LFe C	175	186	193	209
HL-HFe avg.	163	190	186	204
HL-HFe A	162	189	193	196
HL-HFe B	151	192	186	209
HL-HFe C	175	189	180	207

Table 11 NO_3 + NO_2 data for SOSCEx Experiment 1

Experiment 1	NO_3 + NO_2 (µM)			
Days of incubation	0	2	4	6
LL-LFe avg.	9.38	9.13	10.19	8.85
LL-LFe A	9.36	8.82	10.17	9.05
LL-LFe B	9.42	9.19	10.28	8.73
LL-LFe C	9.37	9.39	10.11	8.76
LL-HFe avg.	9.38	9.11	10.04	9.16
LL-HFe A	9.36	8.96	10.04	9.62
LL-HFe B	9.42	9.02	10.01	9.05
LL-HFe C	9.37	9.36	10.05	8.82
HL-LFe avg.	9.38	9.03	9.69	8.45
HL-LFe A	9.36	8.84	9.70	8.74
HL-LFe B	9.42	8.91	9.70	8.22
HL-LFe C	9.37	9.34	9.68	8.41
HL-HFe avg.	9.38	9.07	9.60	7.98
HL-HFe A	9.36	9.16	9.61	8.06
HL-HFe B	9.42	8.78	9.63	7.91
HL-HFe C	9.37	9.26	9.55	

Table 12 NO_3 + NO_2 data for SOSCEx Experiment 2

Experiment 2	NO_3 + NO_2 (µM)			
Days of incubation	0	2	4	6
LL-LFe avg.	13.33	14.17	12.86	13.17
LL-LFe A	13.40	14.14	13.06	13.11
LL-LFe B	13.29	14.19	13.01	13.17
LL-LFe C	13.30	14.20	12.52	13.22
LL-HFe avg.	13.33	14.18	12.89	13.25
LL-HFe A	13.40	14.23	13.28	13.20
LL-HFe B	13.29	14.17	13.03	13.25
LL-HFe C	13.30	14.14	12.37	13.31
HL-LFe avg.	13.33	14.20	12.65	12.81
HL-LFe A	13.40	14.22	12.93	12.88
HL-LFe B	13.29	14.22	12.74	12.79
HL-LFe C	13.30	14.17	12.27	12.77
HL-HFe avg.	13.33	14.10	12.65	12.27
HL-HFe A	13.40	14.22	12.90	12.36
HL-HFe B	13.29	14.06	12.72	12.26
HL-HFe C	13.30	14.00	12.33	12.19

Table 13 PO_4 data for SOSCEx Experiment 1

Experiment 1	PO_4 (µM)			
Days of incubation	0	2	4	6
LL-LFe avg.	0.957	0.802	0.789	0.726
LL-LFe A	0.989	0.906	0.916	0.726
LL-LFe B	0.989	0.625	0.726	0.726
LL-LFe C	0.894	0.875	0.726	0.726
LL-HFe avg.	0.957	0.865	0.800	0.853
LL-HFe A	0.989	0.906	1.011	0.884
LL-HFe B	0.989	0.750	0.758	0.821
LL-HFe C	0.894	0.938	0.632	0.853
HL-LFe avg.	0.957	0.865	0.832	0.779
HL-LFe A	0.989	0.844	0.853	0.821
HL-LFe B	0.989	0.750	0.947	0.726
HL-LFe C	0.894	1.000	0.695	0.789
HL-HFe avg.	0.957	0.875	0.863	0.742
HL-HFe A	0.989	0.875	0.853	0.821
HL-HFe B	0.989	0.813	1.011	0.663
HL-HFe C	0.894	0.938	0.726	

Table 14 PO_4 data for SOSCEx Experiment 2

Experiment 2	PO_4 (µM)			
Days of incubation	0	2	4	6
LL-LFe avg.	1.043	1.137	1.032	0.956
LL-LFe A	1.117	1.200	1.042	0.890
LL-LFe B	0.989	1.105	0.947	1.022
LL-LFe C	1.021	1.105	1.105	0.956
LL-HFe avg.	1.043	1.211	1.053	0.967
LL-HFe A	1.117	1.200	1.074	0.956
LL-HFe B	0.989	1.168	1.011	0.989
LL-HFe C	1.021	1.263	1.074	0.956
HL-LFe avg.	1.043	1.126	1.021	0.967
HL-LFe A	1.117	1.168	1.011	0.989
HL-LFe B	0.989	1.137	1.042	0.890
HL-LFe C	1.021	1.074	1.011	1.022
HL-HFe avg.	1.043	1.137	0.937	0.967
HL-HFe A	1.117	1.042	0.853	0.890
HL-HFe B	0.989	1.232	0.947	0.989
HL-HFe C	1.021	1.137	1.011	1.022

Table 15 SiO_4 data for SOSCEx Experiment 1

Experiment 1	SiO_4 (µM)			
Days of incubation	0	2	4	6
LL-LFe avg.	0.364	0.947	0.528	0.717
LL-LFe A	0.436	0.343	0.564	0.708
LL-LFe B	0.257	1.723	0.513	0.710
LL-LFe C	0.399	0.775	0.508	0.733
LL-HFe avg.	0.364	0.671	0.524	0.718
LL-HFe A	0.436	0.391	0.516	0.719
LL-HFe B	0.257	0.830	0.523	0.712
LL-HFe C	0.399	0.791	0.533	0.724
HL-LFe avg.	0.364	0.618	0.517	0.700
HL-LFe A	0.436	0.406	0.520	0.692
HL-LFe B	0.257	0.661	0.513	0.708
HL-LFe C	0.399	0.787	0.519	0.700
HL-HFe avg.	0.364	0.605	0.509	0.710
HL-HFe A	0.436	0.369	0.488	0.750
HL-HFe B	0.257	0.700	0.535	0.669
HL-HFe C	0.399	0.747	0.505	

Table 16 SiO_4 data for SOSCEx Experiment 2

Experiment 2	SiO_4 (µM)			
Days of incubation	0	2	4	6
LL-LFe avg.	0.268	0.685	0.853	0.849
LL-LFe A	0.261	0.741	0.844	0.902
LL-LFe B	0.272	0.660	0.836	0.914
LL-LFe C	0.270	0.655	0.880	0.731
LL-HFe avg.	0.268	0.731	0.813	0.906
LL-HFe A	0.261	0.726	0.784	0.913
LL-HFe B	0.272	0.710	0.819	0.910
LL-HFe C	0.270	0.758	0.836	0.895
HL-LFe avg.	0.268	0.727	0.871	0.892
HL-LFe A	0.261	0.730	0.858	0.922
HL-LFe B	0.272	0.726	0.905	0.880
HL-LFe C	0.270	0.726	0.849	0.876
HL-HFe avg.	0.268	0.714	0.913	0.838
HL-HFe A	0.261	0.655	0.808	0.853
HL-HFe B	0.272	0.741	0.830	0.811
HL-HFe C	0.270	0.745	1.101	0.850

Table 17 Chl *a* data for SAFePool Experiment 1

Experiment 1	Chl *a* (µg/L)			
Days of incubation	0	2	5	9
LL-LFe avg.	0.946	0.970	1.060	1.195
LL-LFe A	0.642	1.174	0.990	0.677
LL-LFe B	0.982	0.905	1.080	1.427
LL-LFe C	1.214	0.831	1.110	1.480
LL-HFe avg.	0.946	1.198	1.266	1.286
LL-HFe A	0.642	1.126	1.331	1.133
LL-HFe B	0.982	1.131	1.213	1.406
LL-HFe C	1.214	1.337	1.254	1.318
HL-LFe avg.	0.946	0.591	0.920	2.128
HL-LFe A	0.642	0.658	0.823	1.205
HL-LFe B	0.982	0.289	0.782	2.591
HL-LFe C	1.214	0.826	1.153	2.587
HL-HFe avg.	0.946	1.143	1.718	3.281
HL-HFe A	0.642	1.049	1.760	4.014
HL-HFe B	0.982	1.140	1.712	2.298
HL-HFe C	1.214	1.241	1.681	3.531

Table 18 Chl *a* data for SAFePool Experiment 2

Experiment 2	Chl *a* (µg/L)			
Days of incubation	0	3	6	12
LL-LFe avg.	0.625	0.643	0.695	0.694
LL-LFe A	0.675	0.717	0.786	0.520
LL-LFe B	0.650	0.447	0.557	0.759
LL-LFe C	0.550	0.764	0.741	0.801
LL-HFe avg.	0.625	0.494	0.776	0.828
LL-HFe A	0.675	0.635	0.785	0.807
LL-HFe B	0.650	0.575	0.808	0.948
LL-HFe C	0.550	0.273	0.734	0.730
HL-LFe avg.	0.625	0.795	0.754	0.610
HL-LFe A	0.675	0.647	0.781	0.584
HL-LFe B	0.650	0.887	0.783	0.286
HL-LFe C	0.550	0.851	0.699	0.960
HL-HFe avg.	0.625	0.857	0.892	1.675
HL-HFe A	0.675	0.837	0.622	1.967
HL-HFe B	0.650	0.860	0.833	0.970
HL-HFe C	0.550	0.873	1.219	2.087

Table 19 Chl *a* data for SAFePool Experiment 3

Experiment 3	Chl *a* (µg/L)			
Days of incubation	0	3	6	10
LL-LFe avg.	0.638	0.588	1.076	0.740
LL-LFe A	0.592	0.845	1.047	0.485
LL-LFe B	0.683	0.330	1.105	0.994
LL-HFe avg.	0.638	0.879	0.773	1.203
LL-HFe A	0.592	0.891	1.013	1.234
LL-HFe B	0.683	0.867	0.533	1.173
HL-LFe avg.	0.638	1.010	1.023	1.898
HL-LFe A	0.592	0.761	0.919	2.015
HL-LFe B	0.683	1.259	1.126	1.780
HL-HFe avg.	0.638	1.445	3.504	5.649
HL-HFe A	0.592	1.353	4.124	5.008
HL-HFe B	0.683	1.536	2.883	6.290

Table 20 POC data for SAFePool Experiment 1

Experiment 1	POC (µg/L)			
Days of incubation	0	2	5	9
LL-LFe avg.	158.39	169.10	122.31	105.20
LL-LFe A	139.81	129.15	148.35	114.20
LL-LFe B	124.38	144.34	107.51	96.52
LL-LFe C	210.97	233.82	111.07	104.87
LL-HFe avg.	158.39	123.96	126.43	120.78
LL-HFe A	139.81	101.37	121.43	136.11
LL-HFe B	124.38	117.78	115.01	116.61
LL-HFe C	210.97	152.73	142.83	109.63
HL-LFe avg.	158.39	96.72	125.61	239.98
HL-LFe A	139.81	89.63	115.31	228.20
HL-LFe B	124.38	92.92	128.99	248.01
HL-LFe C	210.97	107.61	132.55	243.74
HL-HFe avg.	158.39	150.36	186.73	264.04
HL-HFe A	139.81	147.30	158.80	136.11
HL-HFe B	124.38	151.54	180.48	344.96
HL-HFe C	210.97	152.24	220.90	311.05

Table 21 POC data for SAFePool Experiment 2

Experiment 2	POC (µg/L)			
Days of incubation	0	3	6	12
LL-LFe avg.	96.87	101.79	77.72	78.87
LL-LFe A	103.39	91.79	72.32	81.09
LL-LFe B	92.41	97.56	91.98	73.17
LL-LFe C	94.81	116.01	68.87	82.35
LL-HFe avg.	96.87	94.71	89.57	66.47
LL-HFe A	103.39	102.41	101.46	56.82
LL-HFe B	92.41	90.56	64.50	70.94
LL-HFe C	94.81	91.15	102.74	71.66
HL-LFe avg.	96.87	112.75	118.33	147.01
HL-LFe A	103.39	105.54	131.53	145.44
HL-LFe B	92.41	123.47	109.81	157.40
HL-LFe C	94.81	109.24	113.66	138.19
HL-HFe avg.	96.87	119.84	127.05	181.16
HL-HFe A	103.39	163.35	127.15	172.77
HL-HFe B	92.41	109.10	99.44	170.44
HL-HFe C	94.81	87.07	154.56	200.27

Table 22 POC data for SAFePool Experiment 3

Experiment 3	POC (µg/L)			
Days of incubation	0	3	6	10
LL-LFe avg.	78.45	89.03	73.02	74.99
LL-LFe A	82.38	106.79	63.43	79.43
LL-LFe B	74.52	71.28	82.62	70.55
LL-HFe avg.	78.45	99.27	90.99	68.37
LL-HFe A	82.38	80.23	73.29	72.42
LL-HFe B	74.52	118.30	108.70	64.32
HL-LFe avg.	78.45	125.54	160.45	257.81
HL-LFe A	82.38	134.19	141.25	269.79
HL-LFe B	74.52	116.90	179.65	245.83
HL-HFe avg.	78.45	125.08	174.64	418.59
HL-HFe A	82.38	138.64	181.82	383.07
HL-HFe B	74.52	111.52	167.46	454.12

Cell Counts

Table 23 Condensed cell count data for SAFePool Experiment 2

Experiment 2		T_3				T_6				T_{12}			
Cell diameter (µm)	T_0	LL-LFe	LL-HFe	HL-LFe	HL-HFe	LL-LFe	LL-HFe	HL-LFe	HL-HFe	LL-LFe	LL-HFe	HL-LFe	HL-HFe
2.00	138.05	158.00	150.40	200.35	222.65	118.93	133.40	286.30	322.60	92.20	111.55	553.10	469.00
2.14	132.80	137.45	126.20	193.45	203.40	105.75	122.70	268.05	299.20	94.25	109.80	506.45	401.30
2.29	129.70	128.15	121.25	180.90	208.85	96.13	114.75	244.05	271.40	93.15	95.95	417.50	355.30
2.45	119.25	117.00	111.45	170.30	184.00	85.83	96.30	206.00	232.40	80.70	86.80	294.85	285.90
2.63	120.30	109.70	104.40	161.05	170.95	77.17	93.20	160.70	198.30	73.05	79.65	195.60	214.55
2.81	110.50	101.15	92.65	139.80	145.90	70.02	78.70	119.10	167.75	69.35	73.00	146.75	174.55
3.01	89.80	80.20	82.65	115.20	122.40	61.87	76.10	96.90	145.25	66.05	68.55	124.90	148.05
3.22	77.20	65.70	70.65	98.65	95.75	52.59	67.00	82.60	135.65	55.55	64.45	124.40	146.15
3.45	64.85	58.55	60.65	81.80	83.85	45.70	60.15	76.55	134.15	49.85	64.05	123.70	153.65
3.69	63.45	63.60	62.65	72.55	72.00	54.07	57.40	82.70	141.20	49.10	64.70	132.85	167.60
3.95	68.65	74.75	69.75	68.90	70.60	60.45	63.35	82.05	140.90	57.60	81.45	136.15	181.35
4.23	72.70	74.05	67.40	68.55	69.15	65.56	70.75	79.40	125.85	64.55	86.35	145.75	188.35
4.52	64.10	63.00	63.25	75.80	76.35	52.77	70.40	91.30	136.85	56.55	80.55	142.60	180.80
4.84	50.00	48.65	47.95	65.65	70.30	32.96	57.20	87.90	122.80	40.40	59.55	142.20	176.05
5.18	35.55	35.00	31.90	49.90	54.10	21.86	40.15	74.15	101.25	25.25	42.15	119.45	162.90
5.55	21.70	19.60	20.15	29.40	35.70	12.54	26.35	50.55	67.85	15.55	25.35	82.65	141.00
5.94	13.75	10.40	10.60	17.95	21.65	7.54	14.45	25.60	38.15	9.55	14.65	54.50	101.20
6.36	8.75	7.55	7.50	11.25	13.05	4.14	8.50	12.40	20.60	5.90	9.00	32.10	60.45
6.80	7.60	7.35	6.45	8.55	10.25	3.13	5.15	9.40	12.40	4.95	7.85	21.25	36.85
7.28	6.00	5.70	4.85	7.00	6.70	3.75	5.65	7.70	9.15	4.20	6.50	17.50	27.35
7.80	6.95	5.40	4.75	4.70	5.70	5.38	4.30	6.00	7.85	5.45	6.85	18.05	26.90
8.34	6.05	6.30	6.15	5.20	5.60	4.76	4.65	5.00	7.95	5.15	5.40	15.90	23.90
8.93	9.50	6.50	7.00	5.00	7.35	5.73	5.95	6.80	8.95	5.45	6.60	18.40	24.65
9.56	8.85	7.95	7.10	8.30	6.65	4.65	5.90	7.85	10.10	5.50	6.70	14.25	23.35
10.23	7.05	8.05	6.15	6.25	7.65	3.71	4.40	9.30	11.10	4.05	5.95	13.35	18.35
10.95	6.30	4.90	5.45	5.85	7.55	3.51	4.90	8.45	10.10	4.00	5.75	11.95	18.50

Table 24 Condensed cell count data for SAFePool Experiment 3

Experiment 2		T_3				T_6				T_{10}			
Cell diameter (µm)	T_0	LL-LFe	LL-HFe	HL-LFe	HL-HFe	LL-LFe	LL-HFe	HL-LFe	HL-HFe	LL-LFe	LL-HFe	HL-LFe	HL-HFe
2.00	288.35	366.75	333.35	984.10	953.23	508.80	464.45	1525.00	1575.60	350.65	479.00	1604.95	1167.75
2.14	282.05	290.45	275.95	792.25	815.38	350.25	359.05	1135.25	1348.45	249.45	388.15	1229.30	959.05
2.29	269.95	240.90	237.20	641.30	615.05	240.35	277.55	903.35	1106.40	174.15	301.25	949.05	791.45
2.45	218.60	215.45	202.25	533.55	427.16	193.80	200.50	711.65	877.30	127.75	225.20	691.80	651.70
2.63	165.65	193.30	180.35	474.15	303.24	189.00	153.05	572.45	672.40	90.75	151.40	451.70	534.00
2.81	106.80	163.35	137.05	371.40	204.30	166.00	113.50	479.80	499.20	77.85	99.45	318.05	448.40
3.01	70.60	127.10	104.80	281.65	156.68	141.65	75.10	396.15	354.20	67.20	67.65	236.95	381.45
3.22	59.85	90.80	77.70	181.75	138.85	121.20	57.50	335.75	288.20	58.90	53.80	204.70	334.75
3.45	57.15	65.25	66.50	139.40	132.93	91.75	44.60	292.20	282.80	49.40	51.90	185.05	337.25
3.69	62.30	54.40	60.70	103.00	140.57	70.10	40.35	287.10	289.80	47.45	47.45	206.20	368.80
3.95	59.15	53.25	58.30	98.90	139.74	64.70	39.20	288.40	298.25	55.40	55.55	262.25	398.50
4.23	56.50	45.60	54.60	102.60	135.52	61.60	39.85	266.05	313.85	52.15	59.50	270.25	430.70
4.52	53.95	42.80	46.30	91.95	120.35	63.25	38.80	221.20	301.50	54.80	59.70	263.35	431.20
4.84	44.05	41.00	39.70	80.80	102.21	53.80	30.60	163.65	261.35	45.75	50.85	230.20	423.05
5.18	35.45	30.45	32.10	58.05	72.74	41.45	25.15	128.85	199.95	39.05	37.75	188.75	370.10
5.55	27.40	22.25	24.75	41.65	51.13	31.75	22.30	96.05	152.85	28.85	28.45	157.20	302.20
5.94	21.15	17.15	16.70	32.15	36.19	25.65	15.60	72.50	114.40	21.05	21.00	120.15	239.45
6.36	16.05	11.50	12.20	21.70	27.41	17.85	10.85	58.05	82.15	16.90	16.90	97.85	196.75
6.80	11.80	9.55	8.60	17.95	19.23	14.10	7.05	43.50	59.70	14.90	14.80	73.85	160.75
7.28	8.55	7.90	8.50	12.60	15.52	11.85	6.05	37.25	47.35	13.90	13.70	56.85	135.05
7.80	7.25	5.95	5.40	11.50	11.28	7.90	5.05	29.35	38.40	11.95	11.55	43.25	118.45
8.34	6.35	5.60	4.30	8.80	9.28	5.75	4.45	21.60	31.35	9.60	8.75	34.75	101.75
8.93	5.00	4.70	4.65	8.55	7.76	5.70	4.05	18.15	28.90	6.95	6.05	27.25	88.95
9.56	5.35	4.65	4.15	6.20	7.00	4.60	4.10	14.15	23.85	4.55	5.55	24.90	84.30
10.23	4.65	3.50	3.70	6.15	6.14	4.75	3.90	13.60	20.95	3.85	3.30	27.85	89.30
10.95	3.60	3.10	2.45	5.95	5.66	2.70	2.45	10.40	14.95	2.50	3.20	23.65	77.25

Table 25 F_v/F_m data for SAFePool Experiment 1

Experiment 1	F_v/F_m				
Days of incubation	5	6	7	8	9
LL-LFe avg.	0.412	0.407	0.444	0.418	0.444
LL-LFe A	0.418				0.452
LL-LFe B	0.394				0.455
LL-LFe C	0.418				0.427
LL-HFe avg.	0.402	0.424	0.428	0.408	0.431
LL-HFe A	0.411				0.430
LL-HFe B	0.402				0.431
LL-HFe C	0.393				0.432
HL-LFe avg.	0.332	0.331	0.287	0.310	0.265
HL-LFe A	0.337				0.257
HL-LFe B	0.330				0.219
HL-LFe C	0.328				0.320
HL-HFe avg.	0.301	0.317	0.314	0.285	0.343
HL-HFe A	0.314				0.337
HL-HFe B	0.302				0.336
HL-HFe C	0.281				0.357

Table 26 F_v/F_m data for SAFePool Experiment 2

Experiment 2	F_v/F_m												
Days of incubation	0	1	2	3	4	5	6	7	8	9	10	11	12
LL-LFe avg.	0.444	0.504	0.465	0.481	0.501	0.424	0.477	0.461	0.470	0.390	0.443	0.500	0.463
LL-LFe A	0.442			0.471			0.474						0.451
LL-LFe B	0.448			0.493			0.446						0.465
LL-LFe C	0.440			0.480			0.511						0.475
LL-HFe avg.	0.444	0.487	0.423	0.474	0.484	0.435	0.494	0.494	0.504	0.460	0.461	0.479	0.491
LL-HFe A	0.442			0.471			0.497						0.471
LL-HFe B	0.448			0.465			0.490						0.490
LL-HFe C	0.440			0.487			0.494						0.513
HL-LFe avg.	0.444	0.444	0.368	0.429	0.419	0.403	0.378	0.360	0.338	0.324	0.285	0.283	0.313
HL-LFe A	0.442			0.424			0.366						0.310
HL-LFe B	0.448			0.437			0.398						0.307
HL-LFe C	0.440			0.425			0.370						0.322
HL-HFe avg.	0.444	0.431	0.371	0.450	0.415	0.397	0.465	0.433	0.452	0.420	0.427	0.389	0.377
HL-HFe A	0.442			0.438			0.448						0.384
HL-HFe B	0.448			0.448			0.485						0.378
HL-HFe C	0.440			0.463			0.461						0.369

Table 27 F_v/F_m data for SAFePool Experiment 3

Experiment 3	F_v/F_m										
Days of incubation	0	1	2	3	4	5	6	7	8	9	10
LL-LFe avg.	0.349	0.412	0.452	0.462	0.480	0.466	0.463	0.437	0.429	0.467	0.485
LL-LFe A	0.360			0.463			0.467				0.495
LL-LFe B	0.338			0.461			0.459				0.475
LL-HFe avg.	0.349	0.428	0.470	0.495	0.485	0.492	0.520	0.478	0.498	0.507	0.515
LL-HFe A	0.360			0.490			0.536				0.480
LL-HFe B	0.338			0.500			0.503				0.549
HL-LFe avg.	0.349	0.357	0.383	0.387	0.288	0.338	0.268	0.261	0.255	0.241	0.243
HL-LFe A	0.360			0.404			0.265				0.251
HL-LFe B	0.338			0.370			0.270				0.236
HL-HFe avg.	0.349	0.385	0.426	0.453	0.379	0.456	0.400	0.376	0.340	0.206	0.234
HL-HFe A	0.360			0.447			0.407				0.217
HL-HFe B	0.338			0.458			0.392				0.251

Table 28 σ_{PSII} data for SAFePool Experiment 1

Experiment 1	σ_{PSII} (Å^2/quanta)				
Days of incubation	5	6	7	8	9
LL-LFe avg.	214	200	208	212	225
LL-LFe A	223				229
LL-LFe B	214				225
LL-LFe C	204				222
LL-HFe avg.	224	209	220	212	216
LL-HFe A	224				210
LL-HFe B	211				216
LL-HFe C	234				222
HL-LFe avg.	204	175	195	223	244
HL-LFe A	205				247
HL-LFe B	194				309
HL-LFe C	212				176
HL-HFe avg.	205	184	194	218	206
HL-HFe A	210				215
HL-HFe B	191				209
HL-HFe C	220				194

Table 29 σ_{PSII} data for SAFePool Experiment 2

Experiment 2	σ_{PSII} (Å^2/quanta)												
Days of incubation	0	1	2	3	4	5	6	7	8	9	10	11	12
LL-LFe avg.	222	231	257	215	245	213	253	231	224	206	208	254	234
LL-LFe A	226			221			262						248
LL-LFe B	217			220			234						232
LL-LFe C	225			203			262						220
LL-HFe avg.	222	218	221	213	232	204	221	221	227	208	191	188	217
LL-HFe A	226			219			238						213
LL-HFe B	217			193			207						222
LL-HFe C	225			229			216						217
HL-LFe avg.	222	247	237	223	233	210	242	213	202	197	186	211	206
HL-LFe A	226			239			251						205
HL-LFe B	217			213			255						215
HL-LFe C	225			217			221						197
HL-HFe avg.	222	207	250	212	207	206	213	183	209	203	202	211	210
HL-HFe A	226			202			212						222
HL-HFe B	217			210			222						204
HL-HFe C	225			225			204						205

Table 30 σ_{PSII} data for SAFePool Experiment 3

Experiment 3	σ_{PSII} (Å^2/quanta)										
Days of incubation	0	1	2	3	4	5	6	7	8	9	10
LL-LFe avg.	197	200	230	216	238	225	239	250	230	247	243
LL-LFe A	199			218			238				238
LL-LFe B	195			214			239				248
LL-HFe avg.	197	240	212	224	226	225	238	215	212	233	239
LL-HFe A	199			234			244				228
LL-HFe B	195			215			233				249
HL-LFe avg.	197	202	235	253	301	245	334	263	251	247	237
HL-LFe A	199			255			320				237
HL-LFe B	195			250			349				236
HL-HFe avg.	197	215	197	246	260	208	224	206	205	235	234
HL-HFe A	199			247			212				234
HL-HFe B	195			245			235				235

Table 31 NO_3 + NO_2 data for SAFePool Experiment 1

Experiment 1	NO_3 + NO_2 (µM)			
Days of incubation	0	2	5	9
LL-LFe avg.	39.92	41.54	42.67	37.83
LL-LFe A	34.41	41.03	39.54	35.73
LL-LFe B	42.65	44.29	44.52	41.99
LL-LFe C	42.69	39.30	43.95	35.77
LL-HFe avg.	39.92	42.33	43.24	42.30
LL-HFe A	34.41	44.95	43.42	43.40
LL-HFe B	42.65	41.70	43.87	43.26
LL-HFe C	42.69	40.35	42.45	40.26
HL-LFe avg.	39.92	40.68	40.90	39.12
HL-LFe A	34.41	40.16	35.61	37.62
HL-LFe B	42.65	37.13	43.51	38.83
HL-LFe C	42.69	44.74	43.57	40.91
HL-HFe avg.	39.92	39.14	39.77	35.05
HL-HFe A	34.41	41.15	43.19	37.19
HL-HFe B	42.65	35.90	35.68	30.46
HL-HFe C	42.69	40.38	40.44	37.51

Table 32 NO_3 + NO_2 data for SAFePool Experiment 2

Experiment 2	NO_3 + NO_2 (µM)			
Days of incubation	0	3	6	12
LL-LFe avg,	30.41	32.19	30.54	25.38
LL-LFe A	34.94	27.41	25.83	24.60
LL-LFe B	24.02	33.85	34.82	24.61
LL-LFe C	32.27	35.32	30.99	26.94
LL-HFe avg.	30.41	34.53	23.88	30.72
LL-HFe A	34.94	34.89	22.05	33.13
LL-HFe B	24.02	33.82	20.03	32.22
LL-HFe C	32.27	34.89	29.56	26.81
HL-LFe avg.	30.41	35.13	34.72	27.14
HL-LFe A	34.94	35.10	35.04	21.11
HL-LFe B	24.02	35.75	34.16	28.43
HL-LFe C	32.27	34.53	34.95	31.87
HL-HFe avg.	30.41	31.97	31.85	26.38
HL-HFe A	34.94	38.46	27.85	19.88
HL-HFe B	24.02	21.67	33.02	29.32
HL-HFe C	32.27	35.79	34.66	29.95

Table 33 NO_3 + NO_2 data for SAFePool Experiment 3

Experiment 3	NO_3 + NO_2 (µM)			
Days of incubation	0	3	6	10
LL-LFe avg.	23.51	19.65	21.06	23.75
LL-LFe A	18.38	16.23	20.91	23.96
LL-LFe B	28.65	23.07	21.22	23.54
LL-HFe avg.	23.51	23.23	13.96	22.83
LL-HFe A	18.38	23.23	15.96	22.27
LL-HFe B	28.65		11.95	23.39
HL-LFe avg.	23.51	20.38	16.71	18.33
HL-LFe A	18.38	18.74	18.48	18.82
HL-LFe B	28.65	22.02	14.94	17.84
HL-HFe avg.	23.51	22.83	11.59	5.43
HL-HFe A	18.38	22.52	14.86	4.55
HL-HFe B	28.65	23.14	8.33	6.32

Table 34 PO_4 data for SAFePool Experiment 1

Experiment 1	PO_4 (µM)			
Days of incubation	0	2	5	9
LL-LFe avg.	1.821	1.755	1.646	1.698
LL-LFe A	1.811	1.783	1.486	1.670
LL-LFe B	1.868	1.783	1.755	1.811
LL-LFe C	1.783	1.698	1.698	1.613
LL-HFe avg.	1.821	1.849	1.802	1.792
LL-HFe A	1.811	1.925	1.981	1.811
LL-HFe B	1.868	1.868	1.670	1.811
LL-HFe C	1.783	1.755	1.755	1.755
HL-LFe avg.	1.821	1.811	1.689	1.604
HL-LFe A	1.811	1.783	1.528	1.557
HL-LFe B	1.868	1.840	1.585	1.642
HL-LFe C	1.783	1.811	1.953	1.613
HL-HFe avg.	1.821	1.651	1.604	1.538
HL-HFe A	1.811	1.726	1.613	1.443
HL-HFe B	1.868	1.613	1.585	1.443
HL-HFe C	1.783	1.613	1.613	1.726

Table 35 PO_4 data for SAFePool Experiment 2

Experiment 2	PO_4 (µM)			
Days of incubation	0	3	6	12
LL-LFe avg.	1.078	1.000	0.903	0.981
LL-LFe A	1.019	0.932	0.728	0.903
LL-LFe B	0.845	1.049	0.903	1.019
LL-LFe C	1.369	1.019	1.078	1.019
LL-HFe avg.	1.078	0.981	0.951	1.000
LL-HFe A	1.019	0.932	0.903	1.107
LL-HFe B	0.845	1.049	0.903	0.961
LL-HFe C	1.369	0.961	1.049	0.932
HL-LFe avg.	1.078	0.990	1.029	0.922
HL-LFe A	1.019	0.932	0.990	0.990
HL-LFe B	0.845	1.078	0.990	0.816
HL-LFe C	1.369	0.961	1.107	0.961
HL-HFe avg.	1.078	0.971	0.893	0.903
HL-HFe A	1.019	1.019	0.816	0.757
HL-HFe B	0.845	0.874	0.990	0.903
HL-HFe C	1.369	1.019	0.874	1.049

Table 36 PO_4 data for SAFePool Experiment 3

Experiment 3	PO_4 (µM)			
Days of incubation	0	3	6	10
LL-LFe avg.	0.920	1.061	0.991	0.892
LL-LFe A	0.877	1.019	0.962	0.877
LL-LFe B	0.962	1.104	1.019	0.906
LL-HFe avg.	0.920	1.132	0.849	1.019
LL-HFe A	0.877	1.132	0.849	0.962
LL-HFe B	0.962		0.849	1.075
HL-LFe avg.	0.920	1.118	0.835	0.764
HL-LFe A	0.877	1.047	0.821	0.736
HL-LFe B	0.962	1.189	0.849	0.792
HL-HFe avg.	0.920	1.104	0.693	0.368
HL-HFe A	0.877	1.104	0.792	0.396
HL-HFe B	0.962	1.104	0.594	0.340

Table 37 SiO_4 data for SAFePool Experiment 1

Experiment 1	SiO_4 (µM)			
Days of incubation	0	2	5	9
LL-LFe avg.	67.62	66.29	77.05	62.86
LL-LFe A	65.71	65.71	78.57	59.43
LL-LFe B	72.57	66.86	77.71	72.00
LL-LFe C	64.57	66.29	74.86	57.14
LL-HFe avg.	67.62	69.71	75.62	72.38
LL-HFe A	65.71	69.14	78.86	74.29
LL-HFe B	72.57	70.29	73.14	75.43
LL-HFe C	64.57	69.71	74.86	67.43
HL-LFe avg.	67.62	66.48	68.95	63.62
HL-LFe A	65.71	65.14	57.14	65.14
HL-LFe B	72.57	66.29	72.00	62.86
HL-LFe C	64.57	68.00	77.71	62.86
HL-HFe avg.	67.62	68.76	67.62	63.33
HL-HFe A	65.71	73.71	74.86	66.29
HL-HFe B	72.57	64.00	61.14	54.55
HL-HFe C	64.57	68.57	66.86	69.14

Table 38 SiO_4 data for SAFePool Experiment 2

Experiment 2	SiO_4 (µM)			
Days of incubation	0	3	6	12
LL-LFe avg.	1.070	0.856	0.875	0.775
LL-LFe A	0.843	0.783	0.776	0.740
LL-LFe B	1.505	0.865	0.908	0.798
LL-LFe C	0.861	0.919	0.942	0.787
LL-HFe avg.	1.070	0.846	0.723	0.883
LL-HFe A	0.843	0.832	0.658	0.947
LL-HFe B	1.505	0.861	0.625	0.901
LL-HFe C	0.861	0.846	0.886	0.801
HL-LFe avg.	1.070	0.890	0.899	0.707
HL-LFe A	0.843	0.865	0.850	0.595
HL-LFe B	1.505	0.902	0.898	0.694
HL-LFe C	0.861	0.902	0.948	0.831
HL-HFe avg.	1.070	0.906	0.868	0.594
HL-HFe A	0.843	0.995	0.799	0.470
HL-HFe B	1.505	0.815	0.888	0.634
HL-HFe C	0.861	0.908	0.917	0.679

Table 39 SiO_4 data for SAFePool Experiment 3

Experiment 3	SiO_4 (µM)			
Days of incubation	0	3	6	10
LL-LFe avg.	1.161	1.533	1.699	2.032
LL-LFe A	1.443	1.384	1.619	2.050
LL-LFe B	0.879	1.682	1.778	2.014
LL-HFe avg.	1.161	1.865	1.102	1.881
LL-HFe A	1.443	1.865	1.186	1.831
LL-HFe B	0.879		1.018	1.931
HL-LFe avg.	1.161	1.566	1.487	1.332
HL-LFe A	1.443	1.403	1.549	1.419
HL-LFe B	0.879	1.728	1.425	1.246
HL-HFe avg.	1.161	1.793	0.961	0.599
HL-HFe A	1.443	1.881	1.094	0.612
HL-HFe B	0.879	1.705	0.829	0.587